

ADVANCED ELECTRIC PROPULSION RESEARCH

PREPARED FOR

NATIONAL AERONAUTICS AND SPACE ADMINISTRATION

GRANT NGR06-002-032

REPORT NO. 7

SPACE PROPULSION PROGRAM  
ENERGY CONVERSION PROGRAM  
COLLEGE OF ENGINEERING  
COLORADO STATE UNIVERSITY  
FORT COLLINS, COLORADO



FACILITY FORM 602

N 68-34023  
(ACCESSION NUMBER) (THRU)

104  
(PAGES) (CODE)

CR-96633  
(NASA CR OR TMX OR AD NUMBER) (CATEGORY)

MER 68-69WRM-11

SEMI-ANNUAL REPORT

For the period December 31, 1967 to June 30, 1968

ADVANCED ELECTRIC PROPULSION RESEARCH

Prepared for

NATIONAL AERONAUTICS AND SPACE ADMINISTRATION

June, 1968

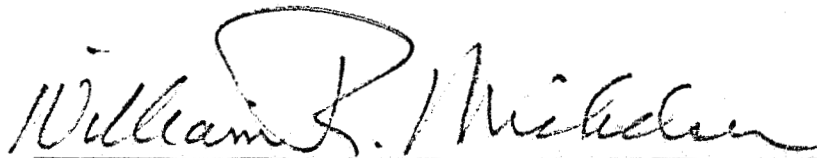
Grant NGR06-002-032

Technical Management

George Pfannebecker

Nuclear Electric Systems Division  
Office of Advanced Research Technology  
NASA Headquarters  
Washington, D.C. 20546

Prepared by:



William R. Mickelsen, principal investigator  
Professor of Mechanical Engineering  
and Professor of Electrical Engineering  
Engineering Center  
Colorado State University  
Fort Collins, Colorado 80521

## CONTENTS

AUXILIARY ELECTRIC PROPULSION - STATUS AND PROSPECTS	1.1
POWER NEEDS FOR ELECTRIC PROPULSION	2.1
COMPARISON OF VARIOUS HEAT ADDITION PROGRAMS TO SUPERSONIC NOZZLE FLOW	3.1
MEASUREMENT OF NEUTRAL-ATOM SPEED IN BOMBARDMENT THRUSTERS	4.1
AN ANALYSIS OF ELECTROSTATIC-SPRAYING FLUIDS IN TERMS OF THEIR ELECTROLYTIC SOLUTION CHARACTERISTICS	5.1

Paper presented at Fifth Symposium on Advanced Propulsion Concepts, April 8-10, 1968, Chicago, Illinois.

## AUXILIARY ELECTRIC PROPULSION - STATUS AND PROSPECTS

by

William R. Mickelsen  
Colorado State University

and

William C. Isley  
Goddard Space Flight Center

### ABSTRACT

Missions for auxiliary electric propulsion are reviewed, including difficult future missions. The present status of electric propulsion applications is summarized. This summary includes electric propulsion systems in missions already flown and in definitely scheduled flights through 1969. Some advanced concepts are described that have promise of providing superior performance. These advanced concepts include thermal augmentation of resistojets for MORL class spacecraft, supersonic power addition in electrothermal thrusters, higher-voltage solar-cell arrays for charged-particle thrusters and for bombardment thruster systems, and radioisotope electrogenerators for charged-particle thrusters and for pulsed-plasma thrusters.

# AUXILIARY ELECTRIC PROPULSION - STATUS AND PROSPECTS

by

William R. Mickelsen\*  
Colorado State University

and

William C. Isley\*\*  
Goddard Space Flight Center

## INTRODUCTION

Mission requirements have played a very important role in the direction of development for electric propulsion systems in the millipound and micropound thrust regimes. As early as 1962, it was recognized by many workers in the field that systems in the "micro-thrust" range would be required for a number of spacecraft applications. Probably the first specific case evolved from studies of 24 hour synchronous spacecraft, where reaction jets were found to be necessary for east-west station keeping. As initial missions involved spin stabilized satellites, the problems were complicated by the requirement for pulsing of jets in synchronism with the spin period in order to provide station keeping. Cold gas nitrogen and peroxide systems emerged as the choice for flight application primarily because propellant weight requirements were small and no alternate electric propulsion approach had been developed to a point suitable for flight use.

The early mission studies gave rise to a wide variety of R&D activities to provide electric thrust systems for the future missions (ref. 1). The resistojets, ion micro-thrusters, and plasma devices were but a few concepts that grew out of the anticipated need for small station-keeping systems. As more serious concern was given to north-south station keeping of spacecraft, attention turned to the higher specific impulse concepts such as bombardment, strip-ion, and colloid thrusters, which could operate at thrust levels from 300 to 500 micropounds. In this case propellant weight has become a strong factor in system selection. A number of application studies were performed to assess

---

\* Professor of Mechanical Engineering and of Electrical Engineering. Participation in this work under NASA Grant NGR06-002-032, Electric Thruster Systems, OART.

\*\* Head, Systems Analysis and Ion Propulsion Section.

optimum thrust levels, the advantages of thrust vector deflection, and propulsion system configuration (refs. 2-4). The results of such investigations generally pointed to the strong influence of onboard electrical power for system operation. For example, approximately 75 watts is required to operate a 350 micropound cesium ion bombardment micro-thruster for north-south station keeping of a 24 hour spacecraft. This power drain would be relatively constant for a spacecraft weight of 1,500 pounds.

The serious consideration of gravity-gradient oriented spacecraft in a 24 hour orbit led to yet another mission application for electric propulsion. It was discovered that thrust levels in the range from 10 to 30 micropounds would be required for east-west station keeping in the presence of gravity stabilizing torques. Elastic body effects associated with the long boom extensions on such spacecraft would cause a motion of the center of mass with resulting attitude disturbance torques on the main body during translational corrections due to thruster misalignments. The maximum permissible thrust level for east-west station keeping was established as that value which could tumble the spacecraft within a prescribed time interval. As an outgrowth of this problem, beam-vectored thrusters appeared quite attractive for minimizing such attitude disturbances.

The most recent mission applications pertain to attitude fine pointing and slewing of large dish antennas in a 24 hour orbit. The use of electric propulsion devices for such purposes has been extensively studied (refs. 5,6) to establish relative advantages with respect to other competitors such as momentum wheels, control moment gyros, and similar concepts. Such studies have indicated that near-term applications will be decided primarily on inherent reliability of competing approaches rather than size, weight, or power alone. Devices such as momentum wheels have a fixed weight penalty, but require electrical power in amounts dictated by slewing rates, solar pressure profile, and required maneuvering action. Generally speaking, such devices also require onboard reaction jets to enable unloading of wheels intermittently, so that this additional weight penalty should be included in comparisons.

From a mission planning standpoint the future prospects for spacecraft auxiliary electric propulsion appear to be promising. In addition to the follow-on flights into 24 hour orbit involving station keeping, it is foreseen that larger spacecraft in spinning modes will be placed in 24 hour orbit, where precise attitude control will be needed for precession of the spin axis. Three-axis stabilized

spacecraft should become larger in size and weight, necessitating greater total impulse for orbit correction. The MORL is but one example of this trend.

As the observer looks further into the potentialities and future prospects of electric propulsion, the trend appears to be turning strongly in the direction of total systems design approach rather than simple physical tradeoffs. The development costs will definitely play an important role in selection of future concepts. To this point, mission requirements have been primarily limited to applications in a 24 hour orbit. There are at least two other interesting missions that will be mentioned here.

The requirements for Earth observation spacecraft using solar power present unique requirements for orbit control. A typical example is a spacecraft located in a nominal 480 nautical mile circular orbit which is inclined 101.9 degrees with respect to the equator. This orbit provides both sun synchronism to maximize power and a near-synchronous earth ground track at the equator crossings. The mission objective is to maintain the ground track with regard to overlap in picture coverage at successive periodic crossings. The sensitivity to orbit variations is demonstrated by the fact that a 0.6 nautical mile change in semi-major axis produces a 10 nautical mile change in overlap out of a total picture width of 96 nautical miles. Studies of the long term maintenance of such an orbit have shown that onboard reaction jets will be required for mission lifetimes in excess of one year assuming perfect initial injection (ref. 7). The total impulse requirements appear to be well suited to a number of electric propulsion concepts.

Another mission possibility is the Hummingbird satellite, which would be located at one of the libration points in the earth-moon system to serve as a communications relay point in Apollo or post-Apollo missions. Early studies have indicated that electric propulsion may be the preferred approach for orbit maintenance against gravitational perturbations. Further study will be required to obtain a firm direction for development activities.

#### CURRENT STATUS SUMMARY

A brief summary is given here of major directions of hardware development and applications in spacecraft auxiliary electric propulsion. A more detailed description of electric propulsion for prime onboard equipment, and for flight experiments, will be found in ref. 1. The status of prime-onboard operational systems (OS) and flight-experiment systems (FE) is summarized in Table I.

## Operational Flight Systems

The resistojet, in a general sense, represents the most basic attempt to improve propulsion system performance over cold-gas and available chemical devices. Two basic avenues were followed in R&D programs for the resistojet. The first approach treated the thruster as a thermal storage device which would be operated under quasi steady state conditions in a pulse mode manner. This technique maximizes realizable specific impulse for brief pulse durations (of the order of minutes) by the use of stored heat to maintain plenum gas temperature. For long-term pulses (continuous operation) such a thruster would degrade in specific impulse to match the end-point energy balance.

Figure 1 shows a single-nozzle version of the TRW Systems resistojet, successfully flown on a Vela III spacecraft in 1965. The design approach was simply to heat the conventional nitrogen propellant to a higher temperature using an electrical heater and thermal insulation on the thruster body. A later version of the TRW resistojet is shown in Figure 2. This represents a multijet thruster flown successfully on an Advanced Vela spacecraft in 1967. Again nitrogen was employed as propellant in a conventional system. Figure 3 presents a single-jet version of a thermal storage resistojet built by General Electric and flown on an NRL spacecraft in 1967. This thruster operates from ammonia propellant, which is stored as a liquid in a tank and fed by capillary action to the thruster.

The second design approach for the resistojet was employed by AVCO Corporation as shown in Figure 4. Here, emphasis was placed upon obtaining fast heatup of the propellant contact surface by minimizing the thermal mass of the heating region. The resulting thruster has a general appearance of a hypodermic needle where propellant is injected through the needle and the ends of the needle are resistively heated. Experimental systems of this type were built and flown on the ATS B and C spacecraft, and advanced versions will be prime-onboard equipment on the ATS D and E spacecraft.

The tradeoff factors between the two design approaches depend heavily upon the intended use, specifically the pulse length and required duty cycle. For attitude control having very low duty cycle, the pulsed-mode resistojet offers significant power savings. For long-term pulsing or high duty cycle the thermal-storage resistojet appears attractive because of the higher obtainable specific impulse.



## Flight Experiment Systems

In addition to the resistojet programs which have attained a flight status, there are a number of flight experiment systems presently under development to assess their performance capabilities in space for mission functions similar to those previously described. These systems are scheduled to fly in the Air Force multi-purpose synchronous satellite program (AFMS), on the ATS D and E spacecraft, and in the LES program (ref. 8).

The General Electric Company ammonia thermal-storage resistojet shown in Figure 5 is designed to demonstrate multiple (redundant) exhaust jets for station-keeping functions in the AFMS program. GE is also developing for NASA Goddard a similar resistojet where the nozzle configuration will provide combined attitude control and station-keeping from a single thruster module and heater. Also included in the AFMS program are the Electro-Optical Systems, Inc. cesium electron-bombardment thruster, for north-south station keeping, shown in Figure 6; and the TRW Systems liquid-spray charged-particle thruster for east-west station keeping and yaw control, shown in Figure 7.

Figure 8 shows a cesium contact ion microthruster with beam vectoring capability which is now under development at Electro-Optical Systems for testing on the ATS D and E spacecraft. In addition to evaluating system behavior this experiment will also permit a demonstration of east-west station keeping thrust levels on a gravity gradient stabilized spacecraft.

Pulsed-plasma thrusters have also reached a development stage where flight experiments can be scheduled. The Republic Aviation Division of the Fairchild Hiller Corporation is preparing a solid-propellant pulsed-plasma thruster system for the LES flight program.

The ATS F and G spacecraft programs presently under study might be vehicles for testing advanced versions of a number of thruster systems discussed so far.

## ADVANCED CONCEPTS

There are a number of advanced concepts in auxiliary electric propulsion that have promise of providing superior performance, greater reliability, and better matching with the spacecraft interface. Some of these concepts have been mentioned previously in reference 9, but are discussed further here, and in addition, some new concepts are presented.

## Radioisojet

A direct alternate to the resistojet class of thrusters is the Radioisojet, which employs a radioisotope thermal source in place of the electrical heater (ref. 10). Early development work for such thrusters has been carried out by General Electric Company and TRW Systems. The GE approach employs promethium-147 oxide as the heat source, and the thruster configuration is shown in Figure 9. The TRW Systems design approach employs Pu-238 as the heat source in a thruster configuration somewhat similar to that previously shown. The major factors in selection of best radioisotope lie in requirements for radiation shielding and aerospace safety for a flight unit.

During tests of the Radioisojet, ammonia propellant temperatures of 1270°K were attained. For reasons that will become clear in the ensuing text, the Radioisojet technology is an important and essential element in a number of advanced electric propulsion concepts.

## MORL Resistojet

The manned orbiting research laboratory (MORL) is a possible unique application for electric propulsion in the foreseeable future. Studies by the McDonnell Douglas Corporation (ref. 11) have shown that a resistojet propulsion system (Figure 10) operating with biowaste propellant would serve well for drag cancellation and for attitude control in conjunction with control-moment gyros. The EC/LS system for a 6-crew MORL could consist basically of an electrolysis unit to produce oxygen from water supplied periodically to the spacecraft. A major constituent of the biowaste would be carbon dioxide gas, which would provide more than sufficient propellant for all propulsion requirements.

Because of oxidizing impurities in the carbon dioxide biowaste, it appears that resistojet operation may be limited to 3000°R plenum temperature. With 40 psia plenum pressure, the performance of such a resistojet would be about 4 watt(electric)/millipound at a specific impulse of 178 seconds (ref. 11).

A possible way of improving this performance is by combining Radioisojet technology with the carbon-dioxide resistojet in the ATEP concept (augmented thermally electric propulsion). Principles and advantages of the ATEP concept are described and analyzed in ref. 12. The diagram in Figure 11 illustrates a hypothetical application to the MORL electric propulsion system. If the radioisotope heater

performance could approach that of the Radioisotjet, then the carbon dioxide could be thermally heated to  $1200^{\circ}\text{K}$ , and then electrically heated to the  $3000^{\circ}\text{R}$  ( $1670^{\circ}\text{K}$ ) compatibility limit. As shown in Figure 12, the ATEP concept with radioisotope pre-heating of the propellant might lower the power/thrust to 1.7 watt(electric)/millipound. This reduction in electric power could be very significant in missions of the MORL type.

#### Supersonic Heat Addition in Electrothermal Thrusters

Another application of the ATEP concept is heat addition to supersonic streams by electrical means. In principle, significant increases in specific impulse are possible, without incurring dissociation or ionization losses in the near frozen flow to be expected in electrothermal thrusters. Analyses reported in refs. 13 and 14 have shown that the mode of heat addition has a very great effect on the nozzle area ratio that is required to reach significantly higher exhaust velocities. The best heating mode reported to date is a linear relation between heat addition and nozzle cross-sectional area, and this mode is used here merely for want of better information.

Theoretical performance of a lithium electrothermal thruster with supersonic heat addition is shown in Figure 13. An area ratio of 100 is assumed for the nozzle, as being representative of an optimum realistic design (ref. 15). Plenum temperature is assumed to be  $2500^{\circ}\text{K}$ , which is in keeping with demonstrated resistojet temperatures (ref. 16), and a negligible exhaust pressure is assumed. Even with the non-optimum mode of supersonic heat addition, significant increases in specific impulse are indicated as the total temperature is increased. This increase in specific impulse appears possible with negligible change in power/thrust. With a fully optimized mode of heat addition, even better performance is anticipated, as discussed in ref. 14.

Even more dramatic improvement in performance is predicted when a combination of thermal augmentation and supersonic heat addition is employed, as shown in Figure 14. Much of the improvement is due to the high heat of vaporization of lithium. As with the carbon-dioxide resistojet, radioisotope thermal heating of the propellant to  $1200^{\circ}\text{K}$  is assumed, which is within the present state-of-the-art for Radioisotjet technology. It must be noted that thermal heating of lithium to  $1200^{\circ}\text{K}$  would provide a vapor pressure of only 1.5 torr, while thermal or electric heating to  $1600^{\circ}\text{K}$  would provide a vapor pressure of 1 atmosphere. For this reason, thermal heating to the higher

temperature would be advantageous. Further improvement in Radioisotjet design could allow increased thermal heating of the lithium propellant, with attendant reduction of the electric power requirements. In addition, further improvement in performance with supersonic heat addition should be possible with optimized modes of heat addition.

#### Higher-Voltage Solar-Cell Arrays

Advantages of higher-voltage solar-cell arrays are discussed in ref. 9 with regard to system weight and reliability of ion thrusters. As more flight-system experience is gained, it becomes increasingly evident that the power conditioning needed to provide kilovolts of electric power for electrostatic thrusters is a serious detriment to system reliability. Operation of solar-cell arrays at hundreds of volts could completely eliminate power conditioning. Some work is presently being done to investigate the feasibility of operating the solar arrays at higher voltage (ref. 17).

In the specific impulse range normally dominated by resistojets, it appears possible to obtain good performance from the liquid-spray charged-particle thruster with voltages in the hundreds of volts. As shown in Figure 15, a solar-cell array voltage of 400 volts could provide a specific impulse of 280 seconds with charged-particle  $q/m = 10,000$  coulomb/kg, which is a presently attainable value (ref. 18). Performance of the liquid-spray thruster at 280 seconds specific impulse is definitely competitive with conventional resistojets. If even higher solar-cell-array voltages were possible, the liquid-spray thruster could exceed the specific impulse of present-day resistojets in the low micro-pound thrust range.

Electrostatic ion thruster performance may be very attractive with only moderate increases in solar-cell-array voltage, as shown in Figure 16. The hypothetical thruster used for these theoretical calculations was assumed to have the demonstrated performance of a cesium hollow cathode, with total-throughput ion optics (ref. 19), and adequate power density by virtue of a composite-grid accelerator structure (ref. 20). Satisfactory operation with composite grid accelerators has been achieved in 100 hour tests with thrusters from 5 cm to 30 cm in size, and with net accelerating voltages from 400 to 1000 volts (ref. 21). Power/thrust for the hypothetical thruster with other alkali propellants was calculated with the assumption that the cathode power consumption (ev/ion) would be proportional to the first ionization potential of the propellant.

From this brief examination of the performance of two extremes of electrostatic thrusters (with respect to charge/mass of propellant), it is evident that much would be gained if solar-cell arrays could be operated at hundreds of volts.

#### The ACCENT System

A new concept in auxiliary electric propulsion is called ACCENT (for autogenically-controlled-cesium-, or colloid-, electro-nuclear-thrust system). This concept offers promise of significant reductions in propellant mass and in demands on the spacecraft power system, and by virtue of the small number of components, the ACCENT system offers greatly improved reliability (ref. 22). High-voltage dc electric power is generated in a radioisotope electro-generator (REG) as described in refs. 22 and 23, thereby eliminating the complex power conditioning needed for conventional electrostatic ion and colloid thrusters, and for pulsed-plasma thrusters.

In ACCENT systems having contact-ion thrusters, radioisotope heating of the ionizer would be required. Low-voltage power for the neutralizer and control circuitry could be provided by incorporating radioisotope thermoelectric generators (RTG).

The REG performance improves as operating voltage is increased, reaching a maximum efficiency at about 50,000 volts when promethium-147 is the fuel. This high-voltage capability makes the ACCENT system especially well suited to the liquid-spray charged-particle thruster. With the bi-polar liquid-spray thruster, there is no neutralizer, and propellant-feed power requirements could be supplied by waste heat from the REG. Low-voltage power for control circuitry could be drawn from the spacecraft power system, or could be generated by an integral RTG within the REG containment vessel. Hypothetical ACCENT systems with 20 micropound and 350 micropound bi-polar liquid-spray thrusters are shown in Figures 17 and 18. Although REG of such designs have not been developed, there is sufficient experimental background to indicate fundamental feasibility (refs. 22 and 23). In fact, some characteristics of the REG would be especially compatible with electrostatic thrusters; for instance, an electric breakdown in the thruster would merely drain the REG much like a capacitor discharge, thereby automatically limiting breakdown damage to the thruster.

Because of the capacitor-like action of the REG, the ACCENT system should be well suited to pulsed-plasma thrusters. There are a number of pulsed-plasma thrusters under development at present. These can be characterized in scope by the solid-propellant Fairchild Hiller thruster described previously, and by the gas-propellant inductive-accelerator system under development at TRW Systems (ref. 24). These thrusters require a capacitive discharge for each thrust pulse, and this discharge could be provided by the REG in an ACCENT system.

With the virtual elimination of all power demand on the spacecraft system, and with reliability through simplicity, the ACCENT system appears to be an advanced concept of great interest.

#### FUTURE TRENDS

The usual criteria for selecting most promising design concepts is basically one of comparing physical parameters such as size, weight, power, and development status. Experience with flight systems and those under development for flight experiments has shown that use of such physical criteria must be replaced with a total systems design evaluation which includes the categories of reliability, design complexity, and cost. For example, the existing resistojet systems rely on an electrical heater for improvement in specific impulse. This heater must ultimately demonstrate high-temperature, long-life capability in order to maintain a competitive position among other approaches. In contrast, Radioisojet uses a radioisotope heat source of inherent high reliability. However, now the problems shift into radiation shielding, spacecraft interfaces, and aerospace safety. Both of these systems require a propellant on-off solenoid valve, which itself must be treated as one of the most important design factors.

For the ion and colloid thrusters, the problems become high-voltage circuitry, electromagnetic interference, reliability of heater elements and electrode degradation. The pulsed plasma devices which are valveless still must deal with electrode deposition and with high-voltage circuitry to obtain competitive performance. A number of design options have been studied to remedy the major reliability problem areas being faced by the conventional ion and colloid systems. For example, the neutralizer could be eliminated on the colloid thruster by employing a bi-polar concept which groups positive and negative needle arrays. Either high-voltage solar-cell arrays, or the ACCENT concept could eliminate most of the complex power conditioning circuitry needed for either engine type. In addition, the

ACCENT system offers complete independence from the spacecraft power system by virtue of complete self-containment. There probably will be an upper practical limit to solar-cell array voltage, which will prevent use of this concept for all applications. Similarly, radiation shielding and aerospace safety requirements probably will limit the thrust range of ACCENT systems.

None of the advanced concepts discussed in this paper are offered as universal solutions for auxiliary propulsion applications. Each has particular advantages and regimes of operation, and all are deserving of some further study to assess their final value to auxiliary electric propulsion.

#### REFERENCES

1. Isley, W. C. and Mickelsen, W. R.: Auxiliary Electric Propulsion for Current Spacecraft Applications. *Astronautics and Aeronautics*, (June, 1968).
2. Duck, K. L., et al: Evaluation of an Ion Propulsion System for a Synchronous Spacecraft Mission. AIAA Paper 67-720 (September, 1967).
3. Barrett, C. C.: Application of Electric Propulsion to Satellite Orbit Adjustment and Station Keeping. AIAA Paper 67-719 (September, 1967).
4. Shattuck, R. D., et al: Electric Propulsion for Satellite Position and Attitude Control. AIAA Paper 67-722 (September, 1967).
5. Isley, W. C.: Optimal Control Applications for Electro-thermal Multijet Systems on Synchronous Earth Spacecraft. AIAA Paper 67-723 (September, 1967).
6. Goddard Space Flight Center: ATS-4 GSFC Concept Design Study. GSFC Report No. X-730-67-10 (January, 1967).
7. Endres, D. L.: The Influence of Ground Track Constraints Upon Orbit Requirements for Sun Synchronous Satellites. GSFC Report X-734-67-598 (December, 1967).
8. Lazar, J., and Peko, P. E.: Potential Applications for Electric Propulsion. AIAA Paper 67-422 (July, 1967).
9. Mickelsen, W. R.: Auxiliary and Primary Electric Propulsion, Present and Future. *Jour. Spacecraft and Rockets*, vol. 4, 1409 (November, 1967).
10. Goddard Space Flight Center: Radioisotjet Program Summary Report. GSFC Report No. X-734-67-475 (September, 1967).

11. Greco, R. V. and Byke, R. M: Resistojet Biowaste Utilization-Evaluation and System Selection. AIAA Paper 68-121 (January, 1968).
12. Mickelsen, W. R.: Thermal Power Augmentation in Electric Propulsion Systems. Annual Report, NASA Grant NGR06-002-032 (January, 1967).
13. Garvey, D. C., and Mickelsen, W. R.: Electrothermal Thrusters in the ATEP System. Semi-Annual Report, NASA Grant NGR06-002-032 (July, 1967).
14. Leon, H. I., Saheli, F. P., and Mickelsen, W. R.: Study of Heat Addition to Supersonic Nozzles. Annual Report, NASA Grant NGR06-002-032 (January, 1968).
15. Murch, C. K., et al: Low-Thrust Nozzle Performance. AIAA Paper 68-91 (January, 1968).
16. Page, R. J., and Short, R. A.: Ten-Millipound Resistojet Performance. AIAA Paper 67-664 (September, 1967).
17. Sellen, J. M., Jr.: Spacecraft-Space Plasma Equilibria for Passive and Active Spacecraft. AIAA Paper 67-702 (September, 1967).
18. Beynon, J. C., et al: Present Status of Colloid Micro-thruster Technology. AIAA Paper 67-531 (September, 1967).
19. Free, B. A., and Mickelsen, W. R.: Plasma Separator Thruster. Jour. Spacecraft and Rockets, vol. 4, 1282 (October, 1967).
20. Nakanishi, S., Richley, E. A., and Banks, B. A.: High Perveance Accelerator Grids for Low Voltage Kaufman Thrusters. AIAA Paper 67-680 (September, 1967).
21. Richley, E. A., and Kerslake, W. R.: Bombardment Thruster Investigations at the Lewis Research Center. Paper to be presented at AIAA 4th Propulsion Joint Specialist Conference (June, 1968).
22. Preliminary Design Study for the ACCENT System. Final Report, Contract NAS5-10366 (December, 1967).
23. Mickelsen, W. R.: Basic Design Considerations for Radioisotope Electrogenators. Paper to be presented at the 3rd Intersociety Energy Conversion Engineering Conference, Boulder, Colorado (August, 1968).
24. Dailey, C. L.: Investigation of Plasma Rotation in a Pulsed Inductive Accelerator. AIAA Paper 68-86 (January, 1968).



TABLE I - Summary of prime-onboard operational systems (OS), and flight-experiment systems (FE).

	'65	'66	'67	'68	'69
<u>VELA-III</u>					
TRW RESISTOJET: NITROGEN, SINGLE-JET, THERMAL-STORAGE	OS				
<u>VASP</u>					
TRW RESISTOJET: NITROGEN, MULTI-JET, THERMAL-STORAGE				OS	
<u>NRL</u>					
GE RESISTOJET: AMMONIA, SINGLE-JET, THERMAL-STORAGE				OS	
<u>ATS B, ATS C</u>					
AVCO RESISTOJET: AMMONIA SINGLE-JET, PULSED-MODE				FE	
<u>AF MULTI-PURPOSE</u>					
GE RESISTOJET: AMMONIA, MULTI-JET, THERMAL-STORAGE					FE
EOS ELECTROSTATIC THRUSTER: CESIUM, ELECTRON-BOMBARDMENT					FE
TRW ELECTROSTATIC THRUSTER: GLYCEROL, LIQUID-SPRAY					FE
<u>ATS D, ATS E</u>					
AVCO RESISTOJET: AMMONIA, SINGLE-JET, PULSED-MODE					OS
EOS ELECTROSTATIC THRUSTER: CESIUM, CONTACT-ION, TWO-AXIS THRUST VECTORING					FE
<u>LES</u>					
REPUBLIC AVIATION PLASMA THRUSTER: SOLID PROPELLANT, PULSED-MODE					FE

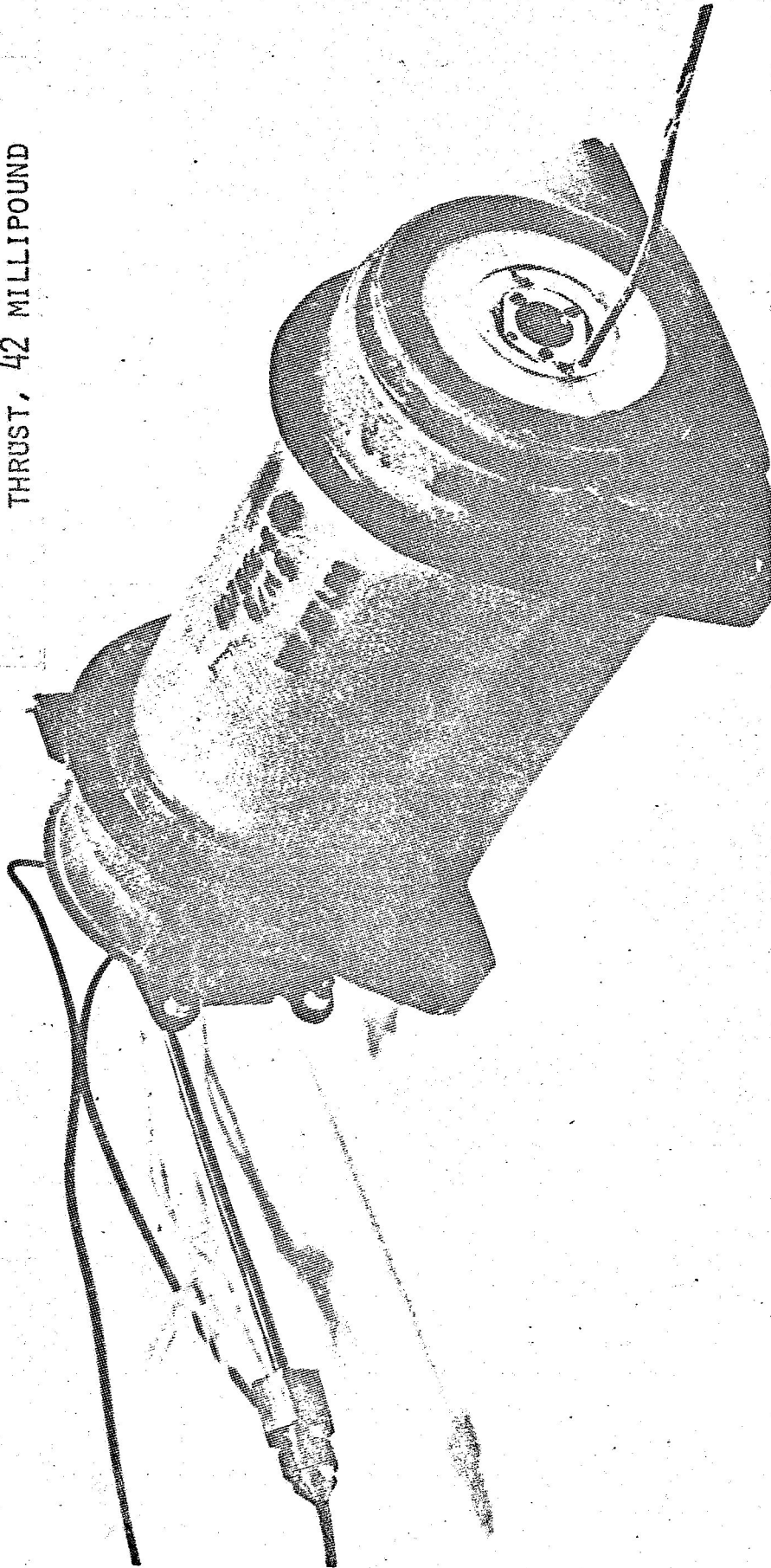
VELA III RESISTOJET

NITROGEN PROPELLANT

SPECIFIC IMPULSE, 123 SEC

POWER, 42 WATTS

THRUST, 42 MILLIPOUND



TRW SPACE TECHNOLOGY LABORATORIES

FIG. 1 - TRW RESISTOJET FOR VELA III SPACECRAFT, SINGLE NOZZLE.

MULTI-NOZZLE RESISTOJET  
FOR ADVANCED VELA  
NITROGEN PROPELLANT  
SPECIFIC IMPULSE 132 SEC.  
POWER, 17 WATTS  
THRUST, 20 MILLIPOUNDS

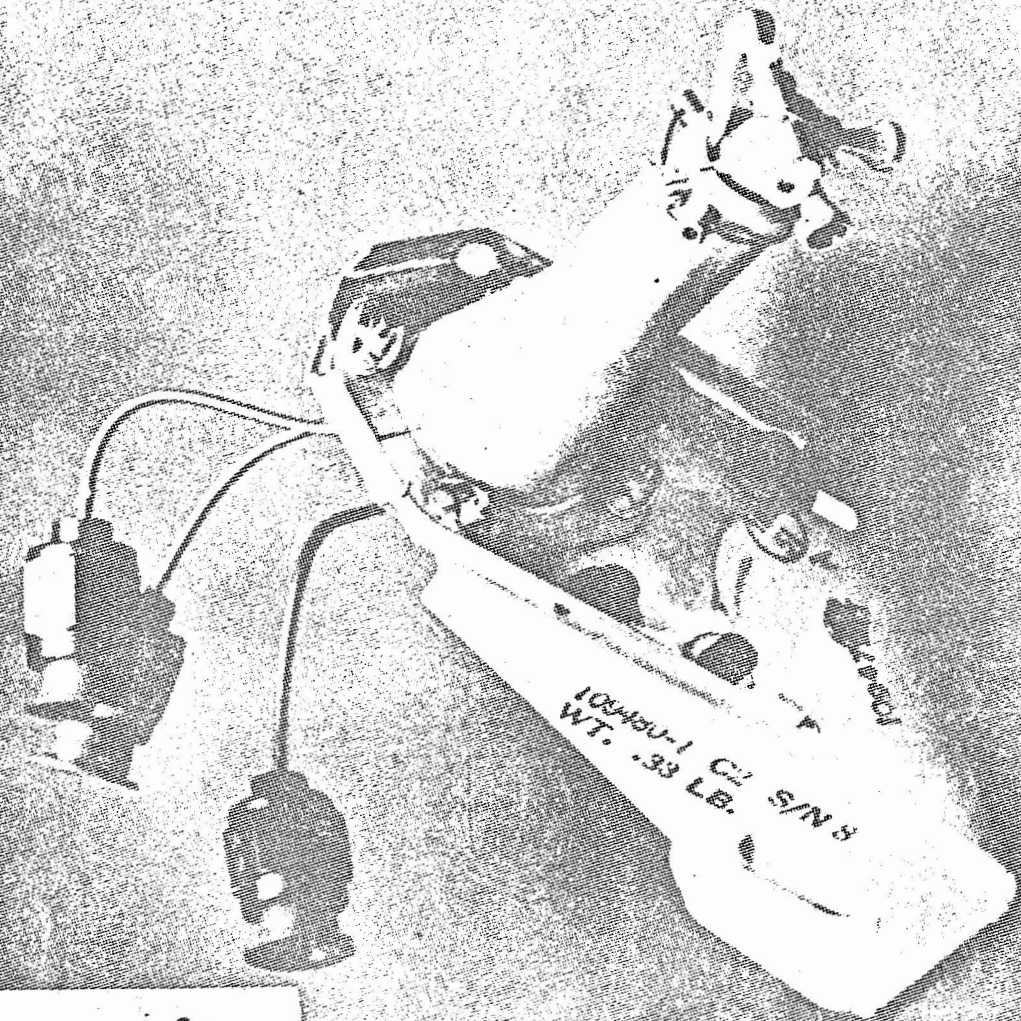
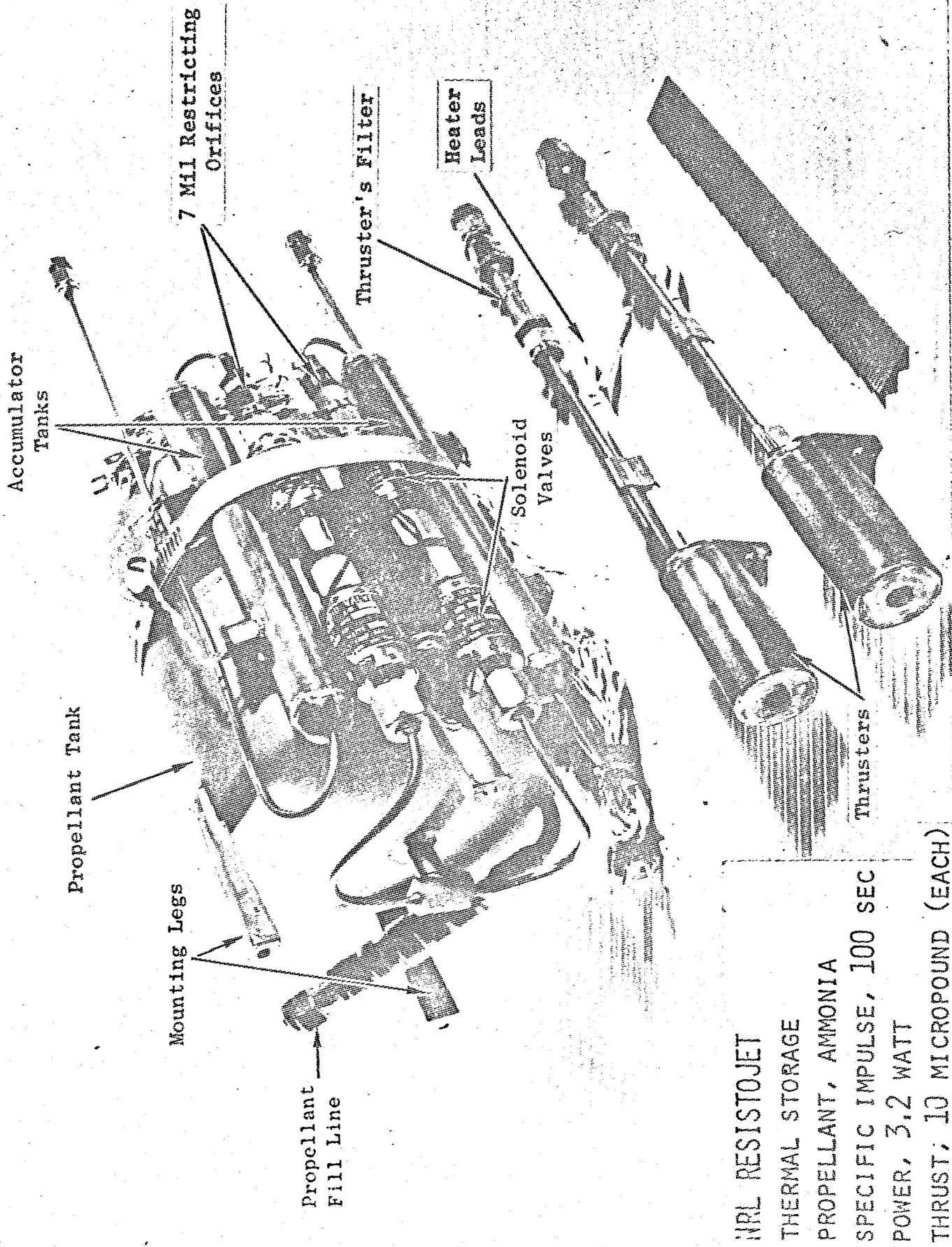


FIG. 2 - TRW RESISTOJET FOR VASP. MULTI-NOZZLE.



NRL RESISTOJET  
 THERMAL STORAGE  
 PROPELLANT, AMMONIA  
 SPECIFIC IMPULSE, 100 SEC  
 POWER, 3.2 WATT  
 THRUST; 10 MICROPOUND (EACH)

FIG. 3 - GE RESISTOJET FOR NRL SPACECRAFT.

ATS-C DUAL RESISTOJET

PROPELLANT, AMMONIA

SPECIFIC IMPULSE, 110 AND 140 SEC.

POWER, 9 AND 10 WATTS

THRUST, 10 AND 100 MICROPOUNDS

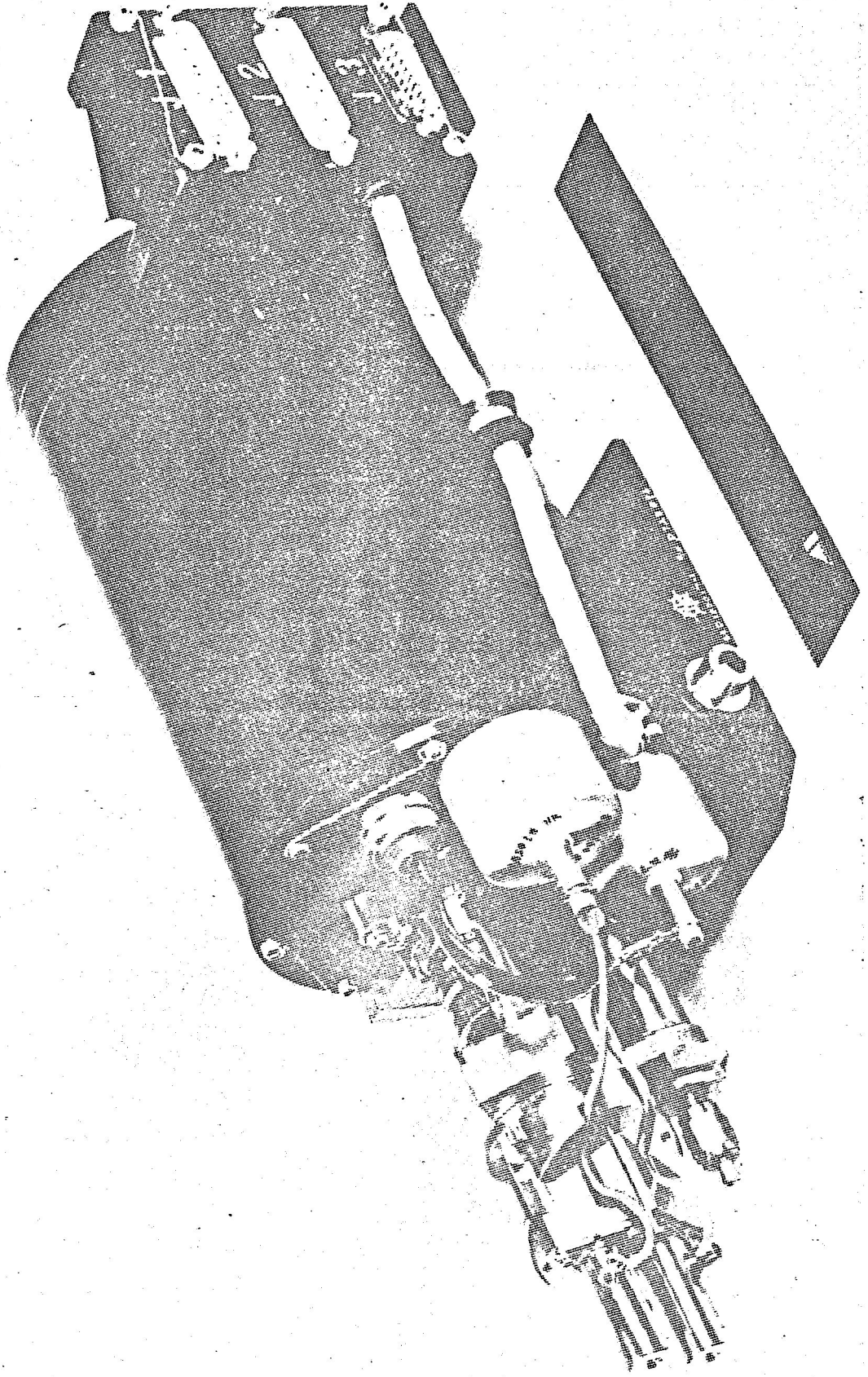


FIG. 4 - AVCO RESISTOJET FOR NASA ATS C SPACECRAFT.

3-NOZZLE THERMAL-STORAGE RESISTOJET  
FOR AIR FORCE MULTI-PURPOSE SATELLITE  
PROPELLANT, AMMONIA  
CATALYST BED IN FLOW PASSAGE

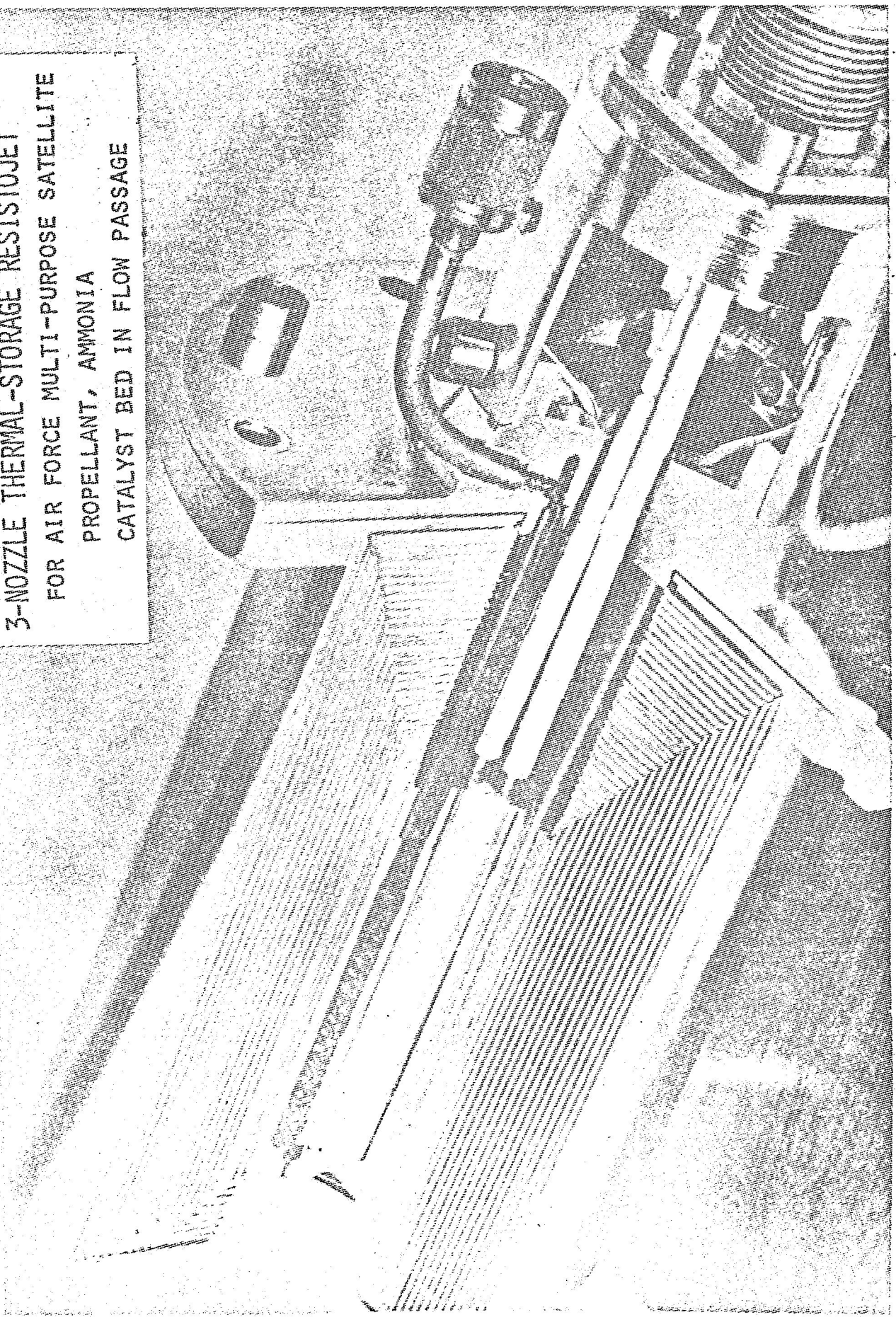


FIG. 5 - GE RESISTOJET FOR AIR FORCE MULTI-PURPOSE SATELLITE PROGRAM, MULTI-NOZZLE.

ELECTRON-BOMBARDMENT THRUSTER  
FOR AIR FORCE MULTI-PURPOSE SATELLITE  
PROPELLANT, CESIUM  
SPECIFIC IMPULSE, 3000-5000 SEC.  
THRUST, 50 MICROPOUND TO 10 MILLIPOUND

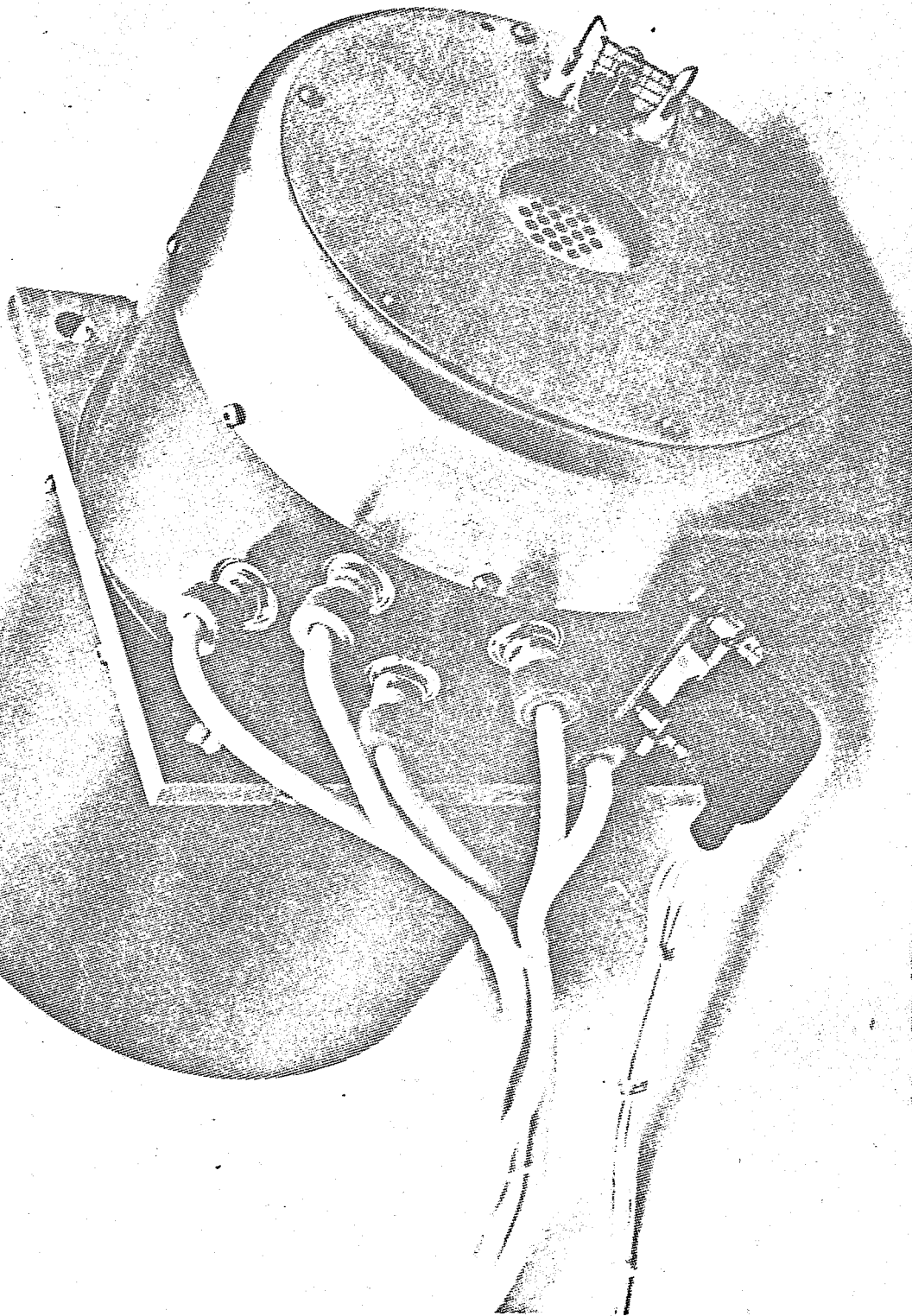


FIG. 6 - EOS CESIUM BOMBARDMENT THRUSTER FOR  
AIR FORCE MULTI-PURPOSE SATELLITE PROGRAM.

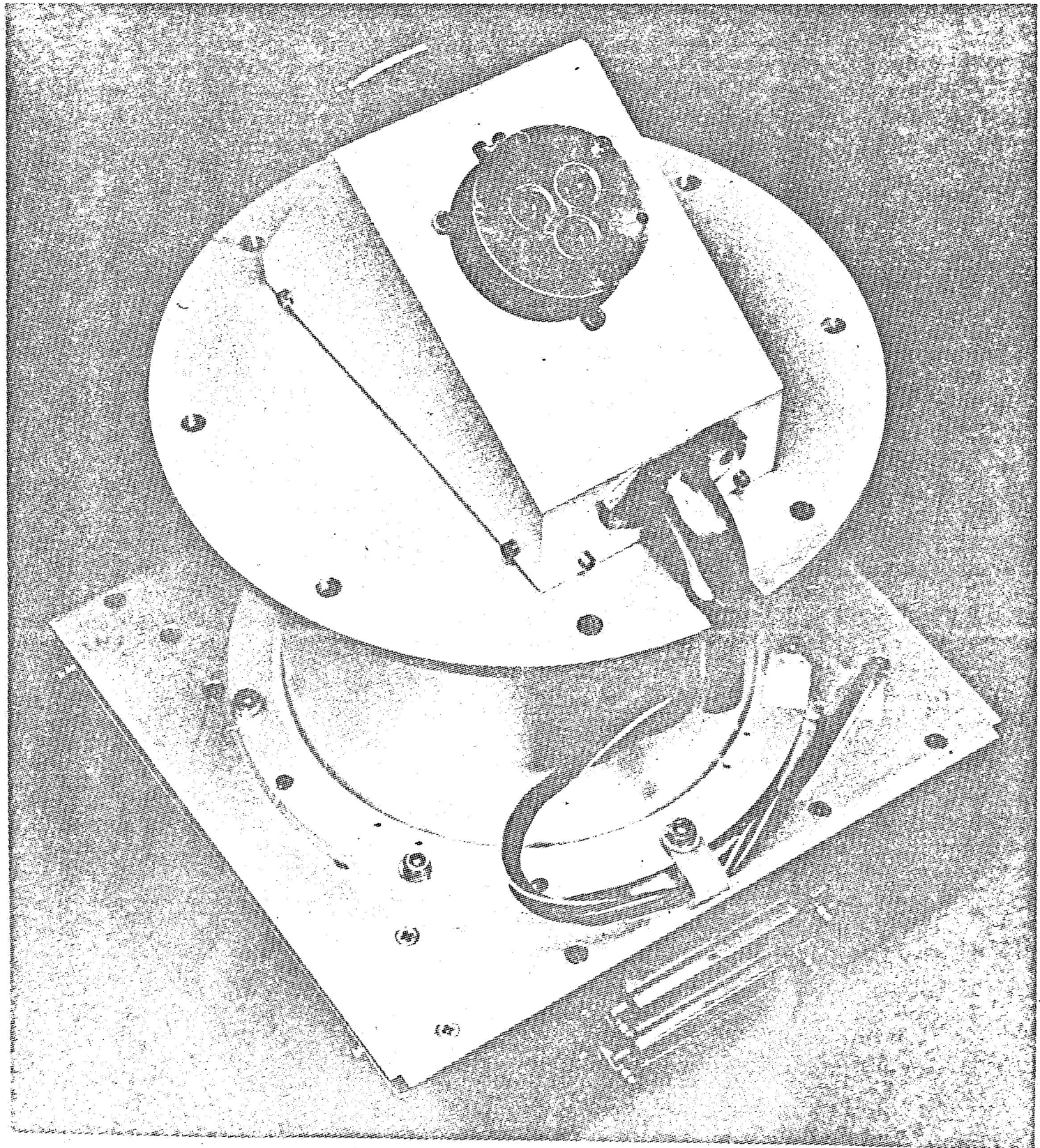
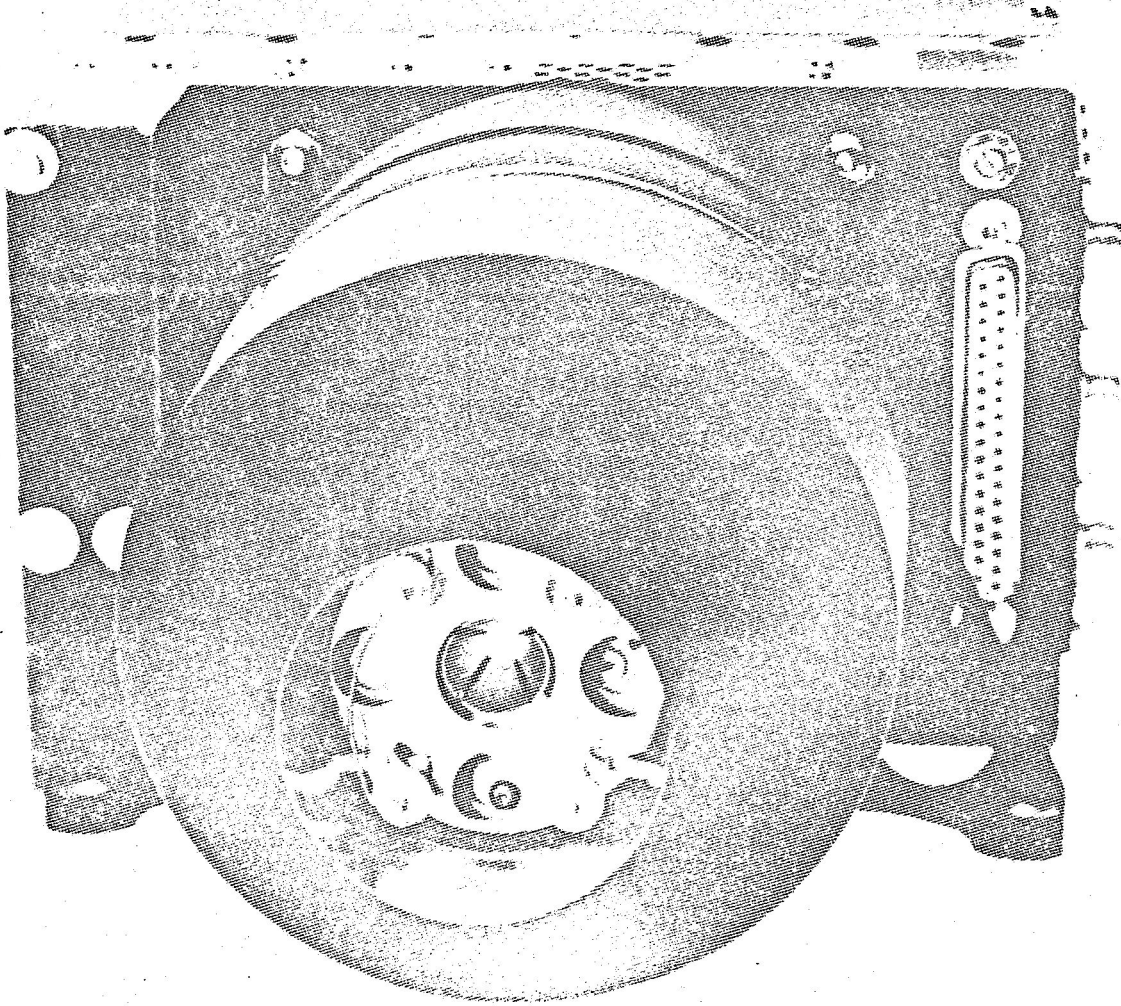


FIG. 7 - TRW SYSTEMS LIQUID-SPRAY CHARGED-PARTICLE THRUSTER FOR AIR FORCE MULTI-PURPOSE SATELLITE PROGRAM. PROPELLANT GLYCEROL; SPECIFIC IMPULSE, 600-1000 SEC.; POWER, 5.2 WATTS; THRUST, 20 MICROPOUNDS.





CONTACT-ION THRUSTER  
FOR ATS-D  
PRECISION THRUST VECTORING  
PROPELLANT, CESIUM  
SPECIFIC IMPULSE, 6700 SEC.  
POWER, 35 WATT  
THRUST, 20 MICROPOUND

FIG. 8 - EOS CESIUM CONTACT ION THRUSTER FOR NASA ATS D SPACECRAFT.

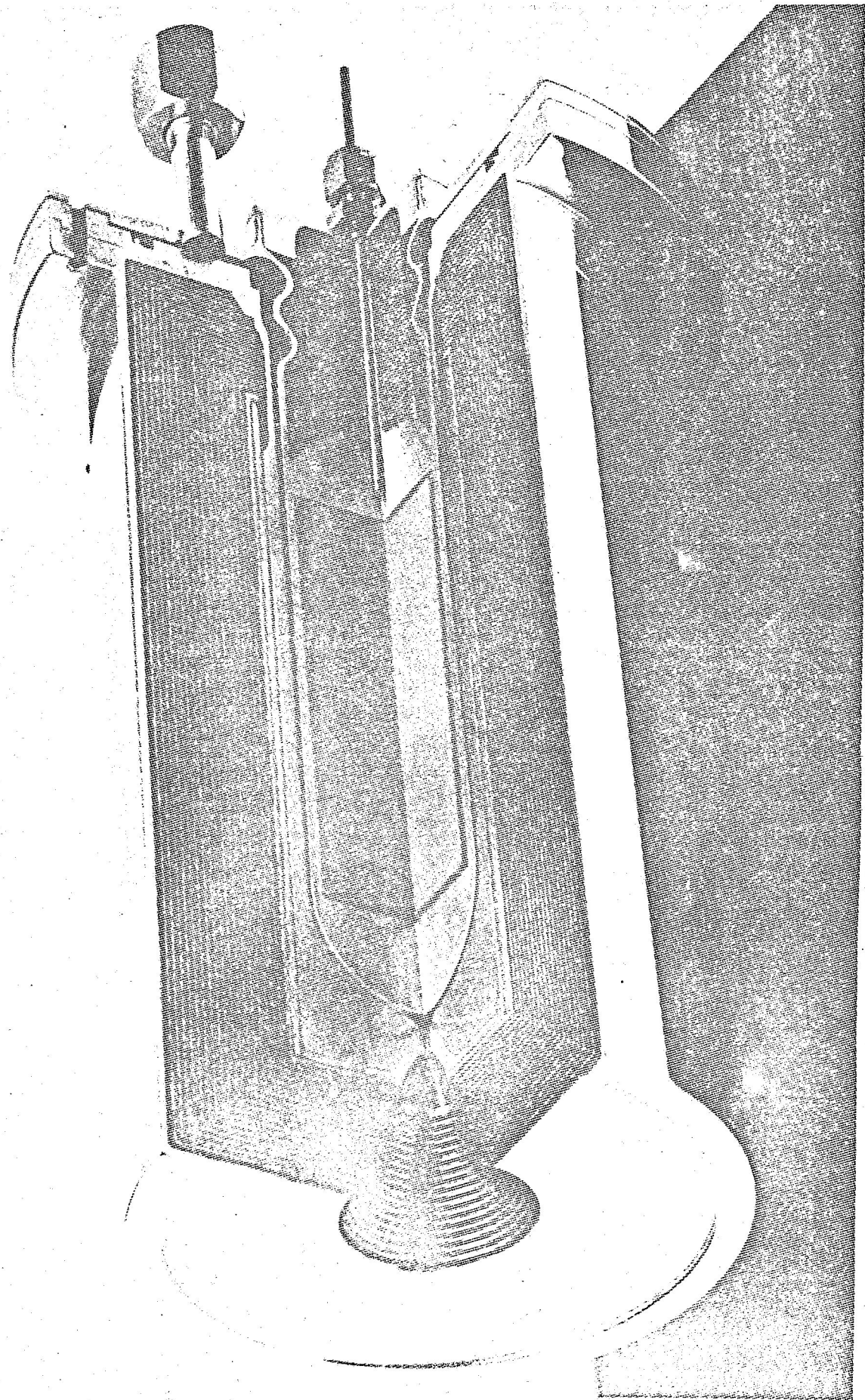
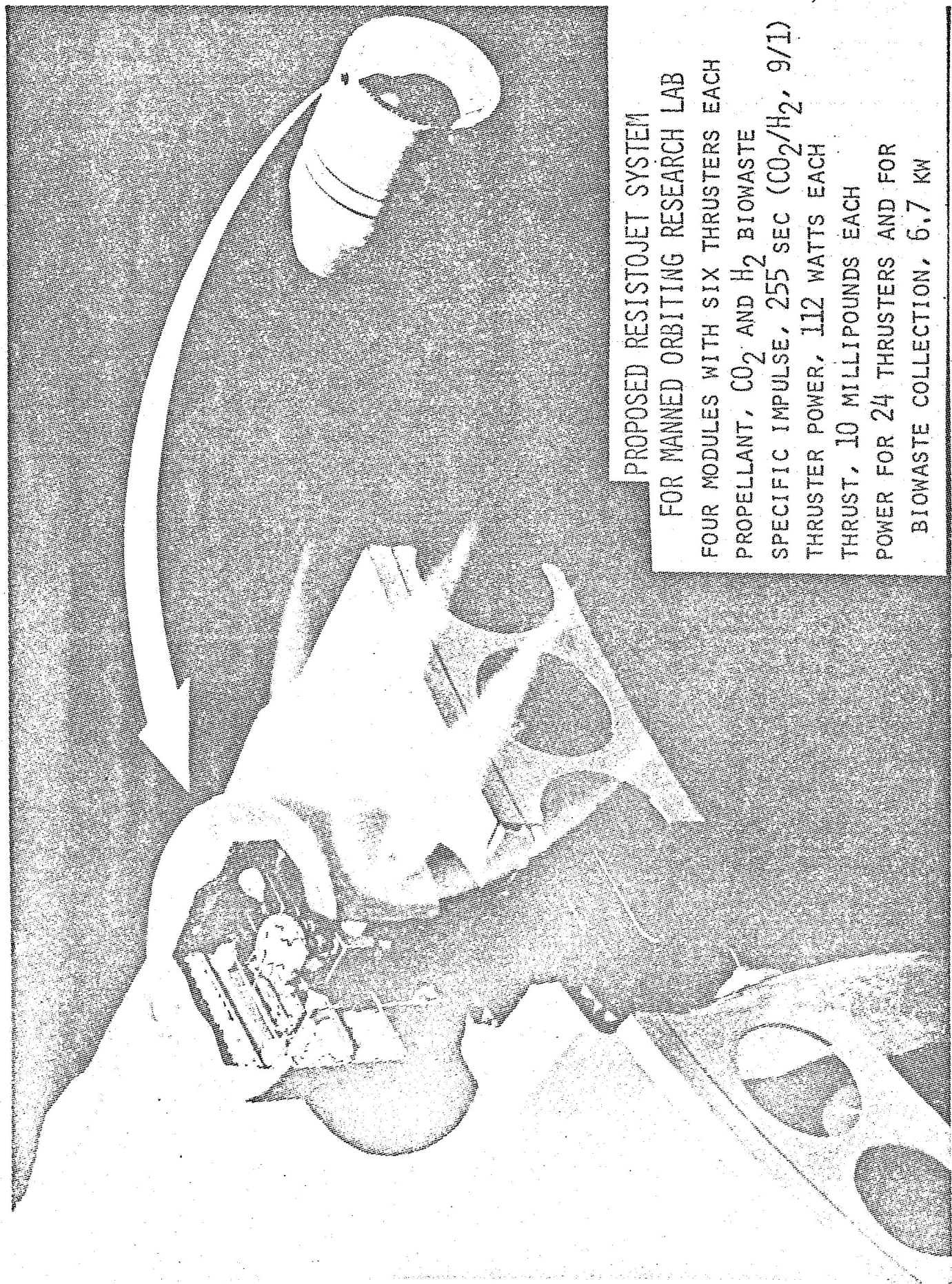


FIG. 9 - GE RADIOISOJET DEVELOPED FOR NASA GODDARD.  
RADIOISOTOPE, 60-WATTS PROMETHIUM-147; PROPELLANT,  
AMMONIA; THRUST, 25 MILLIPOUNDS; SPECIFIC IMPULSE,  
230 SECONDS.



PROPOSED RESISTOJET SYSTEM  
FOR MANNED ORBITING RESEARCH LAB

FOUR MODULES WITH SIX THRUSTERS EACH  
PROPELLANT, CO<sub>2</sub> AND H<sub>2</sub> BIOWASTE  
SPECIFIC IMPULSE, 255 SEC (CO<sub>2</sub>/H<sub>2</sub>, 9/1)  
THRUSTER POWER, 112 WATTS EACH  
THRUST, 10 MILLIPOUNDS EACH  
POWER FOR 24 THRUSTERS AND FOR  
BIOWASTE COLLECTION, 6.7 KW

FIG. 10 - PROPOSED RESISTOJET SYSTEM FOR MORL.

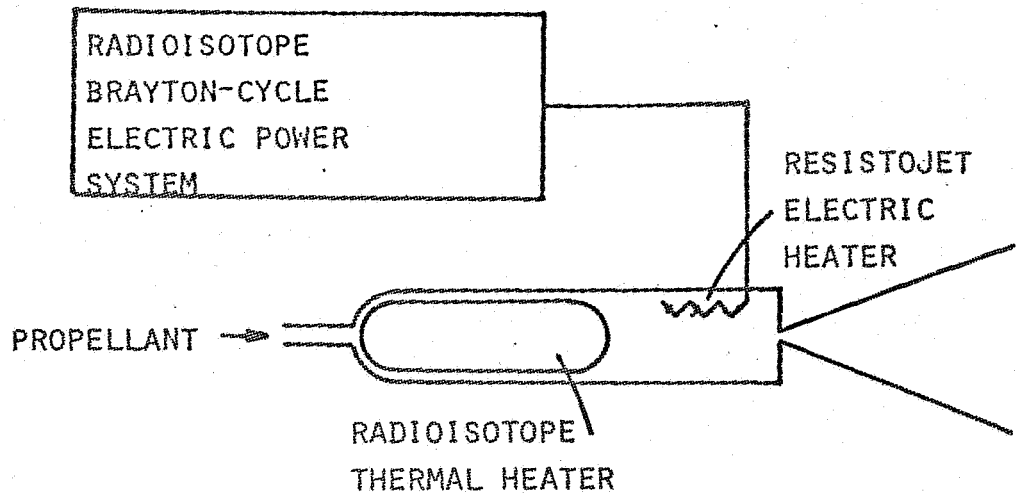


FIG. 11 - Hypothetical application of ATEP concept to MORL resistojet system.

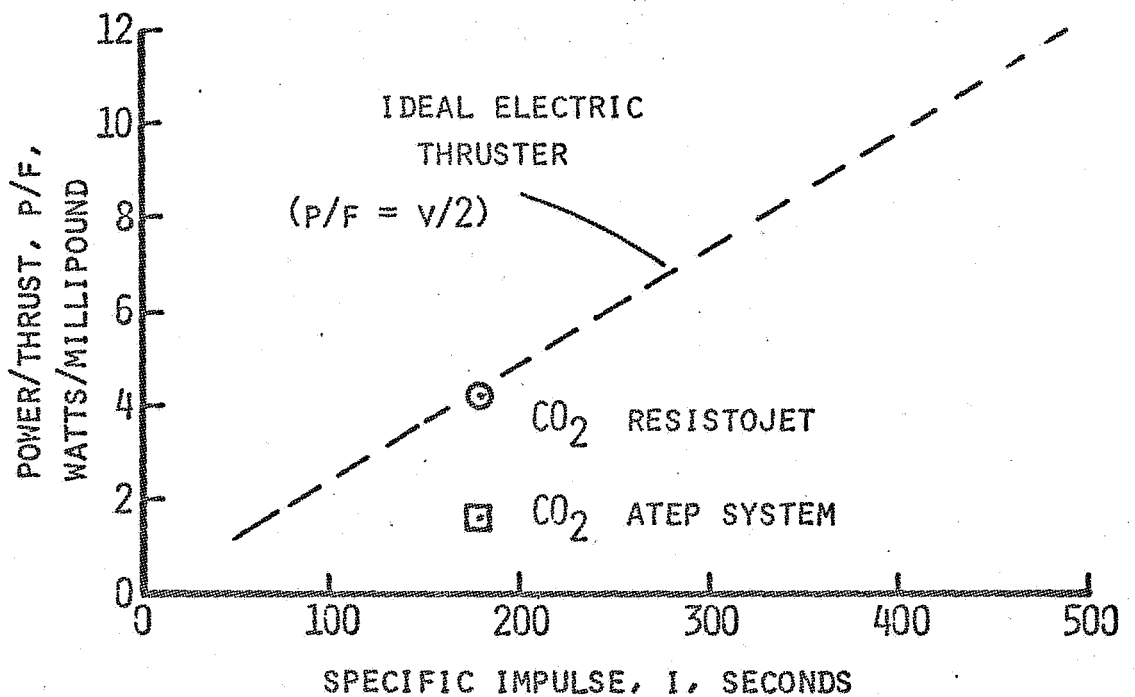


FIG. 12 - CO<sub>2</sub> resistojet performance with ATEP system. Radioisotope thermal-heating to 1200°K (2.46 thermal-watt/millipound) and electric heating to 3000°R (1670°K)

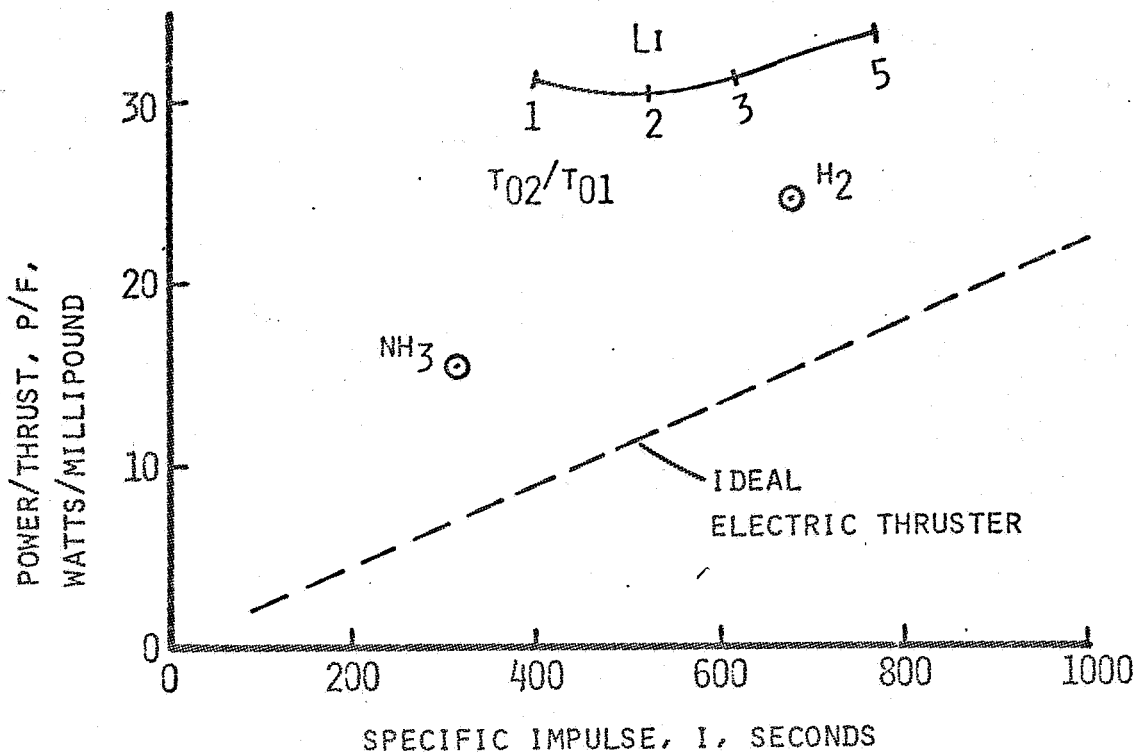


FIG. 13 - Theoretical performance of lithium resistojet with supersonic heat addition. Plenum temperature,  $T_{01} = 2500^{\circ}\text{K}$ ;  $A_2/A^* = 100$ . Ammonia and hydrogen data points for  $T_{01} = 2400^{\circ}\text{K}$ ,  $p_1 = 3$  atmospheres.

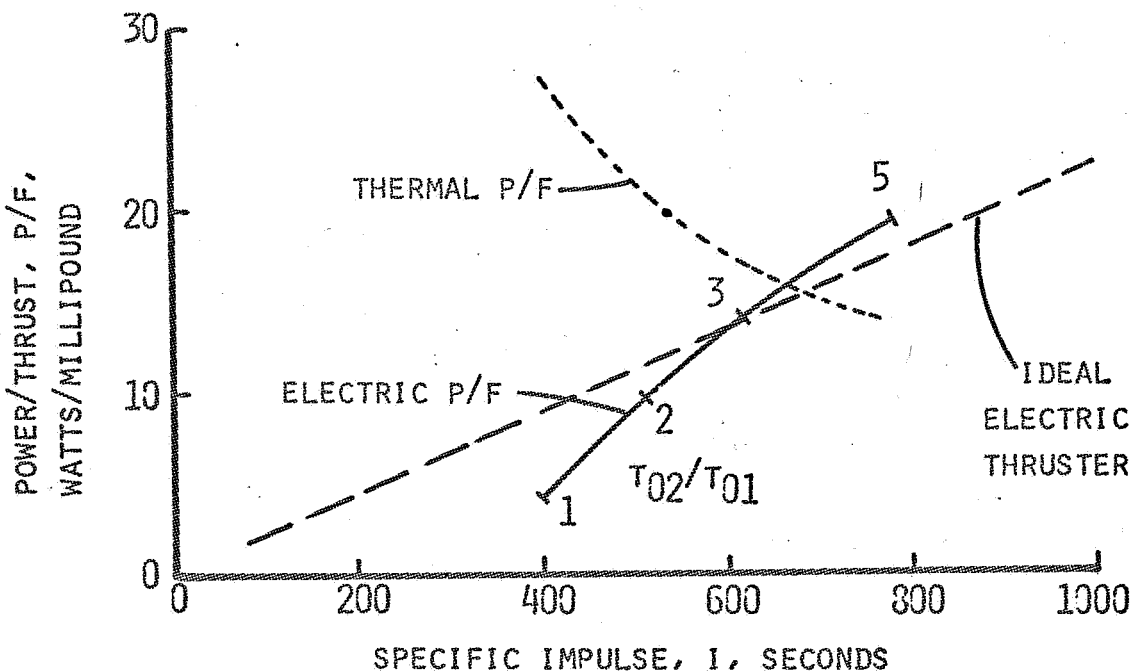


FIG. 14 - Theoretical performance of ATEP resistojet system with lithium propellant. Radioisotope heating to  $1200^{\circ}\text{K}$ , electric heating to  $2500^{\circ}\text{K}$  plenum temperature, electric heating of supersonic stream.

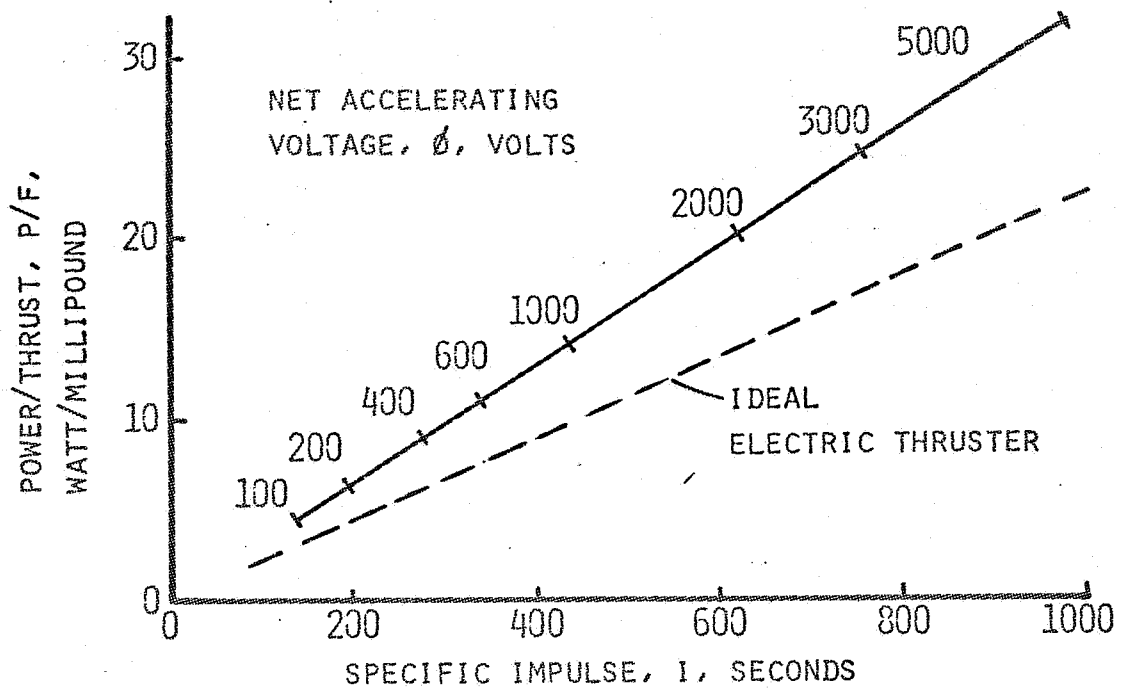


FIG. 15 - Performance of liquid-spray thruster for various net accelerating voltages. Charge/mass, 10,000 coulomb/kg; neutralizer and feed-system power neglected (e.g., bi-polar design).

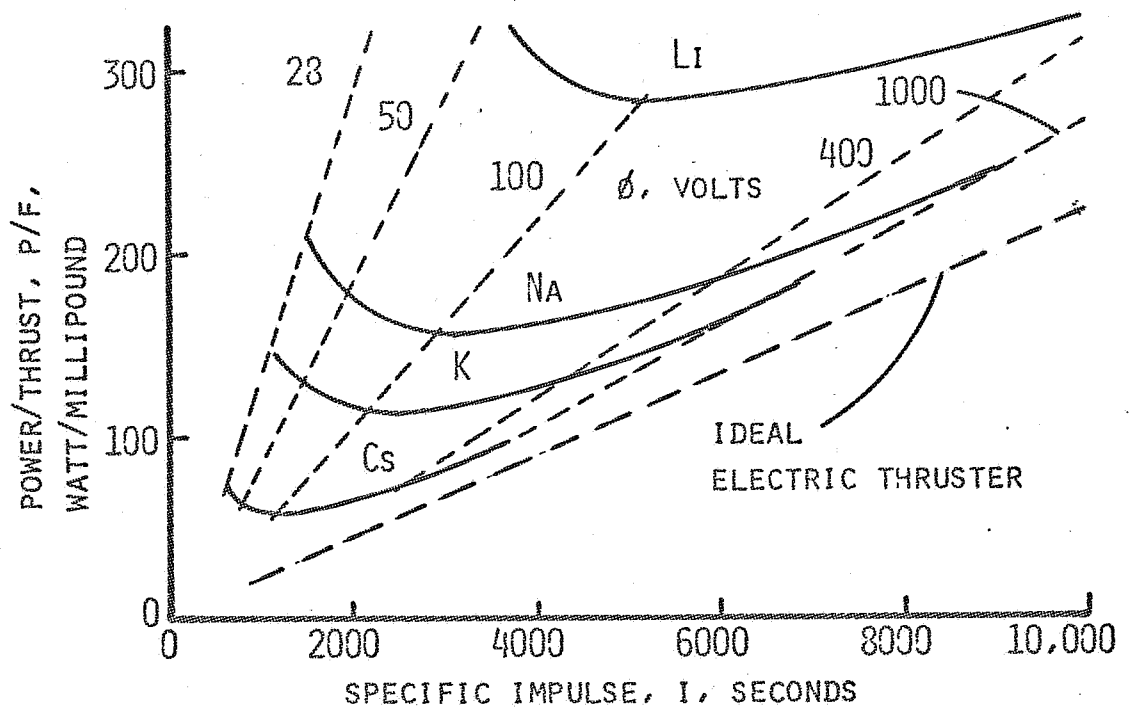


FIG. 16 - Performance of hypothetical ion thruster with various alkali propellants. Hollow cathode, composite grid, total throughput ion optics, 25 ev/ion neutralizer and feed power.

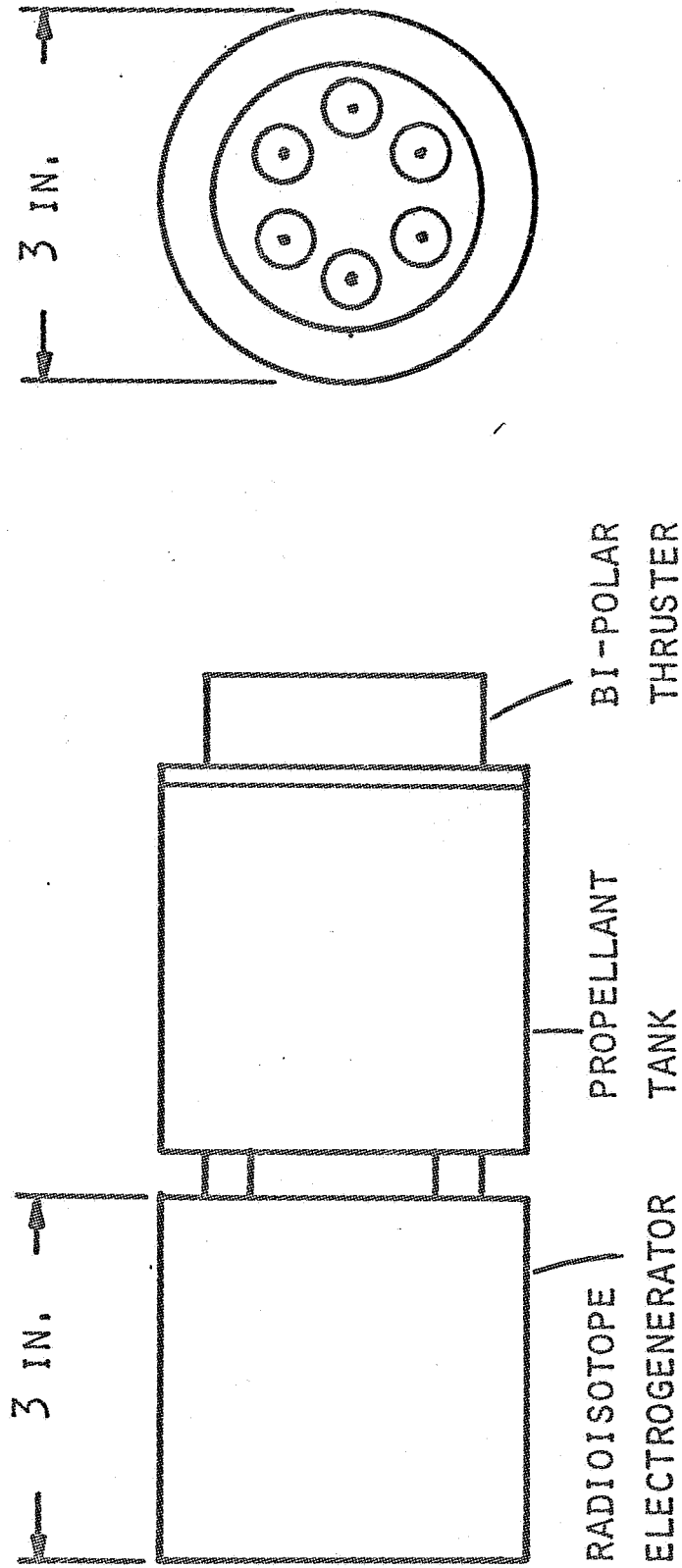


FIG. 17 - Hypothetical ACCENT system with liquid-spray bi-polar thruster. Thrust, 20-micropounds; specific impulse, 3000 sec.; total system weight, approx. 6 lb.; mission duration, 2-years; containment vessel, 1/8-inch tantalum; radioisotope, 27,600 curies of promethium-147.

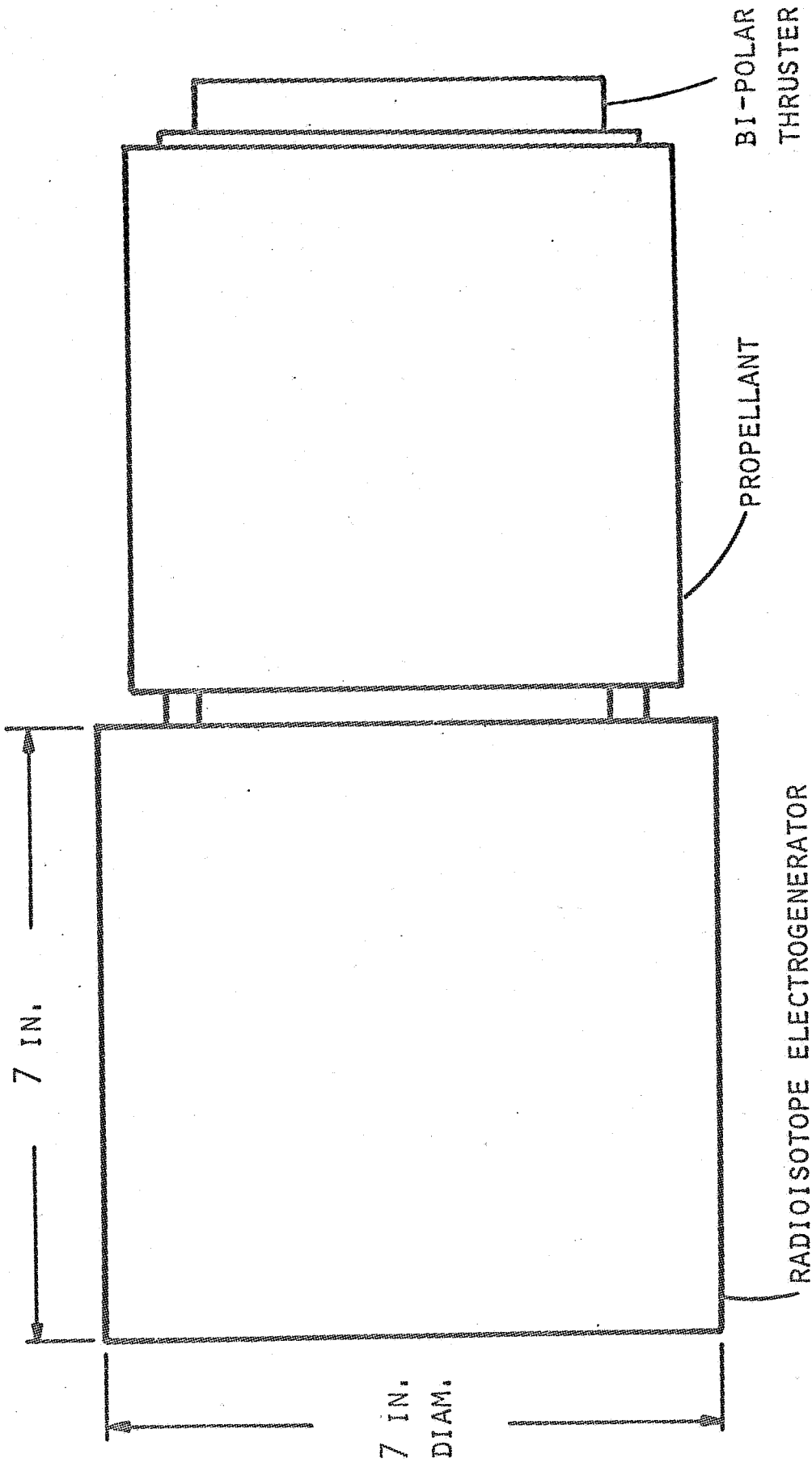


FIG. 18 - Hypothetical ACCENT system with liquid-spray bi-polar thruster. Thrust, 350-micropounds; specific impulse, 3000 sec.; total system weight, approx. 32 lb.; mission duration, 2-years; containment vessel, 1/8-inch tantalum; radioisotope, 483,000 curies of promethium-147.



Invited paper to be presented at the 3rd Intersociety Energy Conversion Engineering Conference, Plenary Session. Boulder, Colorado. August 16, 1968.

POWER NEEDS FOR ELECTRIC PROPULSION\*

by William R. Mickelsen\*\*  
Colorado State University  
Fort Collins, Colorado

ABSTRACT

The present status and future trends of electric propulsion systems and missions are briefly reviewed. Some typical electric propulsion systems are described, these cover a thrust range from 20 micropounds to 65 millipounds, and are intended for space missions ranging from satellite attitude control to primary propulsion for interplanetary unmanned vehicles. Electric power needs for electric propulsion systems are summarized in terms of three general mission classes; auxiliary, intermediate and primary propulsion.

In the auxiliary-propulsion class of satellite missions, it appears that electric propulsion power needs for 2000-pound satellites will range from 2 watts to 200 watts, depending on the thrusting function and on future research and development of advanced concepts.

Intermediate-propulsion missions include the MORL and the raising of satellites to 24-hour synchronous orbits. Power for electric propulsion systems in this class of possible future missions will range from 100 watts to several kilowatts.

Possible future primary-propulsion missions include both unmanned and manned interplanetary spacecraft. Small unmanned spacecraft may require power for electric propulsion in the range from 100 watts to several kilowatts. Still farther in

---

\* Done under NASA Grant NGR06-002-032, Electric Thruster Systems, OART.

\*\* Associate Fellow, AIAA. Senior Member, IEEE. Professor of Mechanical Engineering and of Electrical Engineering.

the future, manned interplanetary vehicles will probably require electric powerplants of several megawatts output power for the primary electric propulsion system.

Power needs are listed for those thruster systems that appear suited to each particular mission. It is intended that this survey paper will serve as a progress report to those in the field of electric power generation, and hopefully can serve as an approximate guide in the synthesis of future electric propulsion systems.

## INTRODUCTION

In the past ten years research and development has brought electric propulsion systems to a flight operational status on some earth satellite spacecraft. Further, complete thruster systems are presently being developed to demonstrate the performance advantages of electric propulsion for interplanetary space flight. The present status and future trends in electric propulsion for this wide range of mission types are discussed in detail in recent articles (refs. 1-6). With electric thruster systems having reached a stage of realistic design, it is of interest to survey the electric power needs of the various thruster systems that may be candidates for possible future space missions.

It is the intent of the present paper to provide those working in the field of electric power generation with a comprehensive survey of the electric power needs of presently existing thruster systems, of thruster systems presently in the research and development phase, and of possible future thruster systems that fall in the realm of advanced concepts. Power needs for existing flight operational systems can be defined quite accurately, while the power needs for advanced concepts can be only approximately assessed at the present time. Because of the brief survey nature of this paper, power assessments are limited to gross power levels, and to listings of the highest voltages needed for each particular thruster system. Details of the numerous auxiliary voltages and currents for each thruster system are available from the referenced literature.

It must be noted that many of the mission applications for electric propulsion that are listed in this paper are merely possibilities for the future and should not be construed as real flight programs at this time. Furthermore, the performance characteristics of thruster systems in the research and development phase are only approximate at best and therefore should be used only as approximate guides in preliminary design studies of future vehicles. Performance parameters for the advanced concepts in electric thruster systems are even more tenuous and are included here only to indicate probable future trends in electric power needs.

#### GENERAL STATUS OF ELECTRIC THRUSTER SYSTEMS

Before proceeding to the assessment of power needs for electric propulsion, it is necessary to clearly define the present status and future trends of electric thruster systems. In defining this status, three general classifications are used: operational, research and development, and advanced concepts. Some thruster systems described here are in transition between these status classifications, and in such cases the judgement for classification hopefully represents the consensus of opinion of those working in the field of electric propulsion.

#### Operational Thruster Systems

Operational systems are those electric thruster systems that have been flown or will be flown on scheduled spacecraft missions. Some of these operational systems are prime onboard equipment to perform thrusting functions that are required for the success of the mission. Other operational systems have, or will, perform thrusting functions more in the nature of flight demonstration equipment (refs. 1 and 2).

Three examples of operational electric propulsion systems are shown in Figures 1 to 3. The resistojet thruster system shown in Figure 1 is representative of an early application of electric propulsion to operational spacecraft. This

resistojet system is used for attitude control and orbit adjustment of the advanced VELA spacecraft.

The contact ion microthruster system shown in Figure 2 is presently being readied for flight on the NASA ATS-D spacecraft as a flight experiment to demonstrate attitude control and east-west station keeping functions. A notable feature of this electric propulsion system is the capability for precision thrust vectoring by means of electrostatic deflection of the ion exhaust beam with the segmented accelerating electrodes shown in the figure. Also notable in the figure is the packaging for the complete power conditioning and control system which draws power from the spacecraft solar-array bus, and provides high voltage d.c. to the thruster system.

The cesium bombardment thruster system shown in Figure 3 is representative of systems intended for north-south station keeping functions on synchronous satellites.

#### Systems in Research and Development

There are a number of electric thruster systems in various stages of research and development. Each of these systems are expected to have improved performance or operational advantages over the present operation systems. The systems that are classified here in the R & D category have a complete compliment of all components that would be required in a flight version of the system. In addition, all have been operated in laboratory vacuum facilities under test conditions and durations adequate to establish their operational feasibility.

A resistojets systems has been proposed as a possible propulsion system for manned orbiting research laboratories to provide thrust for drag cancellation and for attitude control. This proposal is illustrated in Figure 4, and would consist of a total of twenty-four resistojets located in four modules around the periphery of the MORL. A significant feature of this proposed system is the utilization of carbon dioxide biowaste as propellant for the resistojets. Resistojets systems have been operated with carbon dioxide at specific impulse values high enough to provide the required daily total

impulse without exceeding the daily production rate of carbon dioxide biowaste

Another example of an electric thruster system in the research and development stage is shown in Figure 5. This four-thruster array of mercury bombardment thrusters is typical of the system size and complexity that would be required for primary propulsion of interplanetary unmanned spacecraft. This thruster array is presently under development at JPL for purposes of demonstrating the feasibility of solar electric propulsion systems (refs. 3 and 4).

#### Advanced Thruster Concepts

A number of advanced concepts have been proposed that have marked potential improvements in performance or operational characteristics. Some of these advanced concepts are discussed in the recent literature (refs. 2 and 6). All of these advanced concepts are based on demonstrated performance of individual components, but none have been operated as complete thruster systems. These advanced concepts are included in the present survey for the purposes of indicating approximate future trends.

#### POSSIBLE MISSIONS FOR ELECTRIC PROPULSION

Missions for electric propulsion can be roughly divided into three categories: auxiliary, intermediate, and primary propulsion missions. Auxiliary propulsion is generally defined to include thrusting functions of a relatively low magnitude in which the spacecraft velocity is not appreciably affected. The control of satellite attitude is certainly an auxiliary propulsion function, and the station keeping of synchronous satellites may also be included in this category. Intermediate electric propulsion can be defined to include thrusting functions such as drag cancellation for low-level satellites, and significant orbit transfers such as raising a satellite from a low parking orbit to the twenty-four-hour synchronous orbit. Primary electric propulsion missions are those where the electric propulsion system is an upper stage in the overall mission profile.

Propulsion requirements for auxiliary propulsion missions can be defined in terms of an effective vehicle velocity increment,  $\Delta V$  per year, and for a given spacecraft mass a total impulse per year can be determined (refs. 6 and 7). Propellant weight  $W_{pr}$  is simply the ratio of total impulse to specific impulse,  $I$ :

$$W_{pr} = (\text{total-impulse/yr})/I \quad , \quad \text{lb/yr} \quad (1)$$

where  $W_{pr}$  is the propellant consumption per year, total-impulse/yr is the mission requirement, and specific impulse  $I$  is an electric thruster performance parameter. From inspection of equation (1) it is evident that very long missions will require high specific impulse in order to avoid excessive propellant weights.

In general, higher specific impulse in electric thrusters is attained by increasing the electric power input to the thruster. This is illustrated by the following expression:

$$P = 1/2 g_c FI/\eta_{th} \quad (2)$$

where  $P$  is power input to the electric thruster system in watts,  $g_c$  is the gravitational conversion factor 9.81 meters/sec<sup>2</sup>,  $F$  is the thruster system thrust in newtons,  $I$  is specific impulse, and  $\eta_{th}$  is thruster system efficiency. By considering equations (1) and (2) simultaneously it is evident that there will be an optimum value of the specific impulse for each particular set of mission parameters and propulsion system parameters.

Mission and trajectory analysis for electric propulsion spacecraft is not a simple matter as the preceding discussion may imply. However the general features of the influence of specific impulse on propellant weight and powerplant weight are as expressed by equations (1) and (2). This trade-off between propellant weight and propulsion system weight should be kept in mind in considering the text of the next section.

## POWER NEEDS FOR TYPICAL MISSIONS

Power needs for a number of typical electric propulsion missions are shown in Tables I to III. Each of these missions could be flown with any one of several thruster systems. In general, the power needs of the various thruster systems are widely different, depending on the specific impulse, the thruster efficiency, and other factors. For this reason there are quite a few thruster systems listed for each of the missions in Tables I to III.

The missions considered in this paper are merely intended to be representative, particularly with respect to the spacecraft weights that have been assumed. For example, in Table I, it has been assumed that the final satellite in 24-hour synchronous orbit will have a mass corresponding to a ground weight of 2000 lbs. Synchronous satellites of much greater mass are certainly within the realm of possibility, even with existing booster rocket capabilities. The 20-micropound and 490-micropound thrust levels have been determined for 2000-lb satellites with continuous thrusting modes of operation (ref. 7). The 700-micropound thrust level for north-south station keeping has been suggested (ref. 8) as a system redundancy feature where one of a pair of opposing thrusters could do the north-south station keeping in case the other thruster failed. Thrust levels would be higher for more massive satellites.

In Table II, the MORL mission is based on a recent study (ref. 9). Important mission parameters in this study are a 36,000-pound vehicle in a 164 nautical mile circular orbit, requiring a total impulse of 1900 lb-sec/day. Any changes in these mission parameters could be reflected in changes of power levels. The satellite orbit maneuvers mission shown in Table II is based on an estimate of thrust levels that might be required for substantial changes in satellite orbit or position (ref. 8). With one exception, the power levels shown in Table II for the synchronous satellite raising mission were determined from basic trajectory information (ref. 10). These calculations are based on a 300 nautical mile parking orbit, with raising by electric propulsion to the 24-hour

synchronous circular orbit, with the constraint that the electric propulsion system including the solar cell array (or other powerplant) is included in the final 2000-pound spacecraft. It was also assumed that the electric propulsion is done only 1/2 time in each orbit about earth (because of Earth-shadowing of the solar arrays), and no allowance is made for the plane change from the 300 nautical mile parking orbit to the final equatorial synchronous orbit. Trajectory and mission parameters for the 180-day synchronous satellite mission with the mercury bombardment thruster system are reported elsewhere (ref. 11).

Mission parameters for the 600-pound unmanned spacecraft interplanetary mission shown in Table III represent a minimal approach to unmanned spacecraft (ref. 12). The 2300-pound unmanned spacecraft mission shown in Table III is representative of scientific probe missions to the major planets (refs. 3, 4, 13, 14). The 600,000-pound manned interplanetary round-trip mission listed in Table III is representative of possible future applications of electric propulsion (ref. 15).

Electric power needs for the various thruster systems and missions listed in Table I to III were calculated from the information and references summarized in the Appendix. The detailed information in the Appendix is provided primarily for the benefit of those having particular interest in electric thrusters per se, and secondarily as supporting documentation for the power levels shown in Tables I to III.

Operational thruster systems for auxiliary propulsion missions have relatively high electric power needs, particularly at the higher values of specific impulse that will be required for long duration missions. The two thruster systems listed in Table I in the research and development category will not offer much reduction in power requirements at high specific impulse. However, there are several advanced thruster concepts that have promise of significantly lower power needs at high specific impulse. Whether these possible future reductions in electric power are especially advantageous will depend on the size of the spacecraft powerplant. If the spacecraft is a communications satellite



in a 24-hour synchronous orbit, it is possible that the spacecraft powerplant will be in the kilowatt class, and if this is the case then the power savings indicated in Table I may not be sufficiently advantageous to justify the development of the advanced concepts for that particular mission.

There is another important feature of the thruster systems for auxiliary propulsion missions that are listed in Table I in the R & D and the advanced concept categories. This feature is the ability of some of the thruster systems to operate at relatively low voltage levels in comparison with the high voltages required by the operational systems at high specific impulse. For example, the mercury bombardment thruster system presently in the R & D phase has a maximum of 400 volts d.c. in the overall system, which is a voltage level that seems attainable directly from the solar cell array without any intervening power conditioning required (ref. 2). Virtual elimination of the high voltage power conditioning equipment would be an advantage both in cost and in improved reliability. In the advanced concept category the lithium isotope/resistojet offers the possibility of operating directly from the spacecraft bus at practically any voltage, but this thruster system has a relatively low specific impulse, and therefore would have a high propellant weight for long duration missions. In this same category the potassium hollow-cathode ion expansion concept would have a significantly lower voltage than the mercury bombardment thruster in the R & D category, and in addition would have a higher specific impulse. The ultimate in auxiliary electric propulsion systems is represented by the isotope/liquid-spray thruster concept which has a high specific impulse and a very low electric power need, e.g., just enough for the telemetry. This advanced concept would have its own electric power source completely independent from the spacecraft powerplant.

Electric power needs for the intermediate propulsion missions shown in Table II will vary widely, depending on the particular missions and the particular thruster system. In

the MORL class mission where biowaste is used as the propellant, it appears that considerable power savings might be achieved by the advanced thruster concept where an isotope heater is coupled with the electric heater in the resistojet thruster system. This reduction in electric power needs would be achieved in principle by thermally heating the propellant to a fairly high temperature, then raising the propellant to its final high temperature with electric power. The ammonia resistojet and the lithium isotope/resistojet might also be used in the MORL class missions, especially where propellant resupply would not be a significant disadvantage.

The ultimate choice of thruster system for the satellite orbit maneuvers missions will depend primarily on the total impulse requirement of the orbit maneuvers, and on whether or not a considerable amount of electric power is onboard the satellite for other purposes. For instance, direct-broadcast synchronous satellites may eventually have onboard power in the kilowatt range, and if this power were available for orbit maneuvers then the mercury bombardment or the hollow-cathode ion expansion thrusters shown in Table II might be preferable to the resistojets.

Availability of onboard power for electric propulsion may be a very important consideration in possible synchronous satellite raising missions. For instance, if the satellite had somewhat more than 1000 watts of electric power for broadcast functions after positioning, then this power might be used for the lithium isotope/resistojet advanced thruster concept in raising the satellite from a low parking orbit to the 24-hour synchronous orbit. With a specific impulse of 400 seconds, and effectively "free" power this advanced concept should have performance superior to all-chemical delivery systems. Even if additional power were used to reduce the raising time to 40 days, the lithium isotope/resistojet concept appears to offer payload advantage over conventional chemical rockets in this mission. These remarks are not intended to promote electric propulsion for this particular mission, but rather to indicate the great importance of power level assessment in the field of electric propulsion.

Electric power level is of major importance in the primary electric propulsion missions shown in Table III. Because of the high total-impulse requirements of interplanetary unmanned and manned missions, optimum specific impulse is in the 2000 to 3000 second range for propulsion systems having powerplant specific mass of 50 to 100 lb/kwe. The mercury bombardment and the cesium bombardment thruster systems shown in the R & D category in Table III are not very efficient in this range of specific impulse, thereby increasing the electric power requirement. In addition, their voltage requirements are 1000 volts d.c., which may dictate the use of power conditioning in solar electric systems. The hollow-cathode ion expansion thruster system in the advanced concepts category has promise of higher efficiency and lower voltage in the specific impulse range of interest for solar electric unmanned interplanetary spacecraft. This same observation may be made for possible future manned interplanetary spacecraft with nuclear electric powerplants. Although the hollow-cathode ion expansion advanced concept could in principle have a thrust density sufficiently high for reasonable packaging in the payload shroud of very large chemical booster rockets, the MPD arc advanced concept has much promise for a very high thrust density, which may be a definite advantage for the megawatt power levels that would ultimately be required for manned interplanetary electric spacecraft.

#### CONCLUSIONS

From this survey of electric power needs for electric propulsion, it can be concluded that power levels may range from several watts to several megawatts depending on the mission and the propulsion function. Missions with high total impulse will require specific impulse of the thruster system in the range above 2000 seconds in order to avoid excessive propellant requirements. Operation at these high values of specific impulse will require commensurately high electric power needs. In such systems with very high power levels, electric thruster system efficiency will become of crucial

importance in order to minimize powerplant size and mass. There are a number of advanced concepts that offer significant improvements in thruster efficiency.

The need for higher specific impulse in intermediate and in auxiliary propulsion missions will become more acute as mission durations are increased to 5 to 10 year periods. The concomitant increase in power needs for the electric thruster system might be conveniently absorbed in satellites that have high power levels onboard for other functions. However, in the interest of cost reductions, ease in packaging in the booster vehicles, and elimination of sun-orienting mechanisms, there will certainly be many satellites where electric power will be at a premium. In these cases, reduction of power needs by a matter of a few watts will still serve as a strong impetus to the further work on advanced concepts in auxiliary electric propulsion systems.

A final observation can be made with regard to voltage levels required for electric thruster systems. Specific impulse in the range of 2000 to 3000 seconds is of particular interest for solar electric interplanetary spacecraft. In this range of specific impulse, the ion thrusters have accelerating voltages in the range from 100 to 1000 volts d.c. These factors have led to an interest in research and development leading to solar cell arrays having such output voltages. Virtual elimination of power conditioning equipment is a strong motivation in this regard. This trend towards lower voltages may be of direct benefit to future nuclear electric power generation systems for electric propulsion. For example, alternator output voltage in turboelectric systems might be matched directly to the power needs of the primary electric thruster system.

## APPENDIX - THRUSTER SYSTEM CHARACTERISTICS

Information, data, and assumptions that have been used in assessing the power needs for electric propulsion are summarized in this appendix.

## AUXILIARY - PROPULSION

## Operational Thruster Systems

NH<sub>3</sub> resistojet. I = 150 sec. Valves, 2 w; telemetry, 2 w.  
(Ref. 1)

NH<sub>3</sub> resistojet. I = 200 sec. Valves, 2 w; telemetry, 2 w.  
(Ref. 16)

liquid-spray. I = 900 sec. Telemetry, 2 w; neutralizer, 5 w; vaporizer, 5 w. For F = 490 micropounds,  $P = 2 + (14 + 5 + 5) / .7 = 36$  watt, where 14 w thruster power includes a thruster efficiency of 70%, and where power-conditioning efficiency is 70%. (Ref. 17)

pulsed-plasma. I = 1000 sec. (Ref. 18)

Cs-bombardment. I = 5000. Power conditioning efficiency, 70%. (Ref. 19)

Cs-contact. I = 6700 sec. (Ref. 1)

## Thruster Systems in Research and Development

magnetic-expansion MPD. I = 420 sec. at F = 490 micropounds, I = 570 sec. at F = 700 micropounds. Xenon propellant, all permanent magnets. Power conditioning assumed to be not needed. (Refs. 20 and 21)

Hg-bombardment. I = 1700 sec. Power/thrust = 220 watt/mlb. Power conditioning efficiency assumed to be  $\eta_c = 0.7$ .  
 $P = (P/F)(F)/(\eta_c) = 220 \times .49/.7 = 154$  watts. (Ref. 11)

## Advanced Concepts

Li isotope/resistojet.  $I = 400$  sec. Power/thrust = 5 watt/mlb.  
(Ref. 2)

liquid spray.  $I = 1200$  sec. Assumed improved charge/mass.  
Power conditioning efficiency, 0.7.  $P = 2 + (18 + 5 + 5) / .7 =$   
42 watts. (Ref. 22)

K hollow-cathode ion expansion.  $I = 2600$  sec. Potassium  
propellant. Beam current, 300 milliamp. Thruster  
system ev/ion, 97. Net accelerating voltage, 110 v.  
Power conditioning assumed to be not needed. Neutralizer  
power, 5 watt. Vaporizer power, 5 watt. Total power  
 $P = .3(110 + 97) + 10 = 72$  watts. (Refs. 2, 23, and 24)

isotope/liquid-spray.  $I = 4000$  sec. Telemetry, 2 watts.  
Power from radioisotope electrogenerator integral with  
thruster system. (Refs. 2 and 25)

## INTERMEDIATE PROPULSION

## Thruster Systems in Research and Development

CO<sub>2</sub> biowaste resistojet.  $I = 180$  sec. Thruster power/thrust,  
 $P/F = 4.5$  watt/mlb. Power for CO<sub>2</sub> collection, 110 watt  
for 24 millipounds thrust level. (Ref. 9)

NH<sub>3</sub> resistojet.  $I = 300$  sec. Thruster power/thrust,  
 $P/F = 15.7$  watt/mlb. (Ref. 26)

Hg bombardment.  $I = 1900$  sec. Thruster system power/thrust,  
 $P/F = 86$  watt/mlb. Power conditioning efficiency,  
 $\eta_c = 0.88$ . (Ref. 11)

## Advanced Concepts

CO<sub>2</sub> biowaste isotope/resistojet.  $I = 180$  sec. Thruster  
power/thrust,  $P/F = 1.5$  watt/mlb. Power for CO<sub>2</sub>  
collection, 110 watt for 24 millipound thrust level.  
(Ref. 2)

Li isotope/resistojet.  $I = 400$  sec. Thruster power/thrust,  
 $P/F = 5$  watt/mlb. (Ref. 2)

hollow-cathode ion expansion.  $I = 1000$  sec. Thruster power/thrust,  $P/F = 60$  watt/mlb. Power conditioning assumed to be not needed. (Refs. 2, 23, and 24)

#### PRIMARY PROPULSION

##### Thruster Systems in Research and Development

H<sub>2</sub> resistojet.  $I = 740$  sec. Plenum temperature, 2200°K. Thruster power/thrust,  $P/F = 24$  watt/mlb. (Ref. 26)

Hg bombardment.  $I = 2670$  sec. Thruster efficiency,  $\eta_{th} = 0.7$ . Power conditioning efficiency,  $\eta_c = 0.88$ . Power/thrust,  $P/F = (4.45 \times 26,700) / (2 \times 0.7 \times 0.88) = 96.5$  kw/lb. (Ref. 11)

Cs bombardment.  $I = 3360$  sec. Thruster efficiency,  $\eta_{th} = 0.59$ . Power conditioning efficiency,  $\eta_c = 0.88$ . Power/thrust,  $P/F = (4.45 \times 33,600) / (2 \times 0.59 \times 0.88) = 144$  kw/lb. (Ref. 19)

#### Advanced Concepts

Li isotope/resistojet.  $I = 400$  sec. Power/thrust,  $P/F = 5$  watt/mlb. (Ref. 2)

hollow-cathode ion expansion.  $I = 2400$  sec. Cesium propellant. Discharge power, 85 ev/ion. Other powers (neutralizers, vaporizers, etc.), 25 ev/ion. Propellant utilization efficiency,  $\eta_U = 0.99$ . Net accelerating voltage, 400 v. Thruster efficiency,  $\eta_{th} = .99 / (1 + 110/400) = 0.77$ . Power/thrust,  $P/F = 4.45 v_j / (2 \eta_{th}) = 4.45 \times 24,000 / (2 \times 0.77) = 69$  kw/lb. (Refs. 2, 23, and 24)

MPD arc. This thruster concept has promise of high performance in the megawatt power range. It is assumed here that this concept may be developed to a performance level equal to that of the ion expansion advanced concept listed above. The arc voltage is approximately  $60 / \eta_{th} = 60 / 0.77 = 78$  volts. (Ref. 27)

## REFERENCES

1. Isley, W. C., and Mickelsen, W. R.: Auxiliary Electric Propulsion for Current Spacecraft Applications. Astronautics and Aeronautics. June, 1968.
2. Mickelsen, W. R., and Isley, W. C.: Auxiliary Electric Propulsion - Status and Prospects. AFOSR Fifth Symposium on Advanced Propulsion Concepts. Chicago, Illinois. April 8-10, 1968.
3. Kerrisk, D. J., and Bartz, D. R.: Primary Electric-Propulsion Systems Technology and Applications. Astronautics and Aeronautics. June, 1968.
4. Kerrisk, D. J., and Hasbach, W. A.: Primary Electric Propulsion - Status and Prospects. AFOSR Fifth Symposium on Advanced Propulsion Concepts. Chicago, Illinois. April 8-10, 1968.
5. Lazar, J., and Peko, P. E.: Potential Applications for Electric Propulsion. AIAA Paper No. 67-422. July, 1967.
6. Mickelsen, W. R.: Auxiliary and Primary Electric Propulsion, Present and Future. Jour. Spacecraft and Rockets. November, 1967.
7. Duck, K. I., Bartlett, R. O., and Sullivan, R. J.: Evaluation of an Ion Propulsion System for a Synchronous Spacecraft Mission. AIAA Paper No. 67-720. September, 1967.
8. Isley, W. C.: private communication. NASA Goddard Space Flight Center. May 15, 1968.
9. Greco, R. V., and Byke, R. M.: Resistojet Biowaste Utilization - Evaluation and System Selection. AIAA Paper No 68-121. January, 1968.
10. Duck, I. I.: An Approximation Method for Determination of Propulsion Requirements Associated with Low Thrust Coplanar Orbital Transfer in a Central Force Field Under Negligible External Perturbations. Publications of GSFC, 1963: II. Space Technology. 1963.
11. Richley, E. A., and Kerslake, W. R.: Bombardment Thruster Investigations at the Lewis Research Center. AIAA Paper No. 68-542. June, 1968.
12. Meissinger, H. F., and Greenstadt, E. W.: Use of Electric Propulsion for Exploring the Distant Regions of the Geomagnetic Tail. AIAA Paper No. 68-120. January, 1968.
13. Stearns, J. W.: private communication. Jet Propulsion Laboratory. May 21, 1968.



14. Barber, T. A., Edberg, J. R., Goldsmith, J. V.: Spacecraft Electric Propulsion - Now? *Astronautics and Aeronautics*. June, 1968.
15. Layton, J. P.: Propulsion Technology for Manned Planetary Missions. AIAA Technology for Manned Interplanetary Missions Meeting. New Orleans, La. March 5, 1968.
16. White, A.: private communication. NASA Goddard Space Flight Center. May 15, 1968.
17. Zafran, S., Beynon, J. C., and Cohen, E.: Colloid Microthruster System Development. AIAA Paper No. 68-84. January, 1968.
18. Guman, William J., and Peko, P. E.: Solid Propellant Pulsed Plasma Micro-Thruster Studies. AIAA Paper No. 68-86. January, 1968.
19. Sohl, G., Speiser, R. C., and Wolters, J. A.: Life Testing of Electron-Bombardment Cesium Ion Engines. AIAA Paper No. 66-233. March, 1966.
20. Johansen, A. E., Bowditch, D. N., and Burkhart, J. A.: Experimental Performance of a Low-Power MPD Arc Thruster. AIAA Paper No. 67-50. January, 1967.
21. Johansen, A. E.: Lightweight Magnets for MPD Arcs. AIAA Paper No. 67-686. September, 1967.
22. Hunter, R. E.: private communication. NASA Goddard Space Flight Center. May 15, 1968.
23. Free, B. A., and Mickelsen, W. R.: Plasma Separator Thruster. *Jour. Spacecraft and Rockets*, 4, 1282. October, 1967.
24. Free, B. A.: private communication. General Electric Company, Cincinnati, Ohio. February 20, 1968.
25. Mickelsen, W. R.: Basic Design Considerations for Radioisotope Electrogenators. Proceedings of 3rd Intersociety Energy Conversion Engineering Conference. Boulder, Colorado. August, 1968.
26. Page, R. J., and Short, R. A.: Ten-Millipound Resistojet Performance Compared with Theory. AIAA Paper No. 67-664. September, 1967.
27. Jahn, R. G.: private communication. Princeton University. May 18, 1968.

TABLE I - POWER FOR TYPICAL AUXILIARY-PROPULSION MISSIONS  
24-HOUR SYNCHRONOUS SATELLITE  
(ELECTRIC BUS POWER, WATTS)

THRUSTER SYSTEM	HIGHEST VOLTAGE IN THRUSTER SYSTEM	SPACECRAFT, LB	E-W STATION KEEPING AND ATTITUDE	NORTH-SOUTH STATION KEEPING	
	SPECIFIC IMPULSE, SEC	THRUST, MICROPOUNDS			
OPERATIONAL	NH <sub>3</sub> RESISTOJET	150	24	2000	2000
	NH <sub>3</sub> RESISTOJET	200	24	20*	700†
	LIQUID-SPRAY	900	6000 D.C.	12	-
	PULSED-PLASMA	1000	1400 D.C.	-	22
	Cs - BOMBARDMENT	5000	2000 D.C.	5	36
	Cs - CONTACT	6700	3000 D.C.	7	-
	MAGNETIC-EXPANSION MPD	420	60 D.C.	-	159
	Hg - BOMBARDMENT	1700	400 D.C.	35	175
	LI ISOTOPE/RESISTOJET	400	s/c BUS	-	70
	LIQUID SPRAY	1200	6000 D.C.	-	154
ADVANCED	K HOLLOW-CATHODE ION EXPANSION	2600	110 D.C.	-	8
	ISOTOPE/LIQUID-SPRAY	4000	s/c BUS	-	42
				6	55
			-	-	72
			2	2	2

\* INCLUDES PRECISION THRUST-VECTORING CAPABILITY

† FOR SYSTEM REDUNDANCY WHERE ONE FIXED THRUSTER CAN DO N-S STATION-KEEPING

‡ IF OTHER THRUSTER FAILS  
SPECIFIC IMPULSE, 570 SEC.

TABLE II - POWER FOR TYPICAL INTERMEDIATE-PROPULSION MISSIONS  
(ELECTRIC BUS POWER, WATTS)

THRUSTER SYSTEM	HIGHEST VOLTAGE IN THRUSTER SYSTEM	SPACECRAFT, LB	THRUST, MILLIPOUNDS	MORL*	SATELLITE ORBIT MANUEVERS	SYN. SAT. RAISING**	
						40 DAYS	180 DAYS
CO <sub>2</sub> BIOWASTE RESISTOJET	180	6	180	36,000	2,000	2,000	2,000
NH <sub>3</sub> RESISTOJET	300	6	300	24	50	1,000	300
Hg BOMBARDMENT	1900	500 D.C.	1900	240 <sup>+</sup>	-	-	-
CO <sub>2</sub> BIOWASTE ISOTOPE/RESISTOJET	180	s/c BUS	180	380	790	17,400	4,000
LI ISOTOPE/RESISTOJET	400	s/c BUS	400	-	4,300	-	25,000 <sup>++</sup>
Cs HOLLOW CATHODE ION EXPANSION	1000	100	1000	146 <sup>+</sup>	-	-	-
ADVANCED				120	200	5,000	1,200
				-	3,000	-	-

\* TOTAL IMPULSE, 1900 LB-SEC/DAY

+ INCLUDING 110 WATT FOR CO<sub>2</sub> COLLECTION

\*\* FROM 300 N.M., TO SYNCHRONOUS ALTITUDE, ASSUMING ONE-HALF TIME IN EARTH SHADOW, SOLAR-ARRAY INCLUDED IN FINAL 2000 LB.

++ FROM 1000 N.M., FINAL VEHICLE MASS = 7100 LB., INCLUDING 25 KW SOLAR ARRAY, BUT NOT INCLUDING ELECTRIC THRUSTERS, TANKAGE, AND SOME POWER CONDITIONING.

TABLE III - POWER FOR TYPICAL PRIMARY PROPULSION MISSIONS  
(ELECTRIC BUS POWER, WATTS)

THRUSTER SYSTEM	SPECIFIC IMPULSE, SEC	HIGHEST VOLTAGE IN THRUSTER SYSTEM	THRUST, POUNDS	SPACECRAFT, LB	UNMANNED		MANNED
					600	2300	600,000
H <sub>2</sub> RESISTOJET	740	6	430	1,560	-	-	-
Hg BOMBARDMENT	2670	1000 D.C.	1,730	6,300	1.94 MW	-	-
Cs BOMBARDMENT	3360	1000 D.C.	2,600	9,350	2.9 MW	-	-
LI ISOTOPE/RESISTOJET	400	s/c BUS	90	325	-	-	-
Cs HOLLOW-CATHODE ION EXPANSION	2400	400 D.C.	1,200	4,500	1.4 MW	-	-
MPD ARC	2400	78	-	-	1.4 MW	-	-

ADVANCED

R &amp; D

MULTI-NOZZLE RESISTOJET  
FOR ADVANCED VELA  
NITROGEN PROPELLANT  
SPECIFIC IMPULSE 132 SEC.  
POWER, 17 WATTS  
THRUST, 20 MILLIPOUNDS

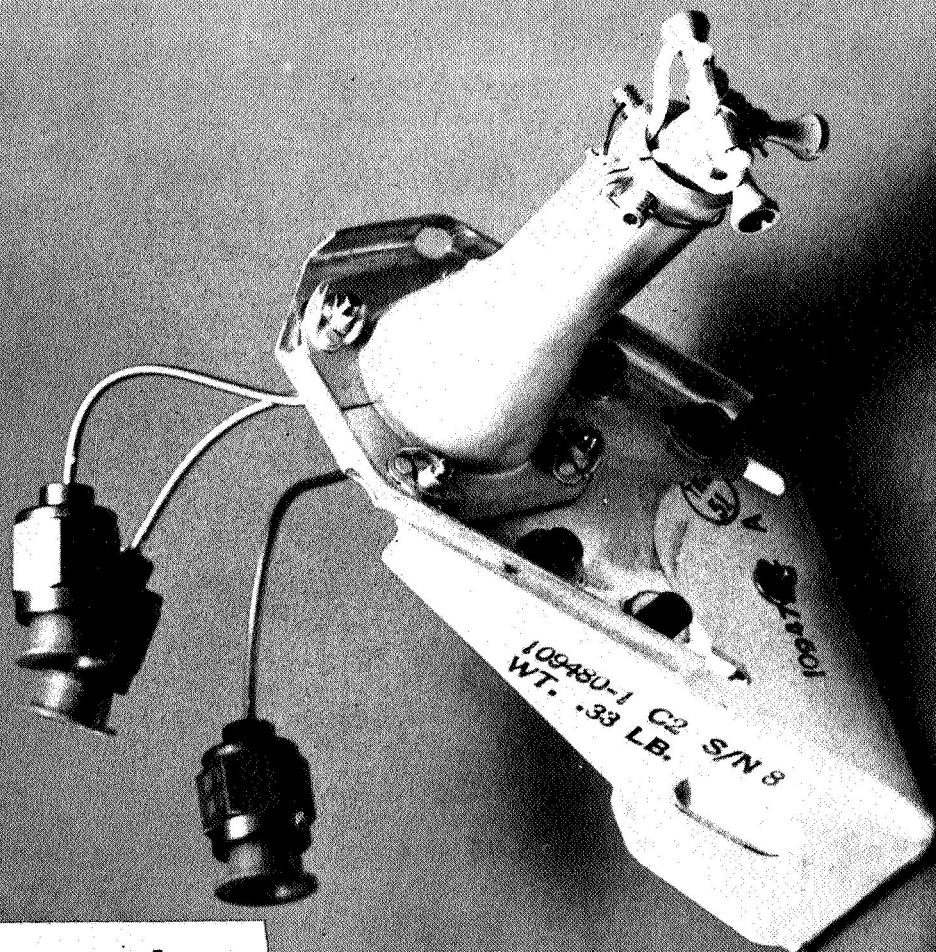
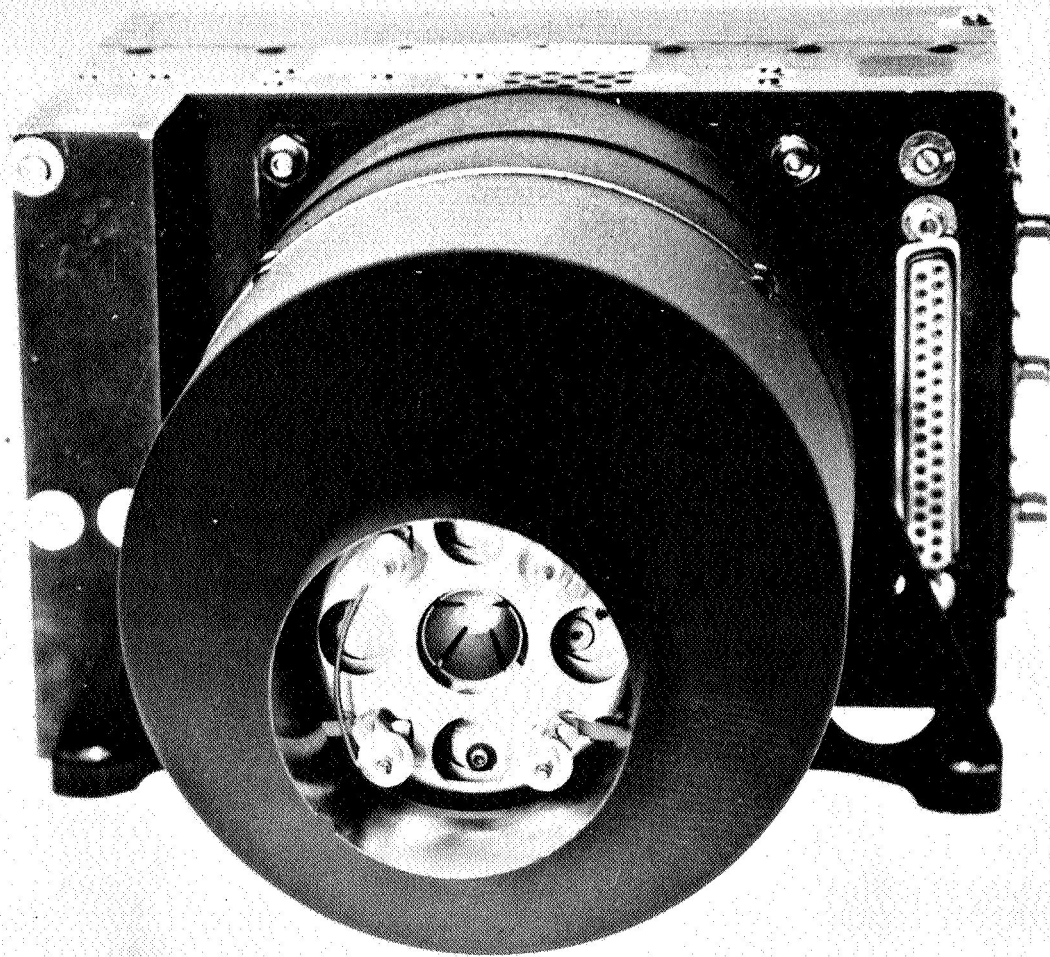


FIG. 1 - TRW THREE-NOZZLE RESISTOJET FOR VELA ADVANCED SPACECRAFT.



CONTACT-ION THRUSTER  
FOR ATS-D  
PRECISION THRUST VECTORING  
PROPELLANT, CESIUM  
SPECIFIC IMPULSE, 6700 SEC.  
POWER, 35 WATT  
THRUST, 20 MICROPOUND

FIG. 2 - EOS CESIUM CONTACT ION THRUSTER FOR NASA ATS D SPACECRAFT.

ELECTRON-BOMBARDMENT THRUSTER  
FOR AIR FORCE MULTI-PURPOSE SATELLITE  
PROPELLANT, CESIUM  
SPECIFIC IMPULSE, 3000-5000 SEC.  
THRUST, 50 MICRPOUND TO 10 MILLIPOUND

23

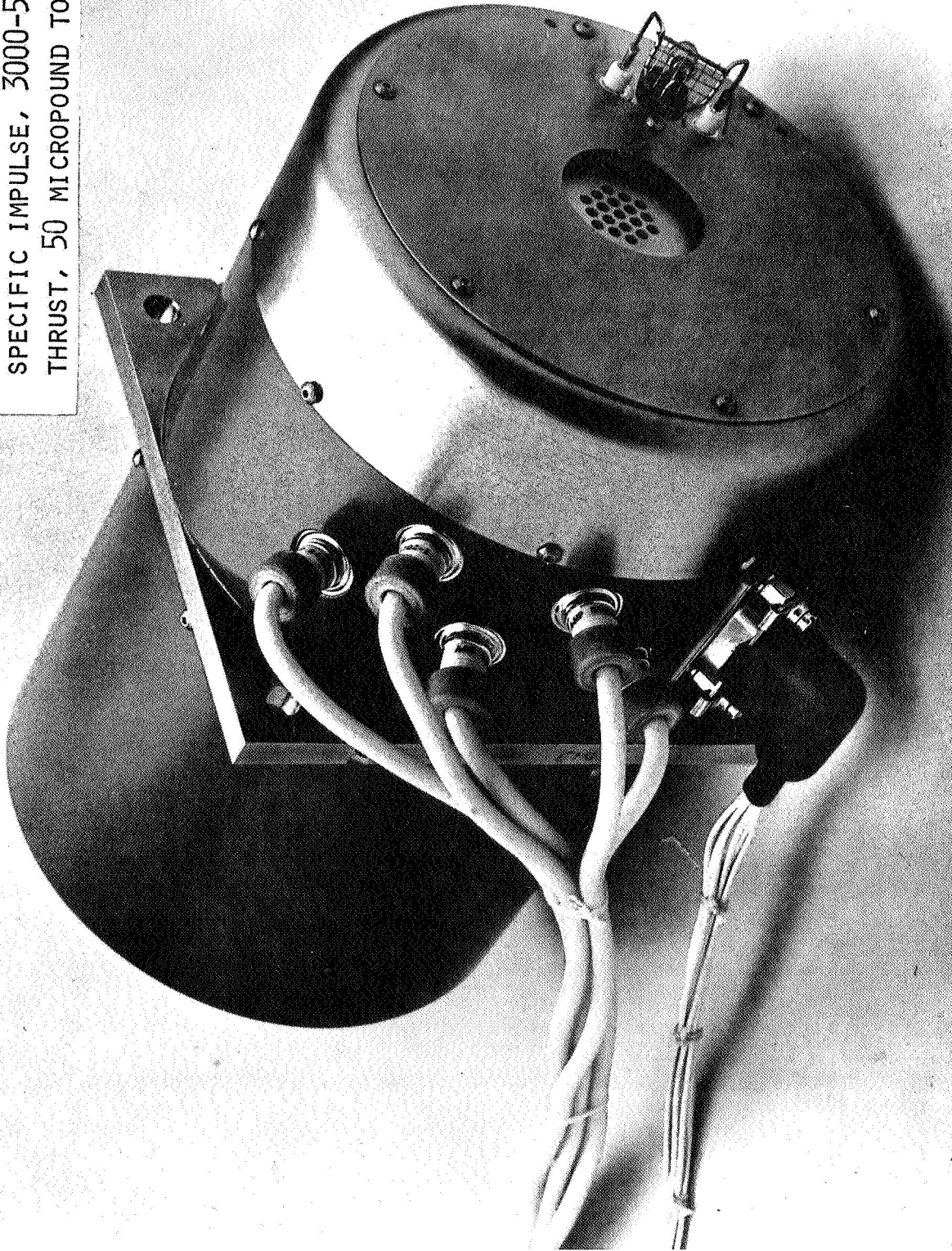
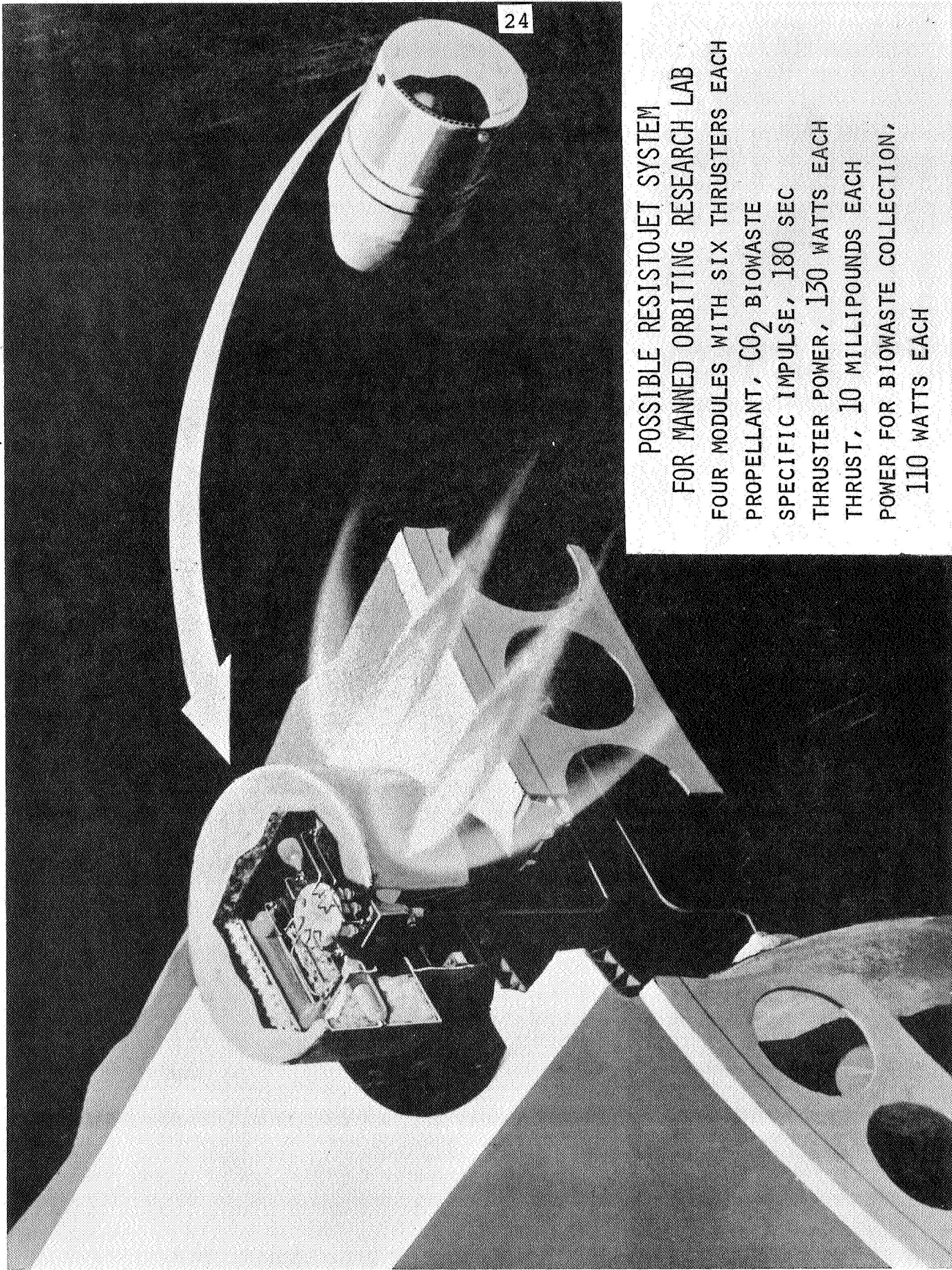


FIG. 3 - EOS CESIUM BOMBARDMENT THRUSTER FOR  
AIR FORCE MULTI-PURPOSE SATELLITE PROGRAM.



POSSIBLE RESISTOJET SYSTEM  
FOR MANNED ORBITING RESEARCH LAB  
FOUR MODULES WITH SIX THRUSTERS EACH  
PROPELLANT, CO<sub>2</sub> BIOWASTE  
SPECIFIC IMPULSE, 180 SEC  
THRUSTER POWER, 130 WATTS EACH  
THRUST, 10 MILLIPOUNDS EACH  
POWER FOR BIOWASTE COLLECTION,  
110 WATTS EACH

FIG. 4 - POSSIBLE RESISTOJET SYSTEM FOR MORL.



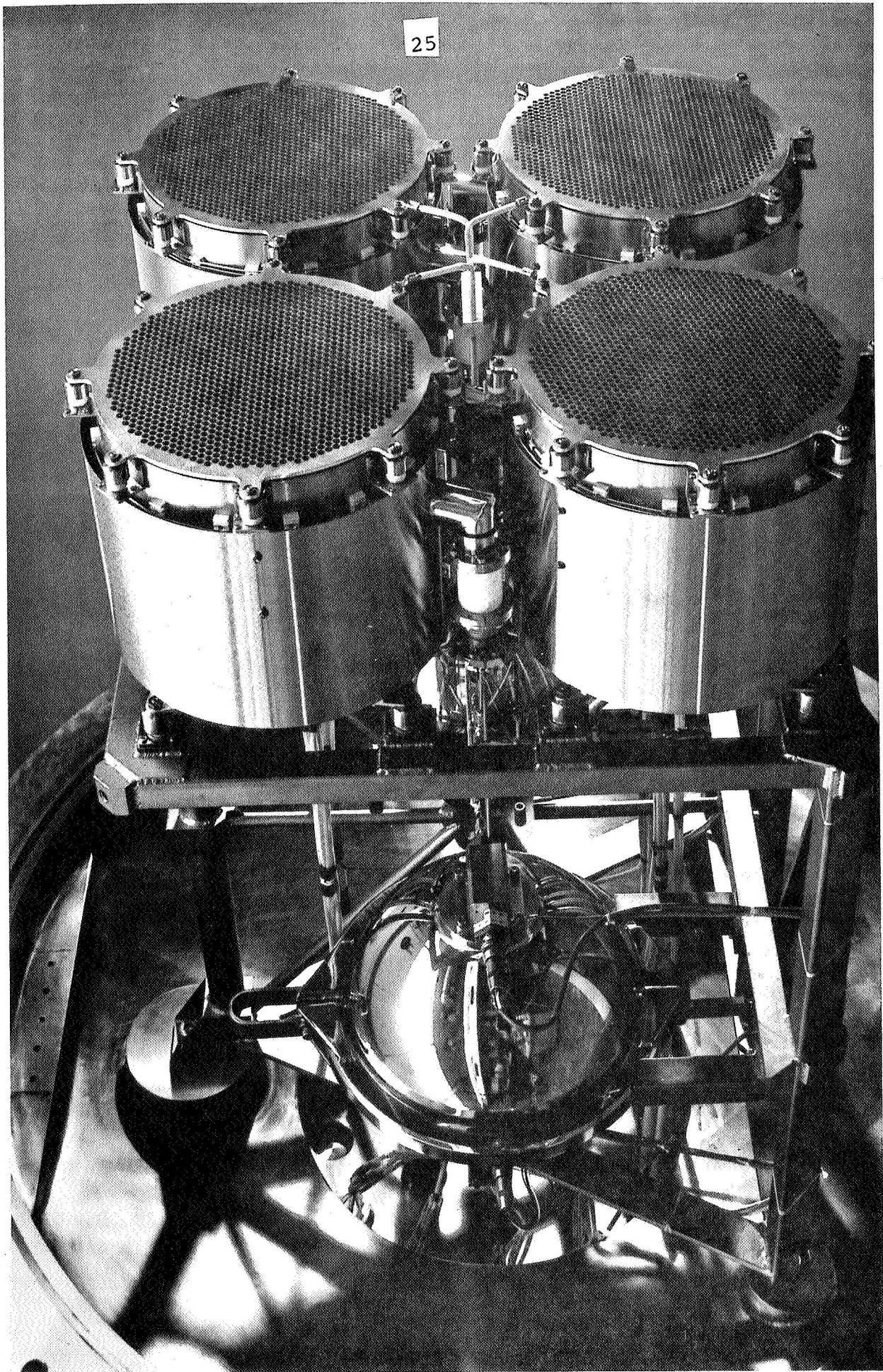


FIG. 5 - ELECTRIC THRUSTER SYSTEM UNDER DEVELOPMENT AT JET PROPULSION LABORATORY FOR POSSIBLE SOLAR-ELECTRIC INTERPLANETARY SPACECRAFT. THRUST, 65 MILLIPOUNDS. SPECIFIC IMPULSE, 2700 SEC. THRUSTER SYSTEM POWER, 10 KILOWATTS.

COMPARISON OF VARIOUS HEAT ADDITION PROGRAMS TO  
SUPERSONIC NOZZLE FLOWby Harry I. Leon, Fariborz P. Saheli and  
William R. Mickelsen

## INTRODUCTION

Previous analysis<sup>3.1</sup> showed that it is possible to have a great increase in the exit velocity of a supersonic nozzle by heat addition in the supersonic section. This greater velocity is highly desirable for increasing the specific impulse of electric thrusters. The velocity increase in the nozzle was found to be a function of both the amount of heat added and of the static temperature of the gas.\* However, the area ratio required for this velocity is very sensitive to the path in which the heat is added.

Three paths of heat addition were studied. For analyzing each of these paths, a computer code was developed. These codes are described in the Method of Analysis and are listed in the Appendix.

Code for Heat Addition Optimization Using  
Steepest Descent Method

With this code, the maximum exit velocity for a given set of initial conditions can be determined by optimizing the nozzle area variations as a function of the optimum heat addition path. The code uses the method of steepest descent optimization and is written in a general manner so as to handle a wide range of optimization problems. It can optimize either by minimizing the entropy increase or by maximizing the velocity increase.

---

\* This is, of course, assuming that there are no discontinuities or friction losses in the flow.

Codes for Nozzle Design with a Combination of  
Heated and Nonheated Supersonic Sections

Continuous Heating. In this code, heat addition was a linear function of the area (see Equation 3.20). A combination of linear heating with nonheating gave the highest velocity per unit area of the paths studied.

Discontinuous Heating. This code is similar to the continuous heating mode except that heat is added very abruptly (to simulate arc heating) and then the gas is allowed to cool by expansion, then again abruptly heated. This process is repeated through the nozzle. This mode of heat addition requires much larger area ratios than for the ideal optimum and for the continuous heating mode, but should provide performance superior to a single-arc-heated nozzle.

METHOD OF ANALYSIS

Heat Addition Optimization Using  
Steepest Descent Method

The equations for the flow assumed a steady one-dimensional variable area nozzle with heat addition, inviscid fluid, and no heat losses. The following equations given by Pai<sup>3.3</sup>, are in a form suitable for optimization:

$$\frac{\dot{V}}{V} = \frac{1}{(1-M^2)} \left( \frac{\dot{q}}{C_P T} - \frac{\dot{A}}{A} \right) \quad (3.1)$$

$$\frac{\dot{T}}{T} = \frac{1-\gamma M^2}{(1-M^2)} \left( \frac{\dot{q}}{C_P T} - \frac{\dot{A}}{A} \right) + \frac{\dot{A}}{A} \quad (3.2)$$

$$\frac{\dot{p}}{p} = \frac{-1}{(1-M^2)} \left( \frac{\dot{q}}{C_P T} - \frac{\dot{A}}{A} \right) \quad (3.3)$$

$$\frac{\dot{P}}{P} = \frac{-\gamma M^2}{(1-M^2)} \left( \frac{\dot{q}}{C_P T} - \frac{\dot{A}}{A} \right) \quad (3.4)$$

where, the Mach Number,  $M$ , is given by  $M = V/(\gamma RT)^{1/2}$ ,  $\gamma$  is the specific heat ratio,  $R$  is the gas constant and  $T$  is the static temperature.

The solution of these equations depends both on the rate of heat addition,  $\dot{q}$ , and on the area variation  $A(x)$ . When heat is added in the supersonic section of the nozzle, the rate of change of area,  $\dot{A}/A$ , must be larger than  $\dot{q}/C_p T$  for a velocity increase. If it is less, the velocity will decrease and the Mach Number will decrease toward 1. At  $M = 1$ , the equations (3.1 - 3.4) will be discontinuous.

All the variables in the above set of equations are differentiated with respect to the nozzle length,  $x$ ; therefore, the solutions will give the flow variable at any point along the nozzle.

Optimization Procedure. In order to maximize the velocity at the exit of the nozzle, the method of steepest descent is used<sup>3,4</sup>. A set of initial conditions are assumed, based on plenum temperature, the initial Mach Number where heat first added, a nominal model for heat addition, and a fixed nozzle length. This nominal model is based on a study previously done at Colorado State University<sup>3,1</sup>.

The set of differential equations used are:

$$\dot{V} = V \frac{1}{(1-M^2)} \left( \frac{\dot{q}}{C_p T} - \beta \right) \quad (3.5)$$

$$\dot{T} = T \frac{1-\gamma M^2}{(1-M^2)} \left( \frac{\dot{q}}{C_p T} - \beta \right) + T\beta \quad (3.6)$$

$$\dot{A} = \beta A \quad (3.7)$$

$$\dot{q} = C\beta \quad (3.8)$$

$$\dot{s} = \frac{\dot{q}}{T} \quad (3.9)$$

where  $C$  in equation (3.8) is an arbitrarily chosen constant and  $\beta = \frac{\dot{A}}{A}$  is the control function.

The method of steepest descent is applied to equations (3.5 - 3.9) as follows:

1. A nominal profile for the area  $A(x)$  is assumed. The nominal model is used for the initial heat addition path.
2. For a given set of initial conditions, the equations (3.5 - 3.9) are forwardly integrated along the nozzle axis to determine the state variables.
3. The adjoint differential equations:

$$\dot{\bar{\lambda}} = - (\bar{F})^T \bar{\lambda} \quad (3.10)$$

can be solved using the control function,  $\beta$ , the velocity,  $V_{x=L}$ , as the payoff, and  $x=L$  as the stopping condition. In equation (3.10),  $\bar{\lambda}$  is the adjoint vector, and  $\bar{F}$  is the matrix given by:

$$\bar{F} = \frac{\partial f}{\partial \bar{Y}} = \begin{bmatrix} \frac{\partial \dot{V}}{\partial V} & \frac{\partial \dot{V}}{\partial T} & \frac{\partial \dot{V}}{\partial A} & \frac{\partial \dot{V}}{\partial q} & \frac{\partial \dot{V}}{\partial S} \\ \frac{\partial \dot{T}}{\partial V} & \frac{\partial \dot{T}}{\partial T} & \frac{\partial \dot{T}}{\partial A} & \frac{\partial \dot{T}}{\partial q} & \frac{\partial \dot{T}}{\partial S} \\ \frac{\partial \dot{A}}{\partial V} & \frac{\partial \dot{A}}{\partial T} & \frac{\partial \dot{A}}{\partial A} & \frac{\partial \dot{A}}{\partial q} & \frac{\partial \dot{A}}{\partial S} \\ \frac{\partial \dot{q}}{\partial V} & \frac{\partial \dot{q}}{\partial T} & \frac{\partial \dot{q}}{\partial A} & \frac{\partial \dot{q}}{\partial q} & \frac{\partial \dot{q}}{\partial S} \\ \frac{\partial \dot{S}}{\partial V} & \frac{\partial \dot{S}}{\partial T} & \frac{\partial \dot{S}}{\partial A} & \frac{\partial \dot{S}}{\partial q} & \frac{\partial \dot{S}}{\partial S} \end{bmatrix} \quad (3.11)$$

where  $\bar{Y}$  is the state vector,  $\bar{Y} = \{V, T, A, q, S\}$ . The terms in the matrix  $\bar{F}$  are evaluated along the nominal path. The initial condition for the adjoint differential equation is:

$$\left\{ \frac{\partial V}{\partial \bar{Y}} \right\}_{x=L} = \{1, 0, 0, 0, 0\} \quad (3.12)$$

4. The matrix  $\bar{G}$  (given below) is then evaluated.

$$\bar{G} = \frac{\partial \bar{f}}{\partial \dot{\beta}} = \begin{bmatrix} \dot{\partial V / \partial \beta} \\ \dot{\partial T / \partial \beta} \\ \dot{\partial A / \partial \beta} \\ \dot{\partial \dot{q} / \partial \beta} \\ \dot{\partial S / \partial \beta} \end{bmatrix} \quad (3.13)$$

5. The new control function,  $\delta\beta(x)$ , can then be evaluated as follows:

$$\delta\beta(x) = \beta_{\text{new}}(x) - \beta_{\text{nominal}}(x) = K\bar{G}^T\bar{\lambda} \quad (3.14)$$

where  $K$  is a constant which determines the step size for the iterative process.

6. The new control variable,  $\beta_{\text{new}}(x)$ , is substituted for  $\beta$  in equations (3.5 - 3.9). These equations are then integrated to obtain the new state variables. The velocity,  $V$  should increase during this iteration. The process is repeated until the constraints on either the maximum area ratio or the maximum heat addition are met.

#### Supersonic Nozzle Design with Combination of Heated and Nonheated Sections

Linear Heating. The velocity increase in the heated section of the nozzle is given by the equation:

$$\frac{dV}{V} = \frac{1}{M^2 - 1} \left[ \frac{dA}{A} - \left(1 + \frac{\gamma - 1}{2} M^2\right) \frac{dT_o}{T_o} \right] \quad (3.14)$$

(See References 3.1 and 3.2). It is noted from this equation that the velocity,  $V$ , will increase as long as:

$$\frac{dA}{A} > \left(1 + \frac{\gamma - 1}{2} M^2\right) \frac{d(T_o)}{T_o} \quad (3.15)$$

where  $A$  is the cross section area of the nozzle,  $\gamma$  is the specific heat ratio,  $T_o$  is the stagnation temperature, and  $M$  is the Mach Number.

The velocity increase in the heated section of the nozzle was analyzed by integrating equation (3.14). Since the path of heat addition (the relationship between  $dA$  and  $d T_o$ ) is not defined, the equation was integrated by numerical methods. In order to accomplish this, equation (3.14) was written in finite difference form as shown below:

$$\frac{V_{n+1}}{V_n} = \left[ \frac{A_n}{A_{n+1}} - 1 - \left( 1 + \left( \frac{\gamma-1}{2} \right) \bar{M}^2 \right) \left( \frac{T_{o_{n+1}}}{T_{o_n}} - 1 \right) \right] \left[ \frac{1}{\bar{M}^2 - 1} \right] + 1 \quad (3.16)$$

where  $\bar{M}$  is the average Mach Number between section  $n$  and  $n+1$ . (The conversion on the average Mach Number for each interval of area and stagnation temperature change was explained in Reference 3.1.)

The value of the area ratio,  $AR$ , where:

$$AR = \frac{A_{n+1}}{A_n} \quad (3.17)$$

was initialized at the nozzle throat. Then the area ratio,  $AR$ , was increased in small steps, called  $DAR$ .  $DAR$  was found to give good results when the value of 0.001 was chosen. Thus the change in area ratio of each step was written as:

$$AR = AR + DAR \quad (3.18)$$

The stagnation temperature ratio,  $TR$ , where:

$$TR = \frac{T_{o_{n+1}}}{T_{o_n}} \quad (3.19)$$

for each step, was then allowed to vary as a function of the area ratio,  $AR$ .

Many paths for heat addition for the nozzle were studied. The best paths analyzed were in the form:

$$TR = AR^{-c} \quad (3.20)$$

where  $c$  was an input constant into the program. The optimum design for the nozzle was found to have values of  $c$  between 1 and 5.

The abrupt heating of the supersonic section of the nozzle was similar to the code above except that the heat was added very abruptly to simulate a special type of arc heating. As noted by equations (3.14) and (3.15), unless the area of the nozzle is changed at a sufficient rate (compared to the stagnation temperature change) the velocity of the gas will not increase. Since the area change is small for a supersonic flow heated at a constant-velocity, it was assumed that the heat was added abruptly. The analysis of the heat addition along this path was made by setting  $dv$  in equation (3.14) equal to zero and integrating in closed form. The area ratio required for a constant-velocity heat addition is given by the expression:

$$AR = (TR)^{1 + \frac{\gamma+1}{2} \bar{M}^2} \quad (3.21)$$

The design for the nozzle heater would then consist of several arcs, each having a section of non-heated expansion between them. The non-heated section of both the linearly-heated and the abruptly-heated nozzles will be discussed below.

Non-Heated Expansion. A study was made of the effect of a non heated section between the heated sections of both the linearly-heated and the discontinuously-heated nozzle. The analysis for the velocity increase with non-heated expansion was made using equation (3.14) with  $d(T_0) = 0$ . The resulting equation was solved by numerical methods similar to equation (3.16) giving:

$$\frac{V_{n+1}}{V_n} = \left[ AR - 1 \right] \left[ \frac{1}{\bar{M}^2 - 1} \right] + 1 \quad (3.22)$$



Thus, when the area is increasing ( $AR > 1$ ), the velocity of the flow increases. Then using the first law of thermodynamics, the stagnation temperature can be written as\*:

$$T_o = T + \frac{v^2}{2C_p} \quad (3.23)$$

where  $T$  is the static temperature. Therefore, when the stagnation temperature,  $T_o$ , is held constant and the velocity is increasing due to the increase in nozzle area, the static temperature will decrease during the expansion.

Combination of Heated and Non-heated Nozzle. The non-heated expansion was incorporated in the nozzle between the heated sections and between the last heated section and the nozzle exit. The gas was heated in the nozzle until the static temperature reached a specified maximum and then was allowed to expand without heat addition until the temperature reached a specified minimum. Then heating was again repeated. Many combinations of maximum and minimum static temperatures were studied. The heating paths were also varied for the linearly-heated path.

## RESULTS

The addition of heat to a supersonic nozzle was found to increase the velocity of the gas if the area is enlarged at a rate sufficient to accommodate this heat. As seen from equation (3.23), the exit velocity is only a function of the exit static temperature and the stagnation temperature, or the total heat addition to the gas. The exit velocity versus the heat added to a lithium propellant is shown on Figure 3.1. The area change required to obtain this exit velocity, is however, a strong function of the path in which the heat is added to the stream.

---

\* In this equation it is assumed that the gas obeys the perfect gas law with constant specific heat, constant molecular weight, and isentropic expansion.

### Heat Addition Optimization Using the Steepest Descent Method

This program was incomplete at the reporting time since the constraints which limit the maximum amount of heat addition and maximum area change were not as yet incorporated into the program. However, the preliminary results of the code are very encouraging. A typical velocity increase on each iteration is shown in Figure 3.2 for a lithium propellant. The corresponding area, heat addition, and temperature change for each iteration is shown in Figures 3.3 and 3.4. The results shown on Figure 3.4 are particularly interesting since the heat addition starts approaching a region of expansion without heating after the heated section. The heating of a nozzle with heat addition in one section, then continued expansion without heat addition, was found in the results below, to give a smaller area ratio for the same velocity than a continuously-heated nozzle.

#### Nozzle Design with a Combination of Heated and Non-heated Supersonic Section

##### 1. Linearly-heated nozzle expansion between non-heated expansions.

Typical results of this study were obtained by using lithium propellant. Figure 3.5 shows the required area ratio versus velocity for two ranges of static temperatures in the linearly-heated path between non-heated sections. The corresponding heat addition required for the velocity, shown in Figure 3.5, versus velocity is plotted on Figure 3.7. If the velocity was corrected to a given static temperature, the amount of heat addition required would be the same as that given on Figure 3.1.

The area required for a continuously-heated nozzle versus velocity is shown on Figure 3.6. A comparison of Figures 3.6 and 3.5 shows that the required area ratio is considerably larger for the continuously-heated path than for the path with non-heated expansion between the heated sections. For example, at a velocity of 6000 m/sec, the linearly-heated nozzle with non-heated expansions required an area ratio of

approximately 10, while the continuously-heated nozzle for the same velocity required an area ratio of approximately 30.

2. Abruptly-heated nozzle between non-heated expansions.

Figure 3.8 shows velocity versus area for a nozzle heated at constant velocity (to approximate arc heating) with non-heated expansions between the heated regions. The corresponding path of heat addition for Figure 3.8 is plotted versus velocity on Figure 3.9. A comparison of the area ratio required for this path of heat addition with other paths studied shows that, at a velocity of 6000 m/sec, an area ratio of approximately 100 is required, compared with an area ratio of 10 for a linearly-heated nozzle between non-heated expansions and 30 for the continuously-heated path.

#### CONCLUSIONS AND FUTURE WORK

##### Heat Addition Optimization Using Steepest Descent Method

1. The preliminary results of this program show that it will be a valuable tool in optimizing the nozzle design.
2. Future work will be in placing constraints of maximum heat addition and area charge into the computer program and in combining this code with the code of heating and non-heating expansion.

##### Nozzle Design with a Combination of Heated and Non-heated Supersonic Sections.

1. The use of a combination of heated and non-heated sections in the nozzle was found to give a much smaller nozzle area than a continuously-heated nozzle.
2. There is little change in the nozzle area required if the temperature limits (i.e. maximum and minimum static temperatures) in the supersonic section of the nozzle are changed. This is shown in Figures 3.5 and 3.8.

3. The abrupt heating with expansion required a greater area ratio for a given velocity than either the continuously-heated nozzle or the nozzle heated linearly between non-heated expansions. However, it should be pointed out that an arc-heated nozzle without non-heated expansions between the heated sections could not obtain an exit velocity of 6000 m/sec with lithium propellant with reasonable static temperatures.

4. Future work will include the real gas effects\*, actual specific heat versus temperature, friction in the nozzle, and dissociation of the gas molecules.

#### REFERENCES

- 3.1. Mickelsen, W. R.: Advanced Electric Propulsion Research, Annual Report for January 1, 1967 to December 31, 1967. Section 5., Prepared for the National Aeronautics and Space Administration. Grant NGR06-002-032.
- 3.2. Shapiro, A. H.: The Dynamics and Thermodynamics of Compressible Fluid Flow, Volume 1, Ronald Press Company, 1953.
- 3.3. Pai, S. I.: Introduction to Theory and Compressible Flow. D. Van Nostrand, Princeton, New Jersey, 1959.
- 3.4. Beyson, A. E., and Denhan, W. F.: "Steepest Descent Method for Solving Optimum Programing Problems." M. Appl. Mech. 29 (1962) 247.

---

\* Lithium is almost a perfect gas in the regions of temperature and pressure which were studied.

## NOMENCLATURE

A	=	area, area per unit flow rate
AR	=	area ratio, equation (3.17)
C	=	proportionality constant, equation (3.8)
c	=	constant density heat path, equation (3.20)
$C_p$	=	specific heat of gas at constant pressure
DAR	=	area ratio increment, equation (3.18)
$\bar{F}$	=	matrix defined by equation (3.11)
$\bar{G}$	=	matrix defined by equation (3.13)
L	=	nozzle length
M	=	Mach Number
P	=	pressure
q	=	heat input
R	=	gas constant
S	=	entropy
$T_{01}$	=	plenum stagnation temperature
$T_{02}$	=	stagnation temperature after heat addition in supersonic section of nozzle
TR	=	stagnation temperature ratio, equation (3.19)
V	=	velocity
x	=	distance downstream of nozzle throat
$\bar{y}$	=	state vector
$\beta$	=	control variable
$\gamma$	=	specific heat ratio
$\bar{\lambda}$	=	adjoint vector
$\rho$	=	density

## superscripts

.	=	total derivative with respect to independent variable ( = $\frac{d}{dx}$ )
-	=	normalized value
T	=	transpose

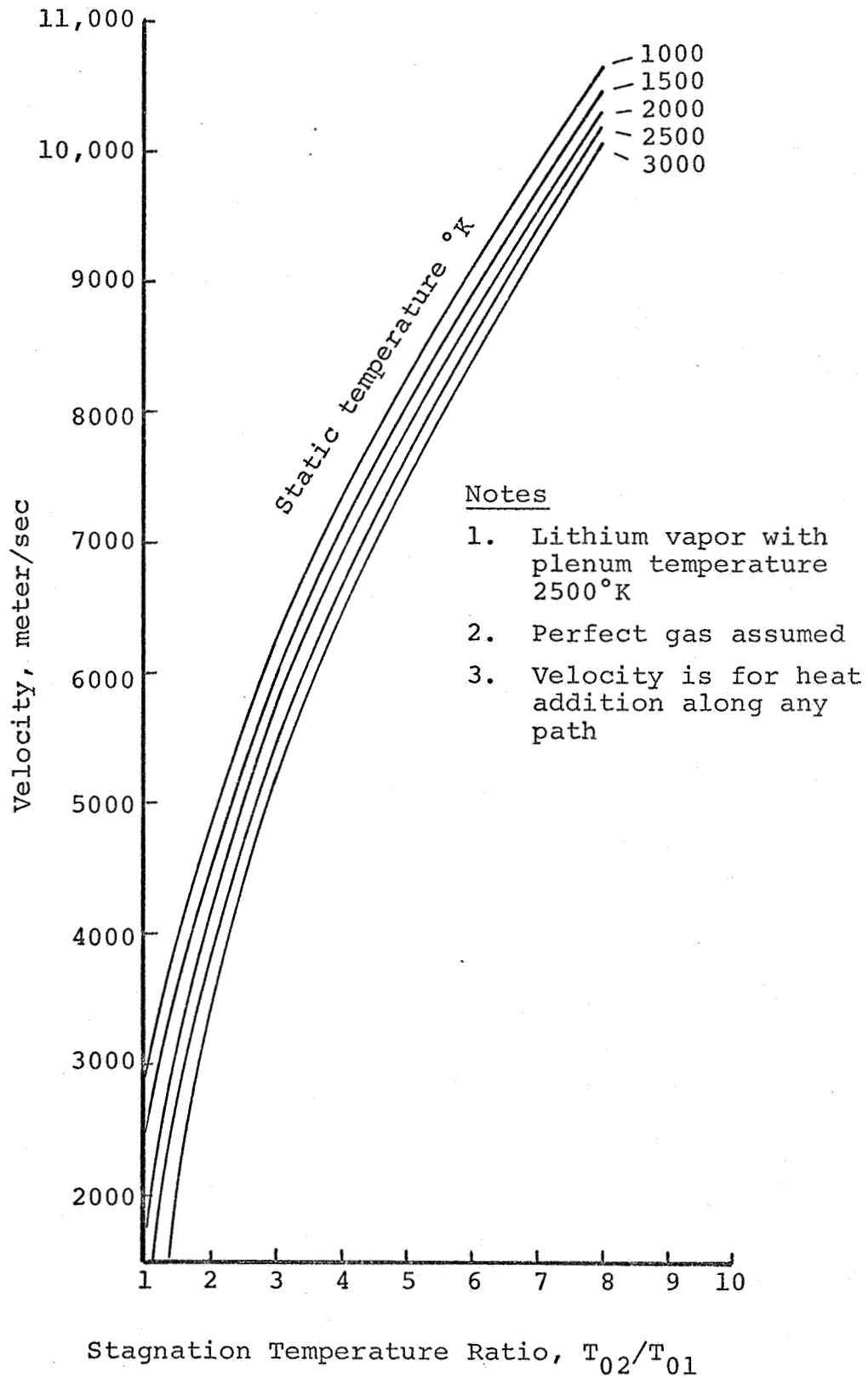
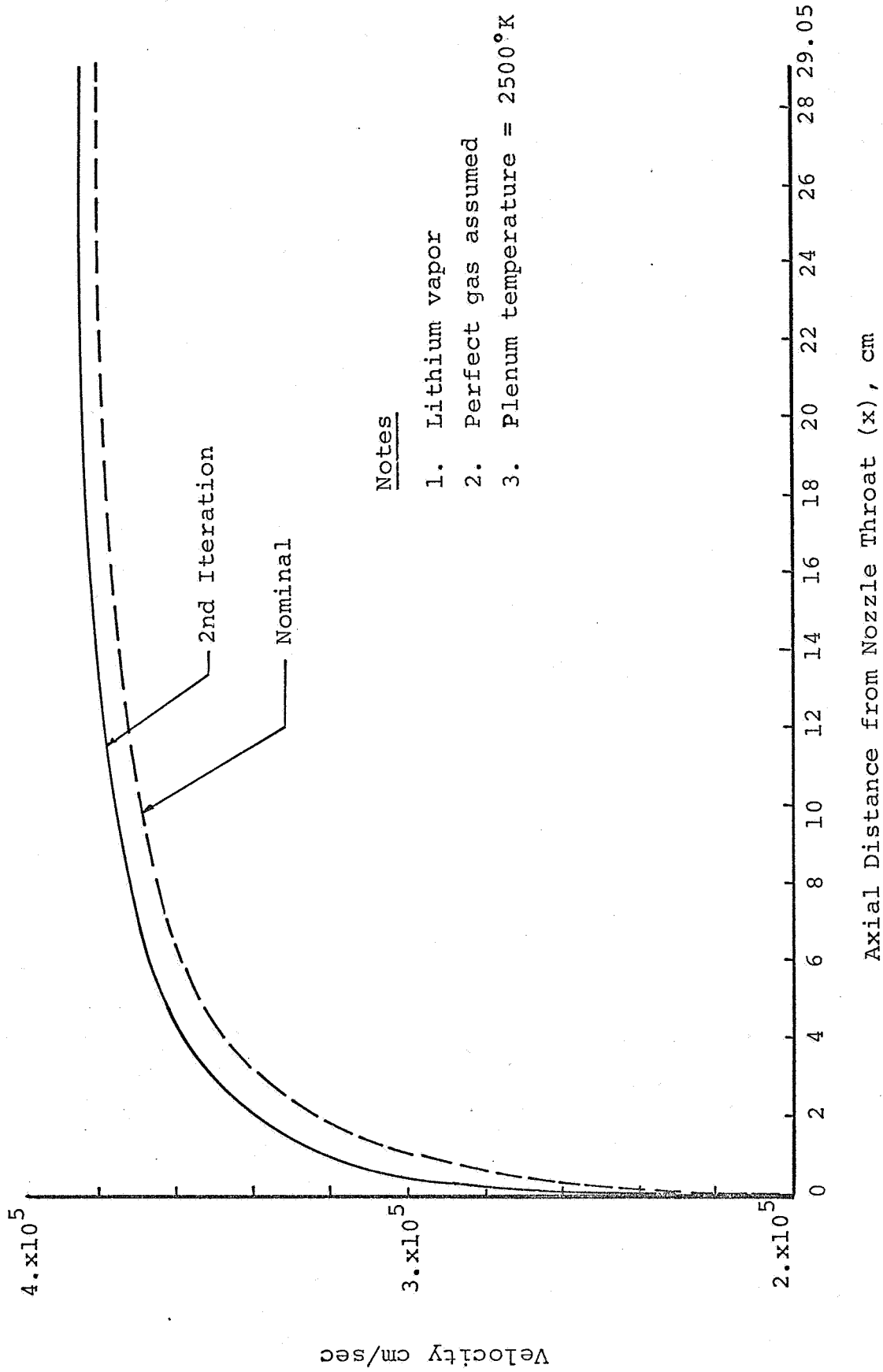


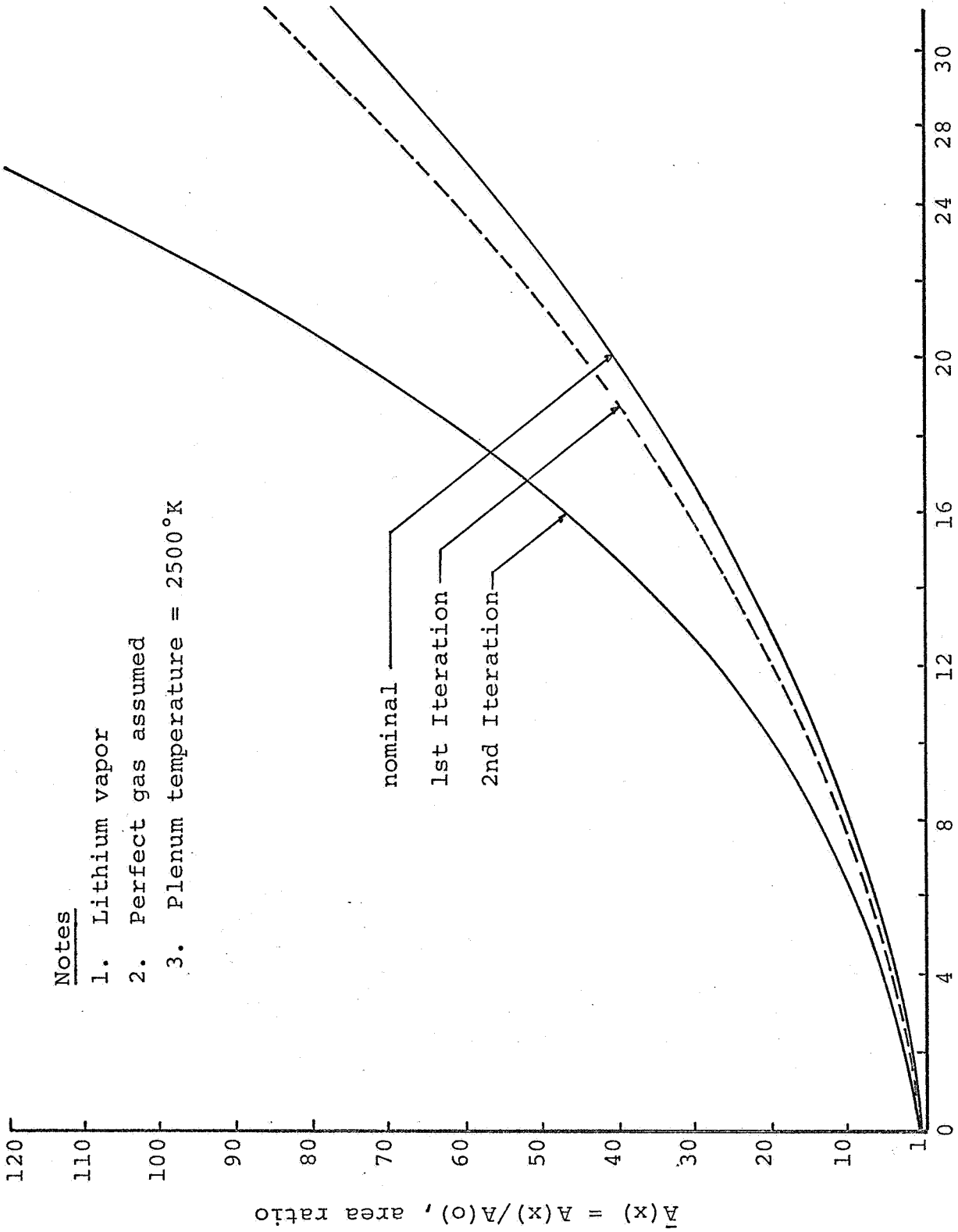
FIG. 3.1 - Velocity Versus Stagnation Temperature Ratio at Various Static Temperatures and Area Ratios.



Notes

1. Lithium vapor
2. Perfect gas assumed
3. Plenum temperature = 2500°K

FIG. 3.2 - Typical Optimization Iteration on Velocity Versus Axial Distance from Nozzle Throat.



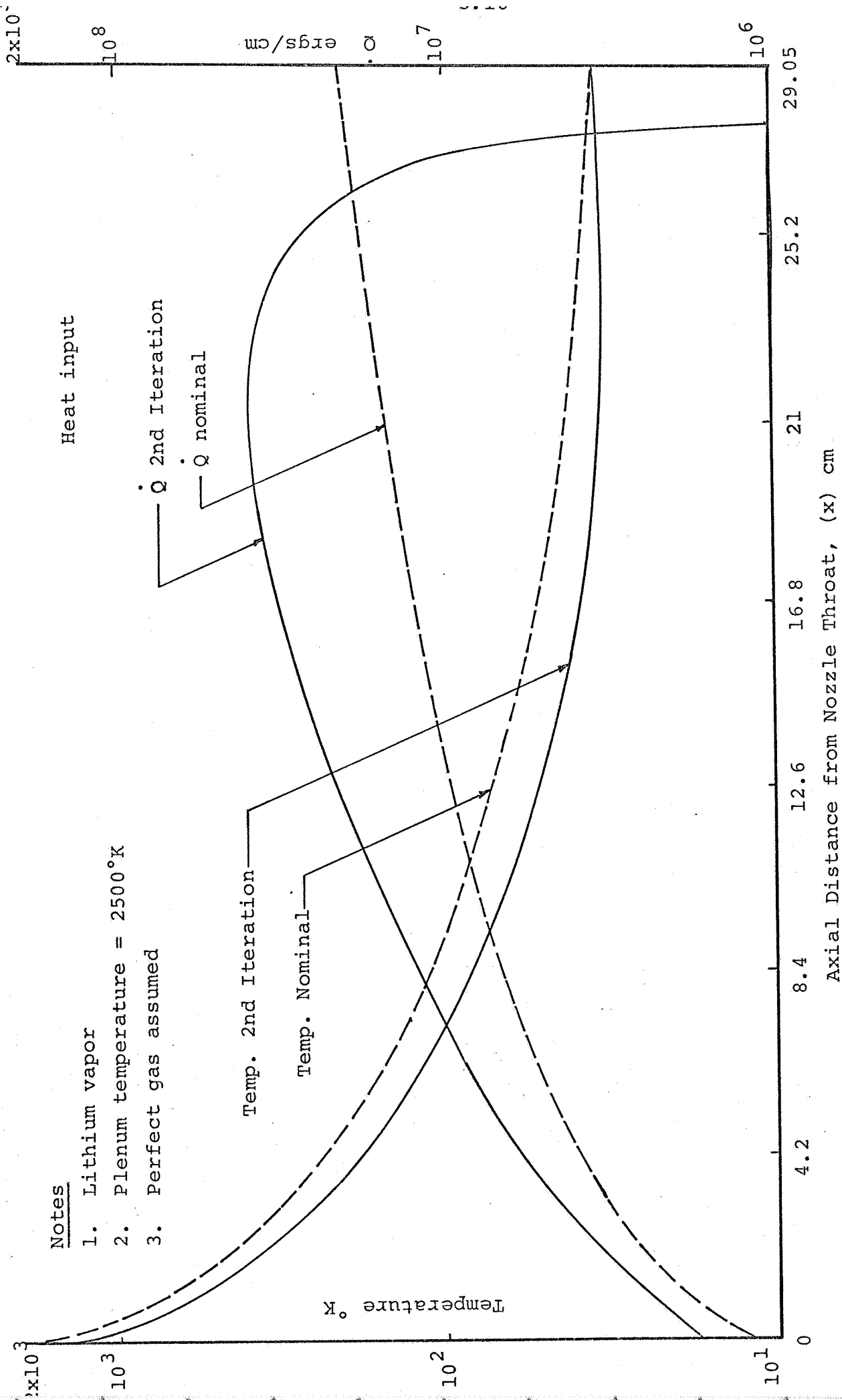
Notes

1. Lithium vapor
2. Perfect gas assumed
3. Plenum temperature = 2500°K

Axial Distance from Nozzle Throat (x) cm

FIG. 3.3 - Typical Optimization Iterations on Area Ratio Versus Axial Distance from Nozzle Throat.





Notes

1. Lithium vapor
2. Plenum temperature = 2500°K
3. Perfect gas assumed

FIG. 3.4 - Optimization Iterations on Static Temperature and Heat Input Versus Axial Distance from Nozzle Throat.

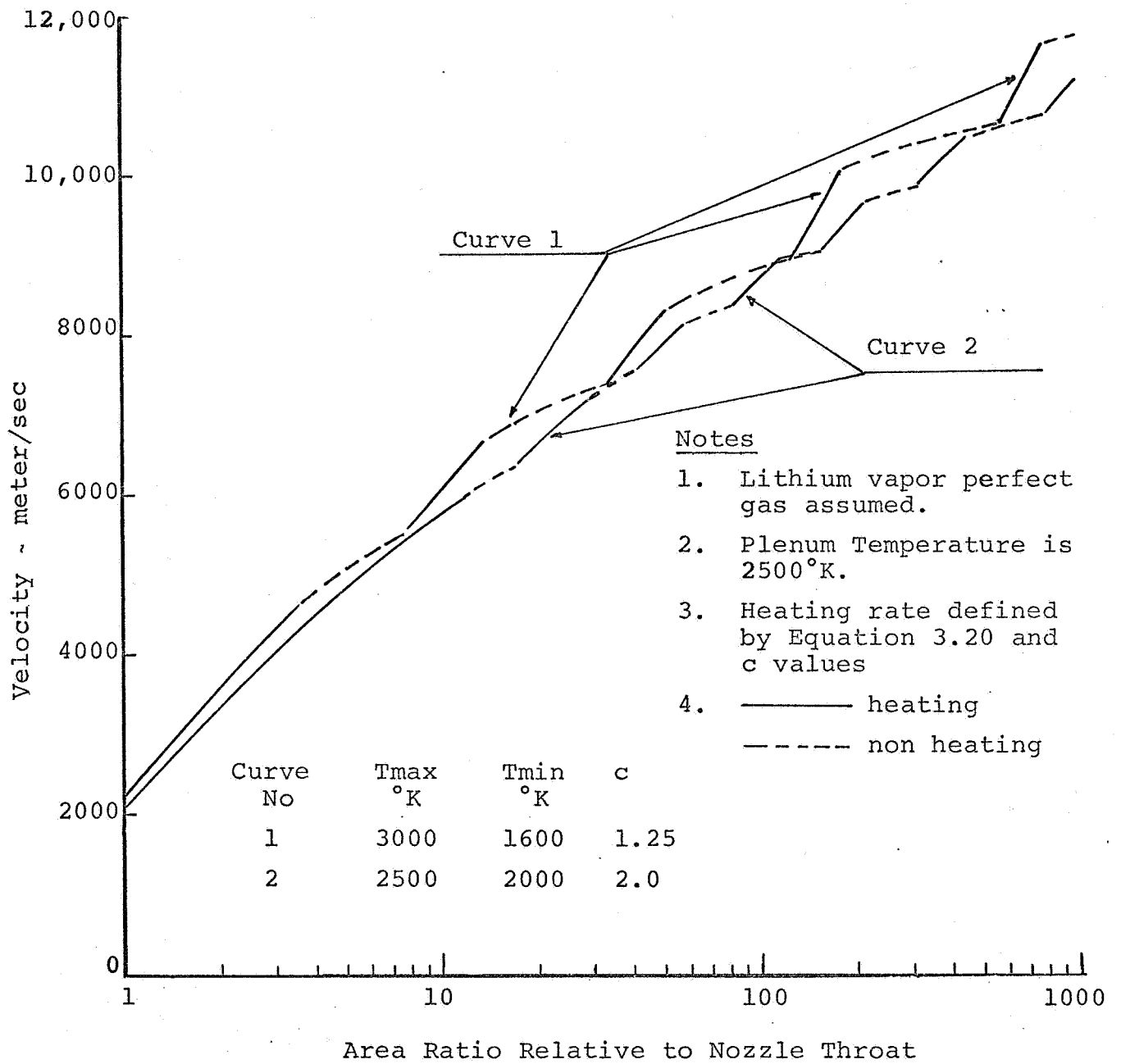
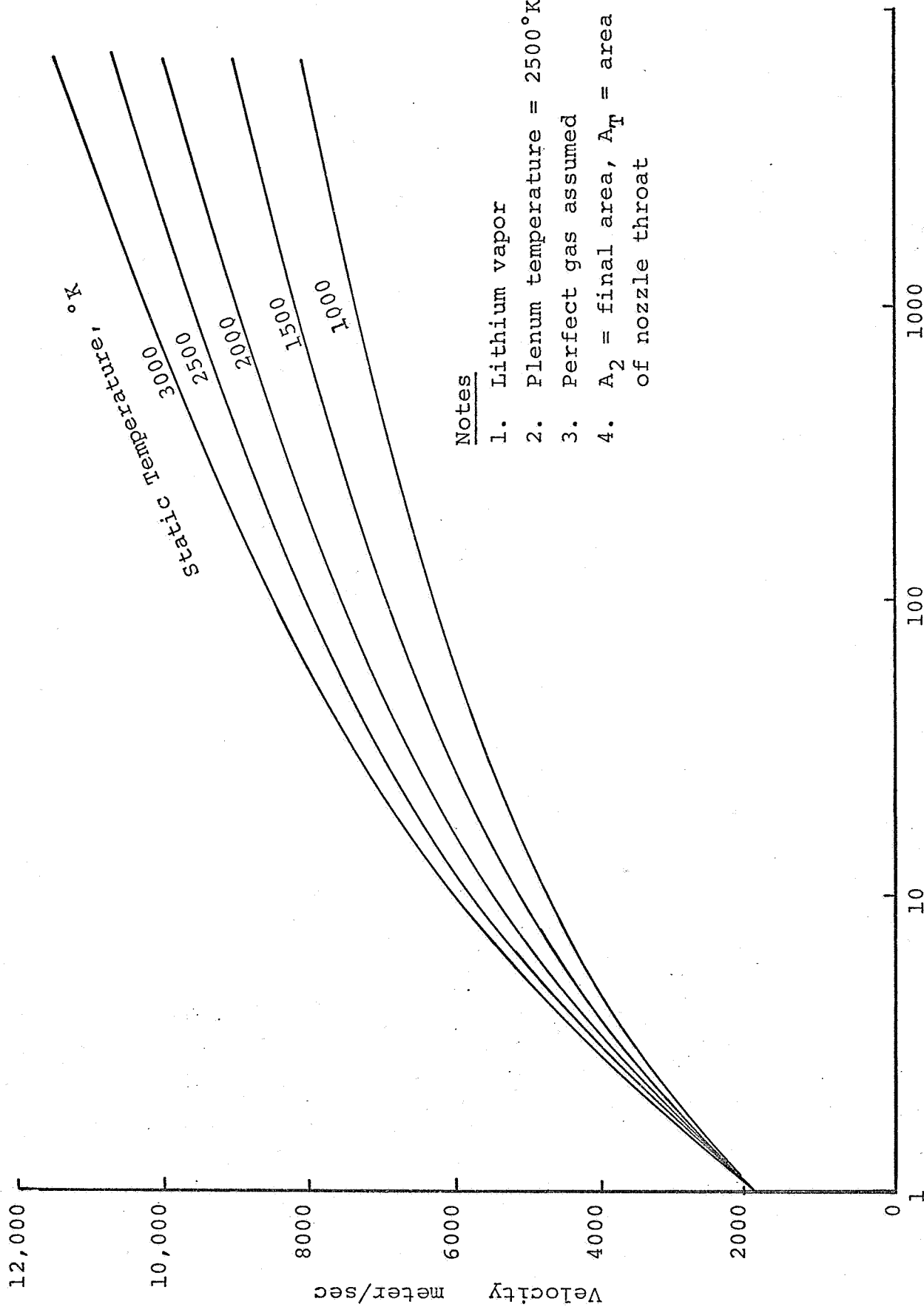


FIG. 3.5 - Velocity Versus Area Ratio for Linear Heat Addition and no Heating Expansion



Notes

1. Lithium vapor
2. Plenum temperature = 2500°K
3. Perfect gas assumed
4.  $A_2$  = final area,  $A_T$  = area of nozzle throat

Cross Section Area Ratio  $A_2/A_T$

FIG. 3.6 - Velocity Versus Cross Section Area Ratio, for Linear Heat Addition Path.

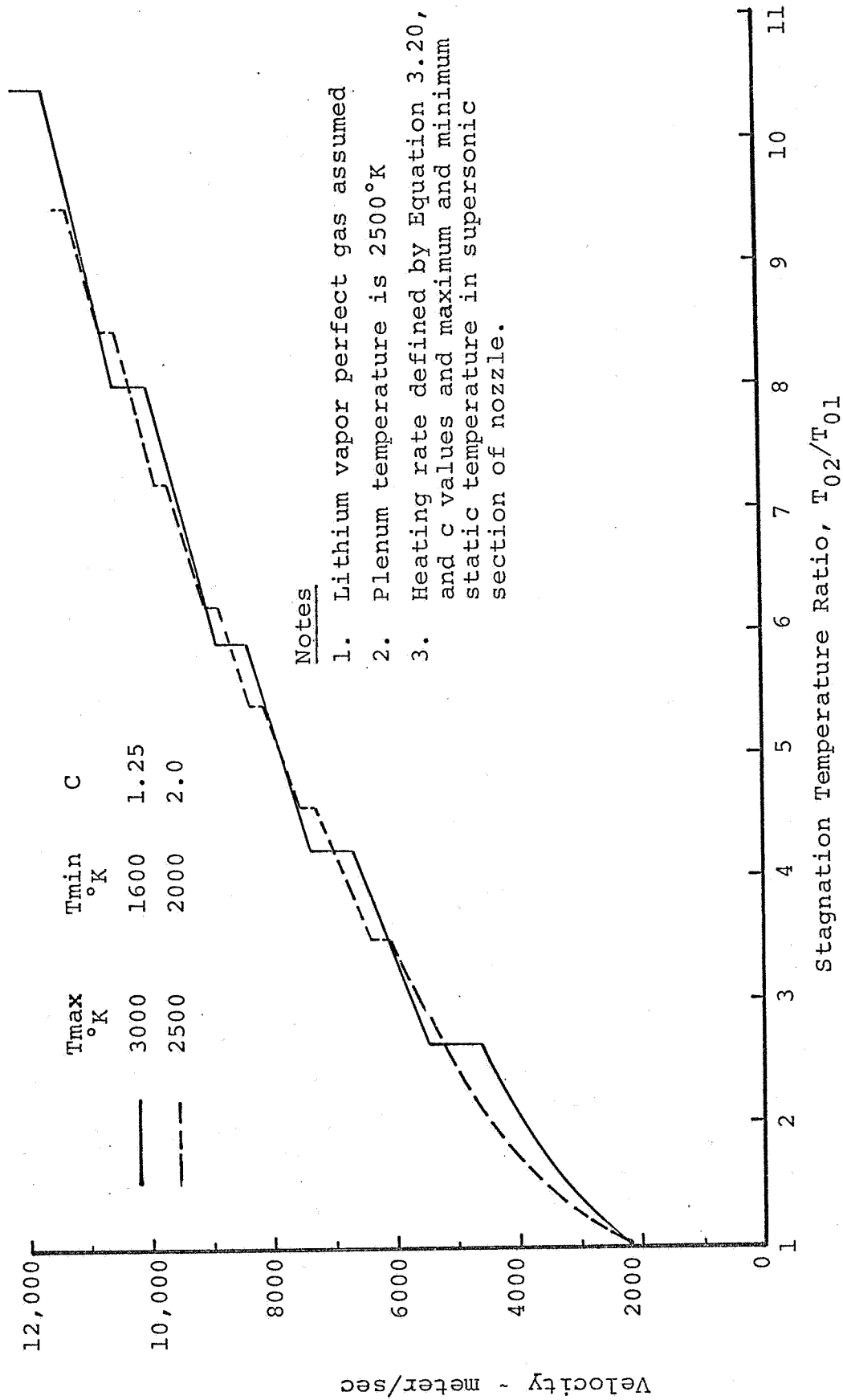


FIG. 3.7 - Velocity Versus Stagnation Temperature Ratio for Linear Heating and No Heating Expansion.

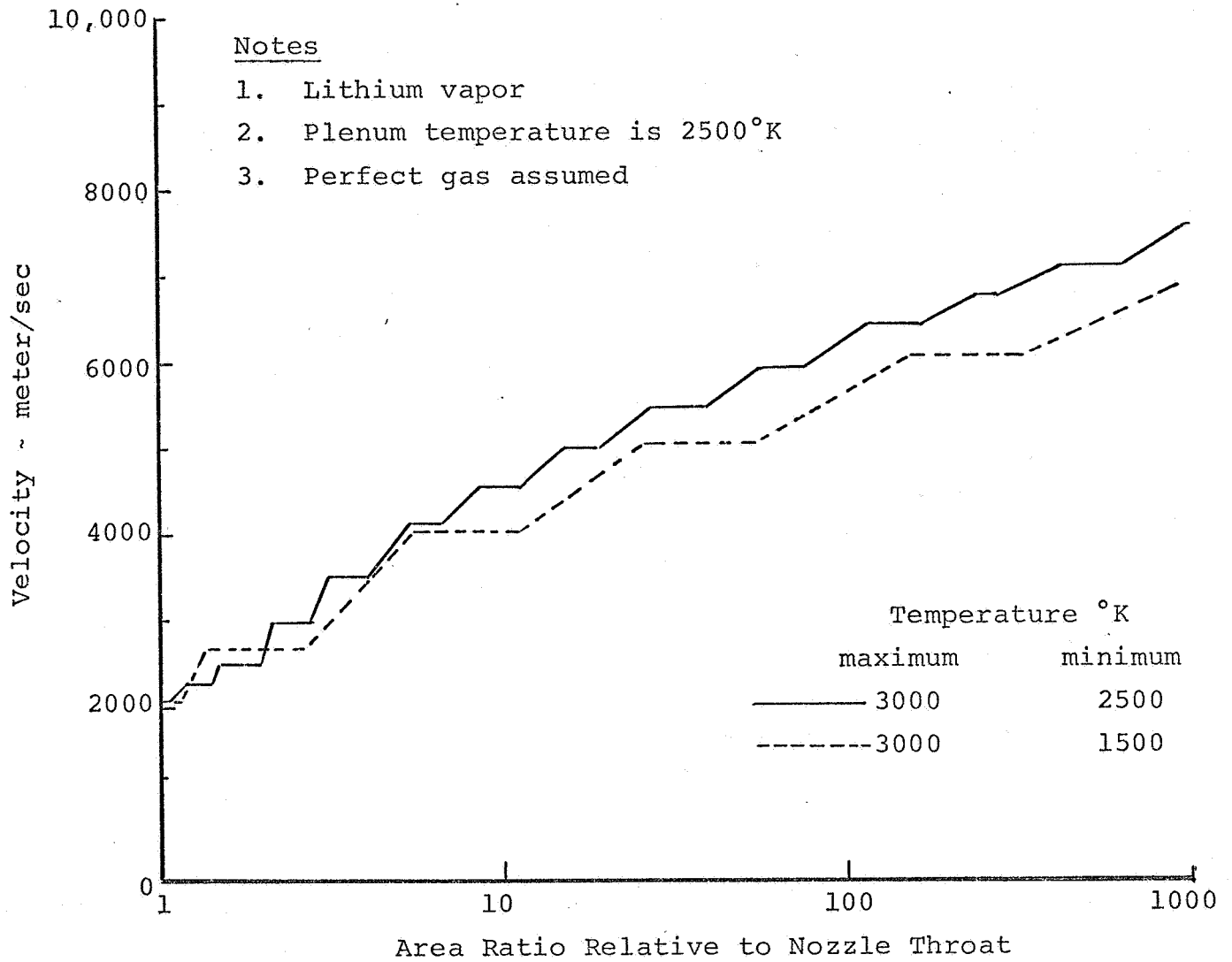


FIG. 3.8 - Heat Addition to Supersonic Nozzle with Constant Velocity Heating - No Heating Expansion Velocity Versus Area Ratio.

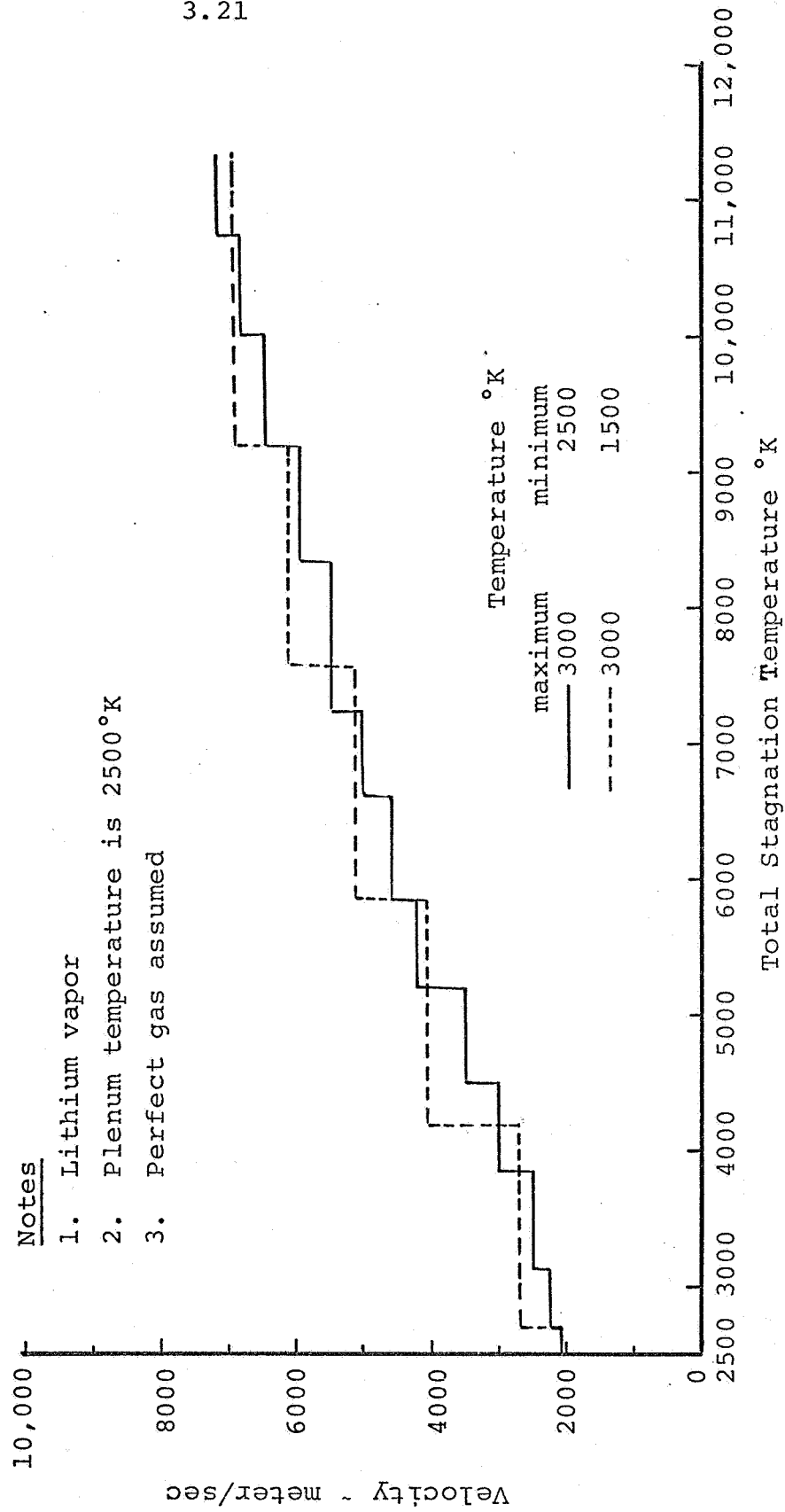


FIG. 3.9 - Heat Addition to Supersonic Nozzle with Constant Velocity Heating - No Heating Expansion Velocity Versus Stagnation Temperature

## APPENDIX

Listing of the Computer Codes Used in this Report.

Nozzle Code For:	Page No.
Optimization Using Steepest Descent Method	3.23
Linear-Heated Expansions Between Non-Heated Expansions	3.27
Constant-Velocity-Heated Expansions Between Non-Heated Expansions	3.31

CODE FOR OPTIMIZATION USING  
STEEPEST DESCENT METHOD

```

*FORTRAN
PROGRAM SYSDE
C THIS PROGRAM IS TO MAXIMIZE VELOCITY BY METHOD OF STEEPEST DESCENT
C M NO OF STATE VARIABLES
C N NO OF POINTS CALCULATED
C NC NO OFCONSTANTS CP,R,MASS,DO=INITIAL DIA.,ETC,
C ITH COUNTER
C Y,S ARE STATE VARIABLES
C FY,S ARE DERIVATIVE w.r.t. DISTANCE
C BETHA=ADOT/A ISCONTROL
C SUBROUTINE FUNC IS SET OF D.E. OF STATE VARIABLES
C SUBROUTINE FUNC1 IS SET OF D.E. ADJOINT TO FIRST SET
C SUBROUTINE FUNC2 IS THE FIRST SET AFTER CHANGE IN CONTROL VARIABLE
C SUBROUTINE RUDSY IS TO INTEGRATE ALONG DISTANCE
DIMENSION YS(10),Y(10),FY(10),C(30),HED(8),SOL(600,5),DSOL(600,5),
1 I TOL(600,5),R(600),BET(600)
COMMON C,Y,YS,FY,ITH,SOL,DSOL,TOL,BETHA,AK,B,BET
FINISH=6HFINISH
2 READ 100,HED
IF(FINISH-HED(1))4,20,4
4 PRINT 101,HED
READ 102,M,N,NC,ITH
PRINT 107,ITH
IF(NC)6,8,5
6 READ 103,(C(I),I=1,NC),C(17),C(18),C(19),C(20)
8 READ 103,H,X,(Y(I),I=1,M)
PRINT 104
PRINT 105
GO TO (10,12,13,12,13,12,13),ITH
10 CALL FUNC(FY,Y,X,C,M,BETHA)
PRINT 110,X,BETHA,FY(4),(Y(J),J=1,M)
DO 19 J=1,M
SOL(1,J)=Y(J)
19 DSOL(1,J)=FY(J)
GO TO 14
12 L=581
46 CALL FUNC1(FY,Y,X,C,SOL,DSOL,L,B,BET)
DO 21 J=1,4
21 TOL(L,J)=Y(J)
HAMIL=TOL(L,1)*DSOL(L,1)+TOL(L,2)*DSOL(L,2)+TOL(L,3)*DSOL(L,3)+TOL
1(L,4)*DSOL(L,4)+TOL(L,5)*DSOL(L,5)
PRINT 110,X,HAMIL,FY(4),(Y(J),J=1,M)
14 CALL RUDSY(M,N,X,H)
GO TO 2
13 AK=.00000001
IK=1
17 CALL FUNC2(FY,Y,X,C,SOL,DSOL,TOL,[K,AK,BETHA,B,BET)
PRINT 109,AK
PRINT 110,X,BETHA,FY(4),(Y(J),J=1,M)
DO 57 J=1,M
SOL(1,J)=Y(J)
57 DSOL(1,J)=FY(J)
CALL RUDSY(M,N,X,H)

```



```

      GO TO 2
    20 CALL EXIT
    100 FORMAT(8A10)
    101 FORMAT(1H1,8A10)
    102 FORMAT(4I4)
    103 FORMAT(8F10.0)
    104 FORMAT(1H0,10X,*RESULTS*/)
    105 FORMAT(1H0,5X,1HX,10X,5HBETHA,5X,5HQDERI,9X,1HV,12X,1HT,14X,1HA,16
      1X,1HQ,16X,1HS)
    107  FORMAT (I4)
    108  FORMAT(1H ,*DERIV*,5X,5E15.7)
    109  FORMAT(* AK=*,F12.8)
    106  FORMAT(1H0,*VAR*,F7.3,5E15.7)
    110  FOKMAT(1H0,F7.3,2X,F12.3,2X,E15.5,2X,5E15.7)
      END

```

```

      SUBROUTINE RUDESY(M,N,X,H)
      DIMENSION Y(10),YS(10),FY(10),C(30) ,PK(4,10),SOL(600,5),DSOL(600,
      15),TOL(600,5),B(600),BET(600)
      COMMON C,Y,YS,FY,ITH,SOL,DSOL,TOL,BETHA,AK,B,BET
      KJ=0
      DO 30 IK=1,N
        I=IK+1
    16  X1=X
        DO 2 J=1,M
          2  YS(J)=Y(J)
          DO 10 K=1,4
            RK=(K+1)/2
          3  GO TO (1,3,7,3,7,3 ,7),ITH
            L=5H2-(IK+K/2)+1
            CALL FUNC1(FY,YS,X,C,SOL,DSOL,L,B,BET)
            GO TO 5
          7  CALL FUNC2(FY,YS,X,C,SOL,DSOL,TOL,IK,AK,BETHA,B,BET)
            GO TO 5
          1  CALL FUNC(FY,YS,X,C,M,BETHA)
          5  DO 4 J=1,M
            4  PK(K,J)=FY(J)*H
            GO TO (90,91,90,91,90,91,90),ITH
          91  IF(K=4) 65,75,75
          65  DO 85 J=1,M
          85  YS(J)=Y(J)-(PK(K,J)/2)*RK
            GO TO (40,35,40,35,40,35,40),ITH
          90  IF(K=4) 5,12,12
            5  DO 8 J=1,M
            8  YS(J)=Y(J)+(PK(K,J)/2.)*RK
            GO TO (40,35,40,40,40,35,40),ITH
          40  X=X1+(H/2.)*RK
            GO TO 10
          35  X=X1-(H/2.)*RK
          10  CONTINUE
          75  DO 28 J=1,M
          28  Y(J)=Y(J)-(PK(1,J)+2.*PK(2,J)+2.*PK(3,J)+PK(4,J))/6.
            GO TO (18,15,17,15,17,15,17),ITH
          12  DO 14 J=1,M
          14  Y(J)=Y(J)+(PK(1,J)+2.*PK(2,J)+2.*PK(3,J)+PK(4,J))/6.
            GO TO (18,15,17,15,17,15,17),ITH
          18  CALL FUNC(FY,Y,X,C,M,BETHA)
            X=X1+1

```

```

IF(KJ-7)213,215
215 PRINT 110,X,BETHA,FY(4),(Y(J),J=1,M)
    KJ=0
213 DO 19 J=1,M
    SOL(I,J)=Y(J)
    19 DSOL(I,J)=FY(J)
    GO TO 30
    15 CALL FUNC1(FY,Y,X,C,SOL,DSOL,L,B,BET)
    KJ=KJ+1
    IF(KJ-7)214,216
216 PRINT 110,X,HAMIL,FY(4),(Y(J),J=1,M)
    KJ=0
214 DO 25 J=1,M
25 TOL(L,J)=Y(J)
    HAMIL=TOL(L,1)*DSOL(L,1)+TOL(L,2)*DSOL(L,2)+TOL(L,3)*DSOL(L,3)+TOL
    1(L,4)*DSOL(L,4)+TOL(L,5)*DSOL(L,5)
    GO TO 30
    17 CALL FUNC2(FY,Y,X,C,SOL,DSOL,TOL,IK,AK,BETHA,B,BET)
    KJ=KJ+1
    IF(KJ-7)217,218
218 PRINT 110,X,BETHA,FY(4),(Y(J),J=1,M)
    KJ=0
217 DO 57 J=1,M
    SOL(I,J)=Y(J)
    57 DSOL(I,J)=FY(J)
    30 CONTINUE
    55 RETURN
    103 FORMAT(8F10.0)
106 FORMAT(1H0,*VAR*,F7.3,5E15.7)
108 FORMAT(1H ,*DERIV*,5X,5E15.7)
    110 FORMAT(1H0,F7.3,2X,F12.3,2X,E15.5,2X,5E15.7)
    .END

```

```

SUBROUTINE FUNC(FY,Z,X,C,M,BETHA)
    DIMENSION FY(10),Z(10),C(30)
    Z(3)=((C(1)+X*C(2))**2)/(C(1)*C(1))
    DAX=(2.*C(2)*(C(1)+X*C(2)))/(C(1)*C(1))
    BETHA=DAX/Z(3)
    DQX=(1.E+10)*BETHA
    AMAC2=((Z(1)*Z(1))/(C(6)*C(19)*Z(2)))
    FY(1)=Z(1)*(1./(1.-AMAC2))*(DQX/(C(7)*Z(2))-BETHA)
    FY(2)=Z(2)*((1.-C(6)*AMAC2)/(1.-AMAC2))*(DQX/(C(7)*Z(2))-BETHA)+
    IZ(2)*BETHA
    FY(3)=BETHA*Z(3)
    FY(4)=DQX
    FY(5)=DQX/Z(2)
    RETURN
    END

```

```

SUBROUTINE FUNC1(FY,Z,X,C,SOL,DSOL,L,B,BET)
    DIMENSION FY(10),Z(10),C(30),SOL(600,5),DSOL(600,5),B(600),BET(600
    1)
    BETHA=DSOL(L,3)/SOL(L,3)
    BET(L)=BETHA
    AM=SQRT((SOL(L,1)*SOL(L,1))/(C(6)*C(19)*SOL(L,2)))
    AM2=AM*AM
    C(21)=1./(1.-AM*AM)
    C(22)=(DSOL(L,4))/(C(7)*SOL(L,2))
    C(23)=(1.-C(6)*AM2)/(1.-AM2)
    B(L)=(AM2)

```

```

C(24)=(DSOL(L,3))/(SOL(L,3)*SOL(L,3))
DQA=(1.E+10)*(-DSOL(L,3)/(SOL(L,3)*SOL(L,3)))
DSA=(1./SOL(L,2))*DQA
FY(1)=-1.*C(21)*(C(22)-BETHA)*Z(1)
FY(2)=SOL(L,1)*C(21)*(1./SOL(L,2))*C(22)*Z(1)+(C(23)*BETHA+BETHA)*
1Z(2)+(DSOL(L,4)/(SOL(L,2)*SOL(L,2)))*Z(5)
FY(3)=-SOL(L,1)*C(21)*(DSOL(L,3)/(SOL(L,3)*SOL(L,3)))*Z(1)-(SOL(L,
12)*C(23)*C(24)-SOL(L,2)*C(24))*Z(2)-BETHA*Z(3)-DQA*Z(4)-DSA*Z(5)
FY(4)=0.0
FY(5)=0.0
RETURN
END

```

```

SUBROUTINE FUNC2(FY,Z,X,C,SOL,DSOL,TOL,I,AK,BETHA,B,BET)
DIMENSION FY(10),Z(10),C(30),SOL(600,5),TOL(600,5),B(600),BET(600)
DQB=5.*(1.E+10)
DELB=AK*(-(SOL(I,1)/(1.-B(I)))*TOL(I,1)+SOL(I,2)*TOL(I,2)*(1.-(1.-
1C(6)*B(I))/(1.-B(I)))+SOL(I,3)*TOL(I,3)+DQB*TOL(I,4)+(1./SOL(I,2))
1*DQB*TOL(I,5))
BET(I)=BET(I)+DELR
BETHA=BET(I)
DAX=BETHA*Z(3)
DQX=(1.E+10)*BETHA
AMAC2=((Z(1)*Z(1))/(C(6)*C(19)*Z(2)))
FY(1)=Z(1)*(1./(1.-AMAC2))*(DQX/(C(7)*Z(2))-BETHA)
FY(2)=Z(2)*((1.-C(6)*AMAC2)/(1.-AMAC2))*(DQX/(C(7)*Z(2))-BETHA)+
1Z(2)*BETHA
FY(3)=BETHA*Z(3)
FY(4)=DQX
FY(5)=DQX/Z(2)
RETURN
END

```

## CODE FOR LINEAR HEATED EXPANSIONS BETWEEN NON-HEATED EXPANSIONS

\*FORTRAN

```

PROGRAM NOZZEL
COMMON I, NC, J, AR, TR, TT, STO, DELTO, K, XMN, VX, V1, V2, VO, VR, ARO, TRO, V, T1
COMMON NP, AMC, XAMC, EX, T01, CPG, R, XK, XNUM, C, AMO, E, NK, DAR, N, AM
COMMON TMAX, TMIN
COMMON XL1, XL2, DL1, DL2, RP21, RP021
C EX=CONVERGENCE EXPONENT ON MACH NO.
C NK=NO. OF C VALUES
C NP=NO. OF COMPUTATION BETWEEN OUTPUT
C NC=TOTAL NO OF COMPUTED POINTS
C T0=INITIAL STAGNATION TEMPERATURE (INPUT)
C AM2= M SQUARED
C E=ERROR IN MACH NO. ALLOWED
C AMO=INITIAL COMPUTED MACH NUMBER, M
C DAR=(A1+1/A1)-(A1/A1-1) CHANGE IN AREA RATIO
C C=D(A2/A1)/D(T02/T01)
C XK=SPECIFIC HEAT RATIO
C NK=NUMBER OF C VALUES USED
C ARO=A1/A0
C TRO=T01/T00
C AR=A2/A1
C VR=V2/V1
C TR=T02/T01
C AMC=COMPUTE MACH NUMBER
C AM=INITIAL ASSUMED VALUE=AMC(I-1)
C INITIAL RATIOS OF AREA, TEMP, VELOCITY
C INTERVALS OF AREA AND TEMP RATIOS
C AMBAR=AVE MACH NO.
C STO=INLET STAGNATION TEMPERATURE OF THE INCREMENT
C TMAX=MAXIMUM STATIC TEMPERATURE IN SUPERSONIC SECTION OF NOZZLE
C TMIN=MINIMUM STATIC TEMPERATURE IN SUPERSONIC SECTION OF NOZZLE
C TT=STATIC TEMPERATURE INLET OF INCREMENT
C DELTO = CHANGE IN STAGNATION TEMPERATURE IN INCREMENT
C XMN=INLET TO INCREMENT MACH NUMBER
C VX=INLET VELOCITY
C DELV IS THE CHANGE IN VELOCITY IN THE INCREMENT
C VELSLOP IS THE CHANGE (DELV /DELTO)
C P10=P1/P01
C P21=P2/P1
C P021=P02/P01
! DIMENSION HED(8)
! READ 100, NHED, NPROB
DO 60 LP=1, NPROB
! READ(5,40) TMAX, TMIN
40 FORMAT(2F10.3)
! DO 2 I=1, NHED
! READ 103, HED
2 PRINT 104, HED
! WRITE(6,41) TMAX, TMIN
41 FORMAT(* TMAX=*F10.1,* TMIN=*F10.1)
! READ 101, XK, XMOLWT, G
R=8314.32/XMOLWT
CP=(XK*R)/(XK-1)
CPG=2.*CP*G
XNUM=(XK-1.)/2.
! READ 101, AMO, T0
T=T0/(1.+((XK-1.)/2.)*AMO*AMO)
CO=SQRT(XK*R*T)
VO=AMO*SQRT(XK*T*R)
! READ 101, F, EX

```

```

READ100,NK
64 DO60 N=1,NK
READ100,NC,NP
READ101,C,DAR
DTR=C*DAR
P10=1./(1.+XNUM*AMO*AMO)**(XK/(XK-1.))
PRINT102,C,DAR,E,AMO,T,TU ,P10
ARO=1.
ARO=(1.0/AMO)*((2.0/(XK+1.))* (1.+XNUM*AMO*AMO))
1**((XK+1.)/(2.*(XK-1.0)))
TRO=1.
AR=1.
VR=1.
TR=1.
AMC=AMO
AM=AMO
T1=T
V1=V0
T01=T0
VX=V0
K=NP
J=0
149 WRITE(6,150)
150 FORMAT(* TT VI V T1 DELV P2/P1
1 PO2/P01 AR XMN STO VR ARO
2 TRO *,1H0)
IF(T1.GT. TMAX ) CALL NONHET
WRITE(6,303)
10 DO60 I=1,NC
GO TO 301
300 WRITE (6,110)
GO TO 140
301 AR=AR+DAR
TR=AR**(1./C)
TT=T01-(VX**2)/CPG
STO=T01
T01=T01*TR
DELTO=(T01-STO)
K=K+1
KM=0
LM=1
XMN=VX/SQRT(XK*R*TT)
12 AMBAR=(AMC+AM)/2.
AM2=AMBAR*AMBAR
AM1=1./(1.-AM2)
KM=KM+1
V=VX*((1./(AM2-1.))*(AR-1.-(1.-XNUM*AM2)*(TR-1.))+1.)
T1=T01-(V*V)/CPG
XAMC=V/SQRT(XK*R*T1)
10 IF(ABS(XAMC-AMC)-E)30,30,20
20 AMC=XAMC*(AMC/XAMC)**EX
IF(KM-15)12,22,22
22 IF(LM-20) 24,24,70
24 LM=LM+1
EX=EX/2.
GO TO 12
30 ARO=ARO*AR
TRO=TRO*TR
P21=(1./ARO)*(AMO/AMC) *SQRT((1.+XNUM*AMO*AMO)/(1.+XNUM*AMC*AMC))
1*SQRT(TRO)
PO21=P21*((1.+XNUM*AMC*AMC)/(1.+XNUM*AMO*AMO))** (XK/(XK-1.))
199 PRINT 201,TT,VX,V,T1,DELV,P21 ,PO21 ,AR, XMN,STO,VR,ARO,TRO
201 FORMAT (1H ,5F10.3,8F10.4 )

```

```

      AM=AMC
      DELV=V-VX
32    VR=V/VO
      VX=V
      K=0
      IF(ARO.GT. 1000.0) GO TO 64
      J=J+1
      IF(11.GT. TMAX ) GO TO 65
      IF(J.EQ. 58) GO TO 300
60    CONTINUE
      65 CALL NONHET
      WRITE(6,303)
      GO TO 10
      70 PRINT108,XAMC,AMC
      GO1064
      303 FORMAT (*           LINEAR HEAT ADDITION *)
      100 FORMAT(1I4)
      101 FORMAT(4F10.0)
      102 FORMAT(1H1,3H C=,F8.3,4X,5H DAR=,F8.7,4X,3H E=,F8.7,4X,5H AMO=,F5.
      13,4X,3H T=,F8.3,4X,4H TO=,F8.3      ,4X,5H P10=,F8.3)
      103 FORMAI(8A10)
      104 FORMAT(1H0.8A10)
      108 FORMAT(2BHOMFAILSTOCONVERGEWITHFINALM=,F10.5,11H ASSUMEOM=,F10.5)
      110 FORMAT(1H1)
      END

```

```

SUBROUTINE NONHET
COMMON I,NC,J,AR,TR,TI,STO,DELTO,K,XMN,VX,V1,V2,V0,VR,ARO,TRO,V,T1
COMMON NP,AMC,XAMC,EX,T01,CPG,R,XK,XNUM,C,AMO,E,NK,DAR,N,AM
COMMON TMAX,TMIN
COMMON XL1,XL2,DL1,DL2,RP21,RP021
DTIM=1.0E-6
WRITE(6,400)
400 FORMAT( * NO HEAT ADDITION EXPANSION )
GO TO 10
149 WRITE(6,150)
J=0
150 FORMAT(*      TT      VI      V      T1      DELV      P2/P1
1      P02/P01      AR      XMN      STO      VR      ARO
2      TRO *,1H0)
10 DO60 I=1,NC
GO TO 301
300 WRITE (6,110)
GO TO 149
301 AR=AR+DAR
TR=1.0
TI=T01-(VX**2)/CPG
STO=STO
T01=T01*TR
DELTO=(T01-STO)
K=K+1
KM=0
LM=1
XMN=VX/SQRT(XK*R*TI)
12 AMBAR=(AMC+AM)/2.
AM2=AMBAR*AMBAR
AM1=1./(1.-AM2)
KM=KM+1
V=VX*((1./(AM2-1.))*(AR-1.))+1.
T1=T01-(V*V)/CPG
XAMC=V/SQRT(XK*R*T1)
16 IF (ABS(XAMC-AMC)-E) 30,30,20
20 AMC=XAMC*(AMC/XAMC)**EX
IF(KM-15) 12,22,22
22 IF(LM-20) 24,24,70
24 LM=LM+1
EX=EX/2.
GOTO 12
30 ARO=ARO*AR
TRO=TRO*TR
P21=(1./ARO)*(AMO/AMC) *SQRT((1.+XNUM*AMO*AMO)/(1.+XNUM*AMC*AMC))
1*SQRT(TRO)
P021=P21*((1.+XNUM*AMC*AMC)/(1.+XNUM*AMO*AMO))**((XK/(XK-1.))
199 PRINT 201,TT,VX,V,T1,DELV,P21 ,P021 ,AR,XMN,STO,VP,ARO,TRO
201 FORMAT (1H ,5F10.3,8F10.4 )
32 VR=V/V0
DELV=V-VX
AM=AMC
VX=V
K=0
J=J+1
IF(T1.LT. TMIN ) GO TO 500
IF(ARO.GT.10000.0) GO TO 500
IF(J.EQ. 58) GO TO 300
60 CONTINUE
70 PRINT10R,XAMC,AMC
108 FORMAT(2BHOMFAILSTOCONVERGEWITHFINALM=F10.5,11H ASSUMEDM=F10.5)
110 FORMAT(1H1)
500 RETURN

```

CODE FOR CONSTANT VELOCITY HEATED EXPANSIONS  
BETWEEN NON-HEATED EXPANSIONS

\*FORTRAN

```

PROGRAM CVNONH
C   CVNONH IS A PROGRAM FOR COMPUTING HEAT ADDITION UNDER CONSTANT VEL
C   OCITY AND NON HEAT ADDITION EXPANSION
C   PROGRAM FOR STUDYING HEAT ADDITION TO SUPERSONIC NOZZLES
C   AM=INIAL ASSUMED VALUE=AMC(I-1)
C   AMBAR=A VE MACH NO.
C   AMC=COMPUTE MACH NUMBER
C   AMO=INITIAL COMPUTED MACH NUMBER,M
C   AM2= M SQUARED
C   AR=A2/A1
C   ARO=A1/A0
C   C=D(A2/A1)/D(T02/T01)
C   CP=SPECIFIC HEAT
C   DAR=(A1+1/A1)-(A1/A1-1) CHANGE IN AREA RATIO
C   DELTO = CHANGE IN STAGNATION TEMPERATURE IN INCREMENT
C   DELVIS THE CHANGE IN VELOCITY IN THE INCREMENT
C   E=ERROR IN MACH NO. ALLOWED
C   EX=CONVERGENCE EXPONENT ON MACH NO.
C   J=AREA RATIO INDEX
C   K=TEMP RATIO INDEX
C   NC=TOTAL NO OF COMPUTED POINTS
C   NK=NO. OF C VALUES
C   NP=NO. OF COMPUTATION BETWEEN OUTPUT
C   P10=P1/P01
C   P21=P2/P1
C   P021=P02/P01
C   ST0=INLET STAGNATION TEMPERATURE OF THE INCREMENT
C   T0=INITIAL STAGNATION TEMPERATURE (INPUT)
C   T1=STATIC TEMP AT AREA,A1,DEG K
C   T2=STATIC TEMP AT AREA,A2,DEG K
C   T01=STAGNATION TEMP BEFORE HEAT ADDITION, K
C   T02=STAGNATION TEMP AFTER HEAT ADDITION, K
C   TR0=T01/T00
C   MOLWT=MOLECULAR WT OF FLUID
C   V1=INITIAL VELOCITY BEFORE HEAT ADDITION,METER/SEC
C   V2=FINAL VELOCITY AFTER HEAT ADDITION, METERS/SEC
C   VELSLOP IS THE CHANGE (DELV /DELTO)
C   VR=V2/V1
C   TR=T02/T01
C   XK=SPECIFIC HEAT RATIO
C   XM1=INITIAL MACH NO BEFORE HEAT ADDITION OF AREA CHANCE.
C   XM2=FINAL MACH NO AFTER HEAT ADDITION AND AREA CHANGE
COMMON AM,AR,AMO,ARO,C,CP,CPG,DAR,DELV,DELTO,E,EX,I,J,NC,NP,NK,N
COMMON P10,P21,P021,R,ST0,T01,T02,TR,T1,T2,TR0,V,VX,V1,V2,V0,VR
COMMON VELSLOP,RELDV,XK,XNUM,XM1,XM2,XMOLWT,TMAX,TMIN,AMC
DIMENSIONHED(8)
READ100,NHED,NPROB
DO60 LP=1,NPROB
DO2 I=1,NHED
READ103,HED
2 PRINT104,HED
READ101,XK,XMOLWT,G
R=8314.32/XMOLWT

```



```

3.32
102 FORMAT(1H ,3H C=,F8.3,4X,5H DAR=,F8.7,4X,3H E=,F8.7,4X,5H AMO=,F7.
13,4X,3H T=,F8.3,4X,4H TO=,F8.3 ,4X,5H P10=,F8.3)
103 FORMAT(2A10)
104 FORMAT(1H0,8A10)
106 FORMAT(1H 10X,6F15.7,2I8,F15.5)
CP=(XK*K)/(XK-1)
CPG=2.*CP*G
XNUM=(XK-1.)/2.
READ101,AMO,TO
T=TO/(1.+((XK-1.)/2.)*AMO*AMO)
CO=SQRT(XK*R*T)
VO=AMO*SQRT(XK*T*R)
READ101,E,EX,DAR
READ 100,NK
64 DO60 N=1,NK
READ101,TMAX,TMIN
P10=1./(1.+XNUM*AMO*AMO)**(XK/(XK-1.))
ARO=(1.0/AMO)*((2.0/(XK+1.))*(1.+XNUM*AMO*AMO))
1**((XK+1.)/(2.*(XK-1.0)))
WRITE(6,55) TMAX,TMIN,AMO
55 FORMAT(6H TMAX=F10.3,5HTMIN=F10.3,4HAMO=F10.3)
TRO=1.
AR=1.
VR=1.
TR=1.
AMC=AMO
AM=AMO
T1=T
V1=VO
T01=TO
VX=VO
K=NP
09 WRITE(6,10)
10 FORMAT(1H1,*SUPERSONIC NOZZLE WITH HEAT ADDITION STUDY*)
149 WRITE(6,150)
150 FORMAT(* T1 V1 V2 T2 DELV P2/P1
1 P02/P01 AR XM1 STO VR ARO
2 TRO *,1H0)
PRINT102,C,DAR,E,AMO,T,TO ,P10
WRITE(6,303)
I=1
DO 20 I=1,60
IF(1.EQ.60)GO TO 9
77 IR=TR+0.001
CALL CONVEL
STO=T01
P21=(1./ARO)*(AMO/XM2) *SQRT((1.+XNUM*AMO*AMO)/(1.+XNUM*XM2*XM2))
1*SQRT(TRO)
P021=P21*((1.+XNUM*XM2*XM2)/(1.+XNUM*AMO*AMO))**((XK/(XK-1.))
199 PRINT 201,T1,VX,V,T2,DELV,P21 ,P021 ,AR,XM1,STO,VR,ARO,IRO
201 FORMAT(1H ,13F10.4)
T1=T2
T01=T02
IF(ARO.GT.10000.0) GO TO 64
IF(T2.LT. IMIN) GO TO 77
IF(XM2 .LT.1.05) CALL NONHET
IF(T2.GT.TMAX) CALL NONHET
WRITE(6,303)
303 FORMAT(* CONSTANT VELOCITY HEAT ADDITION *)
108 FORMAT(2RHOMPFALSTOCONVERGEWITHFINALM=,F10.5,11H ASSUMEDM=,F10.5)
110 FORMAT(1H1)
60 CONTINUE

```

```

20 CONTINUE
100 FORMAT(3I4)
101 FORMAT(4F10.0)
END

SUBROUTINE CONVEL
COMMON AM,AR,AM0,ARO,C,CP,CPG,DAR,DELV,DELTO,E,EX,I,J,NC,NP,NK,N
COMMON P10,P21,PO21,R,STO,f01,f02,TR,T1,T2,TRO,v,vx,v1,v2,v0,VR
COMMON VEL SOP,RELDV,XK,XNUM,XM1,XM2,XMOLWT,TMAX,TMIN,AMC
C CALCULATION OF NOZZLE PERFORMANCE WITH HEAT ADDITION AND AREA
C CHANGE REQUIRED TO HOLD CONSTANT VELOCITY
C1=(V1*V1)/(2.*CP)
T02=T01*TR
XM1=V1/SQRT(XK*T1*R)
T2=T02-C1
XM2=V1/SQRT(XK*T2*R)
XMA=(XM1+XM2)/2.
AR=(TR)**(1.+(XK-1.)/2.)*XMA*XMA
ARO=ARO*AR
DELTO=T02-T01
TRO=TRO*TR
DELTO=(T02-T01)
V2=V1
VELSOP=0.0
DELV=0.0
RELDV=0.0
VR=0.0
RETURN
END

```

```

SUBROUTINE NONHET
COMMON AM,AR,AM0,ARO,C,CP,CPG,DAR,DELV,DELTO,E,EX,I,J,NC,NP,NK,N
COMMON P10,P21,PO21,R,STO,f01,f02,TR,T1,T2,TRO,v,vx,v1,v2,v0,VR
COMMON VEL SOP,RELDV,XK,XNUM,XM1,XM2,XMOLWT,TMAX,TMIN,AMC
AMC=XM2
AM=XM2
VX=V2
149 WRITE(6,150)
150 FORMAT(* T1 V1 V2 T2 DELV P2/P1
1 PO2/P01 AR XM1 STO VR ARO
2 TRO *,1H0)
J=0
WRITE(6,400)
400 FORMAT(* NO HEAT ADDITION EXPANSION *)
10 DO 60 Ix=1,100
DO 60 J=1,60
IF(J.EQ. 60) GO TO 149
301 AR=AR+DAR
T1=T01-(VX**2)/CPG
STO=T01
K=K+1
KM=0
LM=1
XM1=VX/SQRT(XK*R*T1)
12 AMBAR=(AMC+AM)/2.
AM2=AMBAR*AMBAR
AM1=1./(1.-AM2)
KM=KM+1

```

```

V=VX*((1./(AM2-1.))*(AR-1.)+I.)
T2=T01-(V*V)/CPG
XAMC=V/SQRT(XK*R*T2)
16 IF(ABS(XAMC-AMC)-E)30,30,20
20 AMC=XAMC*(AMC/XAMC)**EX
   IF(KM=15)12,22,22
22 IF(LM=20)24,24,70
24 LM=LM+1
   EX=EX/2.
   GOTO12
30 ARO=ARO*AR
   P21=(1./ARO)*(AM0/AMC)*SQRT((1.+XNUM*AM0*AM0)/(1.+XNUM*AMC*AMC))
1*SQRT(TRO)
   PO21=P21*((1.+XNUM*AMC*AMC)/(1.+XNUM*AM0*AM0))**(XK/(XK-1.))
   AM=AMC
   DELV=V-VX
199 PRINT 201,T1,VX,V,T2,DELV,P21,PO21,AR,XM1,STO,VR,ARO,TRO
201 FORMAT(1H,13F10.2)
32 VR=V/VO
   VX=V
   K=0
   IF(T2.LT. IMIN) GO TO 500
   IF(ARO.GT.10000.0) GO TO 500
60 CONTINUE
70 PRINT108,XAMC,AMC
   GO TO 10
100 FORMAT(3I4)
101 FORMAT(4F10.0)
102 FORMAT(1H1,3H C=,F8.3,4X,5H DAR=,F8.7,4X,3H E=,F8.7,4X,5H AM0=,F7.
1,4X,3H T=,F8.3,4X,4H T0=,F8.3,4X,5H P10=,F8.3)
103 FORMAT(8A10)
104 FORMAT(1H0,8A10)
106 FORMAT(1H 10X,6F15.7,2I8,F15.5)
108 FORMAT(28H0MFAILSTOCONVERGEWITHFINALM=,F10.5,11H ASSUMEDM=,F10.5)
110 FORMAT(1H1)
500 V1=V
   RETURN
   END

```

MEASUREMENT OF NEUTRAL-ATOM SPEED  
IN BOMBARDMENT THRUSTERS

by Richard Moore

During this grant period several changes were made in order to improve the experiment. A larger d.c. motor with three times the power rating of the original motor was purchased to drive the velocity selector. This was necessary because it was found that the smaller motor would not start the selector from rest in the vacuum chamber unless the selector bearings has just been lubricated<sup>4.1</sup>. With the new motor installed no more problems have been encountered with the velocity selector. The new motor will drive the selector up to speeds of 12,000 RPM. This means that in order for a mercury atom with an average speed, given by  $(2.55kT/m)^{1/2}$ , to get through the velocity selector, the temperature of the gas would have to be  $\approx 4000^\circ\text{K}$ . Therefore, if the neutral gas is at the temperature of the thruster walls, which is  $\approx 500^\circ\text{K}$ , the velocity selector will stop all but a small fraction of the mercury atoms which make up the beam from the thruster.

In order to detect the number of molecules which make it through the selector an ion gauge and lock-in amplifier are being used. The function of the lock-in amplifier<sup>4.2</sup> is to pick out a weak signal which is superimposed on top of a large unwanted signal. This is accomplished by making the desired signal along with a reference signal, usually a photo cell and light source, appear at a certain frequency and phase angle. The lock-in amplifier is then set to look at the frequency at which the signal will appear. Since most of the unwanted signal will have random frequencies and phase angles, only the desired signal along with a small component of noise, which appears at the set frequency, should be recorded.

In our case the flux of neutral atoms from the thruster is first chopped at a frequency of 330 C.P.S. Then atoms move on through the velocity selector into the ion gauge where a

fraction of them are ionized. The signal from the ion gauge is sent to the lock-in amplifier where the desired information is recorded on strip chart paper.

When the above set up was first run, the lock-in amplifier did not function correctly. In order to determine if this was a fault of the amplifier, a high intensity beam was produced which could be easily measured. The beam was produced by closing off the front end of the thruster and introducing argon gas into the thruster at a flow rate of  $\approx 5 \times 10^{17}$  molecules/sec with the discharge off. When equilibrium in the thruster is obtained, the flow in equals the flow out. Of the total flow out of the thruster only  $7.8 \times 10^{14}$  molecules/sec make up the beam which enters the ion gauge. This is compared to a flux of  $10^{12}$  molecules/sec when the thruster is operated with no cover on the front. A mechanical shutter was placed in such a position that the beam can be turned off and on by hand.

The lock-in amplifier was then operated using the intense beam. It still did not work correctly. It was later found that the chassis of the lock-in amplifier was not grounded correctly. When this was corrected a signal of 100 microvolts was obtained, using an emission current of 8 ma in the ion gauge. The signal was due to beam molecules because when the shutter was placed in front of the beam the signal dropped by 100 microvolts. It has since been found that when the velocity selector is used, the signal from the lock-in amplifier does not behave the way it should. We are now at the point of trying to determine the reason and correct it. As a diagnostic tool, some rough measurements will be taken using the oscilloscope as the signal detector.

## REFERENCES

- 4.1. Advanced Electric Propulsion Research, Annual Report for the period January 1, 1968 to December 31, 1968. NASA Grant NGR06-002-032.
- 4.2. Foner, S. N.: Mass Spectrometry of Free Particles. Advances in Atomic and Molecular Physics, Vol. 2. Academic Press, New York, 1966.

AN ANALYSIS OF ELECTROSTATIC-SPRAYING FLUIDS IN  
TERMS OF THEIR ELECTROLYTIC SOLUTION CHARACTERISTICS

by V. Steadman and G. W. Tompkin

The study of the behaviour of electrolytic solutions at high electric fields is a valuable means of interpreting the results of electrostatic spraying experiments. The primary basis for thinking that one can isolate the contribution of the conductivity of the propellants in these experiments is furnished by Pfeifer's theory<sup>5.1</sup> and its agreement with experiment. In this theory, it is established that:

$$q_s \approx K \left[ \frac{\sigma(E_o) E_o}{\dot{M}} \right]^{\frac{3}{7}} \quad (5.1)$$

where

$$K = \left[ \left( \frac{4\pi}{\epsilon} \right)^2 \frac{(9\delta)^2 \epsilon_o^5}{\rho^4} \right]^{\frac{1}{7}}$$

$\dot{M}$  = mass flow rate,

$\delta$  = surface tension,

$\rho$  = density,

$E_o$  = electric field strength at the capillary tip,

$\sigma(E_o)$  = conductivity as a function of  $E_o$ .

For NaCl-doped glycerine, the empirical dependence of the specific charge  $q_s$  on  $\sigma(E_o)$  has been found to be<sup>5.2</sup>:

$$q_s = 6.5 \times 10^{-6} \left[ \frac{\sigma E_o}{\dot{M}} \right]^{0.575} \quad (5.2)$$

(Theoretically, for this Na-Cl glycerine system,  $K = 6.0 \times 10^{-6}$  in MKS units.) Such accuracy in the theory is fortuitous, but marked similarities between  $q_s$  as a function of  $E_o$  and conductivity as a function of  $E_o$  are expected in general. In fact, it appears that:

"Thorough understanding of electrostatic spraying requires thorough understanding of the ionic conduction at high fields. Excessive high field conductivity studies of doped organic solutions appear to be necessary."<sup>5.1</sup>

Problem areas in the generation of charged particles by electrostatic spraying in which knowledge of electrolyte behaviour is capable of aiding in analysis are:

- (1) inefficiency as evidenced by non-narrow particle distributions
- (2) factors which enhance the conductivity of a particular propellant at otherwise fixed system conditions
- (3) interferences which make a given propellant suitable for electrostatic spraying at only one needle potential polarity
- (4) inefficiency occurring from energy loss in the droplet extraction process.

There are two rather distinct aspects to the characteristics of propellants which affect their average charge-to-mass ratio and the beam efficiency  $\eta_s$ . These aspects are the tendency to form both ions and macromolecular charged particles under the same conditions and the tendency to produce several distinct species of charged colloid particles in a given beam. A correlation between the variation of the degree of ion (or aggregate) production with needle potential and changes in the numbers of ions (or aggregates) in a given solution with applied potential may be possible. Many observations<sup>5.3-5.5</sup> on the variation of  $q_s$  and  $\eta_s$  with needle potential in electrostatic spraying experiments indicate:

- (1) the number of ions in the beam increases with increasing potential, and
- (2) the beam efficiency decreases with increasing applied needle potential.

A good illustration of this situation is seen in Figure 5.1, taken from Ref. 5.5. (No research propellants at present have  $q_s$  and  $\eta_s$  values such that their points lie within the dotted "V" region.)



This increase in the number of ions with applied field agrees qualitatively with Onsager's ion-pair dissociation theory<sup>5,6</sup>. In the electrostatic spraying case, entities (not necessarily ion-pairs) which tend to form charged colloids increasingly "dissociate" at higher electric field strengths to form ions (or smaller ionic entities). The following equation, due to Onsager, indicates the increased conductivity to be expected with an increase in field strength in the case of ion-pairs:

$$\frac{\kappa}{\kappa_0} = 1 + \frac{e^3}{4\epsilon k^2 T^2} E, \quad (5.3)$$

where  $\kappa(\kappa_0)$  is specific conductivity at an electric field  $E$  ( $E_0$ ), and  $\epsilon$  is permittivity of the dielectric. There is an accompanying increase in ionic species since  $\frac{\Delta\kappa}{\kappa} = \frac{\Delta\alpha}{\alpha}$ , where  $\frac{\Delta\alpha}{\alpha}$  is the increase in the percentage of dissociated ion-pairs. By analogy then, one would expect the increase in average  $q_s$  to be accompanied by lowered beam efficiency (due to an increase in the relative number of different species present), as has been found. A propellant in which monotonicity in the relationships between applied needle potential,  $q_s$ , and beam efficiency exists is NaOH-glycerol. Partial data for this system are as follows<sup>5,4</sup>:

<u>Needle potential (kv)</u>	<u>Pressure ("Hg)</u>	<u><math>\eta_s</math> (%)</u>	<u><math>q_s</math></u>
6	10	89.2	157
7	10	81.5	295
8	10	73.9	516
9	10	69.9	770
10	10	70.0	871

Thus, whereas Pfeifer's theory only accounts for an overall increase in the average  $q_s$  with increasing potential, it may be further possible to account for the overall decrease in efficiency by consideration of electric-field-enhanced dissociation processes.

A case in which quite large distinct aggregates must be present in the beam is that of tetraethylammonium chloride (TEAC) in oleic acid ( $\langle q_s \rangle = 41.2$  coul/kg;  $\eta_s = 86\%$ <sup>5.5</sup>). Three distinct peaks corresponding to particles with small  $q_s$ 's have been found in the velocity distribution of this solution. Such a result is not surprising since ammonium salts with long hydrocarbon side-chains commonly form distinct polymer species in organic solutions<sup>5.7</sup>. The dipole moments and molecular radii of such species have been measured in some cases<sup>5.7</sup>. (A "molecular" radius of 25 Å and a dipole moment corresponding to a charge separation of 1.6 Å are typical of such aggregates<sup>5.7</sup>. The effects of most of the charges are cancelled by symmetry<sup>5.7</sup>.) Such species--or a tendency to form such aggregates in the developing droplet--may have led to the peculiar peaks mentioned above for TEAC-oleic acid. It would be of interest, then, to correlate the concentrations of various aggregates under non-electrostatic spraying conditions (but still high electric field) with those found to be present in the charged beam. Dipole absorption techniques superimposed on a d.c. electric field would allow one to determine variations in the size and types of these aggregates with increasing  $\vec{E}$ . (Dipole absorption occurs at megacycle frequencies for such aggregates. Due to the finite alignment time of the ionic atmosphere, one would not see increased conductivity (and possibly not increased dissociation) with increased applied  $\vec{E}$ , if only an a.c. field is present<sup>5.7</sup>.)

To find propellants which lie within the region of high efficiency for high  $q_s$  (the dotted "V" region in Figure 5.1), one must consider factors which favor an enhanced conductivity of one propellant over another at fixed system conditions. Electrolytes are known for which an increase in concentration greatly enhances the average  $q_s$  value but does not alter the efficiency. An example is NaI-glycerol, the data for which is as follows<sup>5.8</sup>:

<u>Needle dimensions (mil)</u>	<u>Conc. (g NaI/100 ml glycerol)</u>	<u>Needle potential</u>	<u><math>\langle q_s \rangle</math></u>	<u><math>\eta_s</math></u>
8 x 4	15	6kv	70 $\frac{\text{coul}}{\text{kg}}$	81%
"	20	"	5000 "	81%
"	20	6.3kv	8000 "	79%

This phenomenon should be even more enhanced for electrolytes which form micelles at and above a rather definite concentration region. For instance, in aqueous solutions, it has been found that  $2 \times 10^{-3}$  M solutions of cetylpyridonium chloride have a conductance 30% greater than that of solutions of the same salt at infinite dilution<sup>5.6</sup>. \* Similar increases in the conductance of  $\text{MgSO}_4$  in glycerol-water mixtures have also been attributed to micelle formation in the past<sup>5.6</sup>. \*\* The hypothesis is that multi-charged micelles make a greater contribution to conductance than a corresponding number of single ions on the basis of decreased overall viscosity effects<sup>5.6</sup>. Certainly such micelle solutions seem likely candidates for the production of high specific charge propellants with high beam efficiency. (The increase in conductivity seems to rule out the possibility that these micelles are actually multiple ion-pair aggregates, in which there is an overall cancellation of charges rather than a multiply-charged entity.)

A second factor which tends to increase the conductivity of a particular electrolytic solution is the ability to

---

\* The applied voltage was 200kv/cm for both aqueous solutions. The conductivity difference increases with applied field strength in accordance with usual results as the electric field is increased. Further, nonaqueous solutions are expected to exhibit much larger differences with increased electric field strength.<sup>5.2</sup> The field strength at the needle in electrostatic spraying experiments is estimated to be on the order of  $10^5$  V/cm for a 1kv applied needle potential. Cf. Ref. 5.1.

\*\*However, the author failed to mention whether the high field conductance  $\Lambda$  exceeded that at infinite dilution  $\Lambda_\infty$ . Hence, he may have seen the increased dissociation of ion-pairs, for which  $\Lambda < \Lambda_\infty$ <sup>5.6</sup>.

conduct by a "chain" mechanism. This phenomenon may be operative whenever protons or hydroxyl ions are present in the doping agent for glycerol-solvated systems. One suspects that the extraordinarily linear dependence of  $\log q_s$  on the needle potential  $V_N$  for NaOH-glycerol solutions is due to the fact that the mechanism of conduction and dissociation does not change with increased potential. This mechanism - of whatever origin - evidently takes precedence over other conduction means. Figure 5.2 (from Ref. 5.9) gives a comparison of the electrostatic spraying behaviour of NaOH-glycerol with that of other propellants. The slope of  $\log q_s$  versus  $V_N$  for NaOH-glycerol is much steeper than for the other electrolytes with two exceptions - NaI-glycerol and sulfuric acid-glycerol. Increased conductivity due to the "chain" mechanism would explain the hydroxide and acid cases, but the performance of NaI-glycerol is peculiar. (As for the other results given in Figure 5.2, past studies<sup>5.6</sup> of the high field conductivity of polyvalent electrolytes in aqueous solutions as compared to monovalent electrolytes are in agreement with the relative trends seen there. Polyvalent electrolytes have greater increases in conductivity with increased electric field<sup>5.6</sup>.) Work needs to be done to confirm whether the increased mobilities of protons and of hydroxide ions in glycerol solutions can be accredited to the "chain" mechanism. The increased mobilities of these ions in aqueous solution have been shown experimentally to be the result of such a mechanism. Further, no experiment has, as yet, been run on the NaOH-glycerol and the sulfuric acid-glycerol systems to establish the dependence of the actual conductivity on the applied electric field strength.

Another facet of electrostatic spraying in which further knowledge of electrolytic solution behaviour may aid in analysis is the inequality in the performance of most propellants as needle voltage polarity is changed. This problem is especially important in the development of bipolar thrusters. Difficulties specific to this research area include:

- (1) the tendency of certain ionic species to be reduced at the needle, producing either a gas which leads to arcing instabilities or a needle-clogging deposit
- (2) solvation, complexation, and ion neutralization phenomena which prevent, or impede, the formation of charged particles at one needle polarity.

Cases of all these situations have been found. One such is that of silver nitrate in glycerol-glycol<sup>5.10</sup>. A dc beam of charged particles can be formed for silver nitrate-glycerol for both needle voltage polarities below 3kv<sup>5.10</sup>. But, for AgNO<sub>3</sub>-glycol and AgNO<sub>3</sub>-glycol solutions, dc (Mode III) spraying occurs only for negative needle potentials below 3kv in magnitude<sup>5.10</sup>. A similar failure has also been noted for NaI-glycerol: "Extended examination of NaI/glycerol revealed that this fluid was not capable of producing a DC beam at negative potentials"<sup>5.9</sup>. For NaI-glycerol, the neutralization of Na<sup>+</sup> ions is hindered by the fact that the electron in the metal is at a lower energy than it would be if it were transferred to the sodium ion<sup>5.9</sup>. Hence, the failure may stem from this phenomenon. But, is such an explanation applicable to the AgNO<sub>3</sub>-glycol result? The ease of neutralization of either Ag<sup>+</sup> or NO<sub>3</sub><sup>-</sup> should not differ significantly for the glycol and glycerine systems, in which solvation of these ions should be similar. Nevertheless, measurements of the transference numbers of silver ion and nitrate ion in these various solvents were made to determine whether there are significant differences in their degree of solvation. (A reduction in mobility (or transference number) for a given ion is indicative of the tendency to maintain a solvent shell during migration\* or to form complexes with the counterions.) Our initial results

---

\* At low electric fields in aqueous solutions, a 50% reduction in ionic mobility has been found for solvated lithium ion.

for the transference numbers of silver ion and nitrate ion were:\*

$$(1) \quad t_+ = 0.57, \text{ 0.11N AgNO}_3 \text{ in glycerol;}$$

$$(2) \quad t_+ = 0.48, \text{ 0.06N AgNO}_3 \text{ in glycol.}$$

(The possibility that silver ion or nitrate ion transferred a solvent shell was considered in the experimental approach, so that "true" transference numbers were obtained.) From the transference number for silver ion in glycol, it appears that the nitrate ion has a greater mobility than the silver ion, whereas the reverse is true in glycerol. Hence, the relative mobility of the silver ion is more affected by the change in solvent. A determination of the average number of solvent molecules migrating with a given ion for these various solutions is needed to ascertain more precisely the changes in degrees of solvation with solvent for the two ionic species. Methods are known for making such a measurement at low electric fields. In general, further study should be made of the effects of similar solvents on the ability of a given salt (in solution) to give rise to a dc charged particle beam.

Finally, the inefficiency in charged droplet generation which arises during droplet formation must stem from energy consumed in one of the following processes:

- (1) charge grouping to form a multiply-charged droplet (from Faraday cage experiments it is known that these particles are so charged<sup>5.1,5.2</sup>)

---

\* It should be noted that these measurements of the transference numbers (or relative mobilities) of the ions were made at low field strength. No method exists at present to distinguish the mobility of the individual types of ionic species at high electric field strengths. In organic solutions, where very large dependencies (often 200% or greater increases for moderate field strengths (Ref. 5.2, 5.6, 5.6)) of the conductivity on applied electric field are observed, knowledge of the individual mobilities could be of prime importance to electrostatic spraying analysis. In fact, it has been found that "if the ion being neutralized had a higher mobility than the ion ejected from the capillary, then much better specific charge distributions resulted..."<sup>9</sup> (These mobilities were evidently extrapolated from "zero-field" transference number measurements.)

- (2) Joule heating
- (3) extraction of the charged colloid particle from the fluid-vacuum interface
- (4) field distortion.

Such "intrinsic" inefficiency has been measured by utilizing a retarding potential method to determine the "actual" kinetic energy of charged particles as a function of applied needle voltage<sup>5.11</sup>. A 23% energy loss was "consistently"<sup>5.11</sup> noted. Such a large energy loss is "of the order of the molecular formation energy of the glycerol itself"<sup>5.11</sup>. \* No dissipative mechanism can be found to explain this large an energy loss<sup>5.11</sup>. Hence, it was suggested that part of the "energy" loss is actually due to evaporation. (The experiment performed could not distinguish between such mass and energy losses.) It seems necessary to hypothesize further that there is an "intense local heating of the glycerol droplets which then partially evaporate in flight"<sup>5.11</sup>. The heating, if occurring, must be due to migration of the ions in the electric field. If so, for a fixed needle potential, propellants having different conductivities should produce differing amounts of Joule heating.\*\* The breakage of solvent-solvent bonds in the extraction of the droplet, on the other hand, reduces the heat content of the liquid. Similarly, neither the energy consumed in moving charges into the region of multiple like charges, nor that lost due to field distortion would result in heating increase. Thus, it is critical that the degree of evaporation of particles in flight be determined. This degree of evaporation could be increased by heating the needle or possibly by bombarding the particles with light from an intense source. A greater "energy" loss should then be observed with the retarding field method.

---

\*  $\Delta H(\text{formation})$  for glycerol = 159.8 kcal/mole. Unfortunately, data for the experiment under consideration were omitted in Reference 5.11.

\*\* Also, measurements of the absolute mass loss could be made with a Faraday cage in conjunction with a retarding potential for particles of  $q_s < 100$  coul/kg. A thrust balance could be used for a multiple<sub>s</sub> needle arrangement.

To obtain an order of magnitude estimate of the pre-droplet-extraction energy loss, one could apply a high potential pulse to the needle of duration shorter than that of the droplet formation time. (The droplet formation time is on the order of microseconds<sup>5.2</sup>.) The resistivity of the solution will be greater for such a short voltage pulse due to the fact that the solution has a finite alignment time<sup>5.6</sup>. This energy loss would be equal to the integral of the product of the current flowing to the needle and the applied voltage at a particular instant of time, integrated over the period of a voltage pulse. Some current must flow since the charges are separated and neutralized prior to droplet extraction. The voltage pulse technique may also provide information on Joule heating. Such heating of electrolytic solutions under high applied electric fields has been detected even for high voltage pulses of microsecond duration<sup>5.6</sup>. This heating lowers the resistivity of the solution and should be detectable as a rise in needle current flow with time for a given applied needle voltage (of pulse duration).

Field distortion also appears to be a possible problem. Analysis of it can best be handled by comparing the  $q_s$  of ions as measured by time-of-flight and quadrupole mass spectrometers.\*

In summary, several areas in charged colloid generation research have been considered in which further knowledge of electrolytic solution characteristics at high electric fields could be utilized. More detailed information on the types of ionic species, and their respective mobilities under high field conditions, should lead to greater understanding of the origin of beam inefficiencies. Such information should aid in the selection of propellants having high beam efficiencies as well as high charge-to-mass ratios. In addition, further experiments on the overall high field conductivity of doped organic

---

\* In one case, results obtained from TOF analysis indicate a beam current which is 42% ionic and contains an ion having a  $q_s$  of 590,000 coul/kg (Ref. 5.4) -- 13% is too high for an ion composed of two molecules of glycerol. Field distortion could explain the discrepancy.



solutions are needed. The inefficiency of the droplet extraction process may also be traceable to Joule heating occurring during ion migration.

## REFERENCES

- 5.1. Pfeifer, R.: Parametric Studies of Electrohydrodynamic Spraying. Ph.D. thesis, University of Illinois. June, 1965.
- 5.2. Pfeifer, R., and Hendricks, C.: Parametric Studies of Electrohydrodynamic Spraying. AIAA Paper No. 66-252. March, 1966.
- 5.3. Cohen, E.: Research on Charged Colloid Generation. APL TDR 64-75. June, 1964.
- 5.4. Cohen, E., and Huberman, M.: Research on Charged Particle Electrostatic Thrusters. AFAPL TR 66-94. September, 1966.
- 5.5. Perel, J., Bates, T., Mahoney, J., Moore, R., and Yahiku, A.: Research on a Charged Particle Bipolar Thruster. AIAA Paper No. 67-728. September, 1967.
- 5.6. Eckstrom, H., and Schmelzer, C.: The Wien Effect: Deviations of Electrolytic Solutions from Ohm's Law Under High Field Strengths. Chem. Rev., 24, 367 (1939).
- 5.7. Sharbaugh, A., Schmelzer, C., Eckstrom, H., and Kraus, C.: Dielectric Behaviour of Solutions of Electrolytes in Solvents of Low Dielectric Constant I. A Calorimetric Method for Measuring Losses. J. Chem. Phys., 15, 47 (1947). A. Sharbaugh, H. Eckstrom, and C. Kraus. "...II. Dielectric Absorption." Loc. cit., p. 54. H. Strobel and H. Eckstrom. "...III. The Influence of Constitution on Dielectric Absorption." J. Chem. Phys., 16, 817 (1948). "...IV. A. Dielectric Absorption of Butyl Alcohol, B. The Second Wien Effect." Loc. cit., p. 827.
- 5.8. Hunter, R., and Wineland, S.: Charged Colloid Generation Research. Space Electronics Symposium, AAS Science and Technology Series V.6, 1965, p. II-1.
- 5.9. Wineland, S., Burson, W., and Hunter, R.: The Electrodynamic Generation of Charged Droplet Beams. AFAPL TR-66-72. August, 1966.

- 5.10. Steadman, V., and Tompkin, G. W.: The Production of Charged Colloid Particles from Waste-Type Materials. Advanced Electric Propulsion Research, NASA Grant NGR06-002-032. January, 1968.
- 5.11. Beyon, J., Cohen, E., Goldin, D., Huberman, M., Kidd, P., and Zafran, S.: Present Status of Colloid Microthruster Technology. AIAA Paper No. 67-531.
- 5.12. Handbook of Chemistry and Physics 41st ed. 1959-60, Chemical Rubber Pub. Co., p. 1916, 1922.

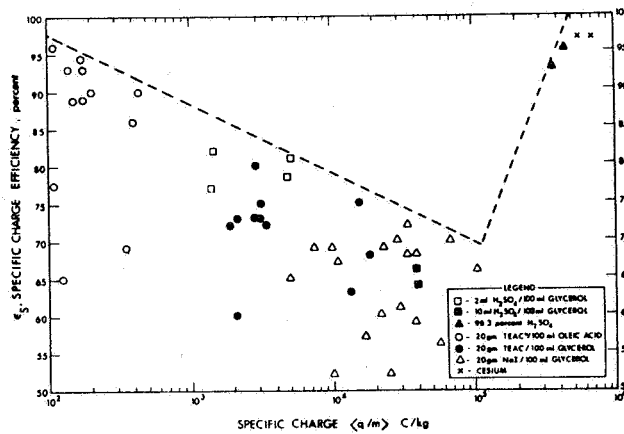


FIG. 5.1 (From Ref. 5.5, page 5).

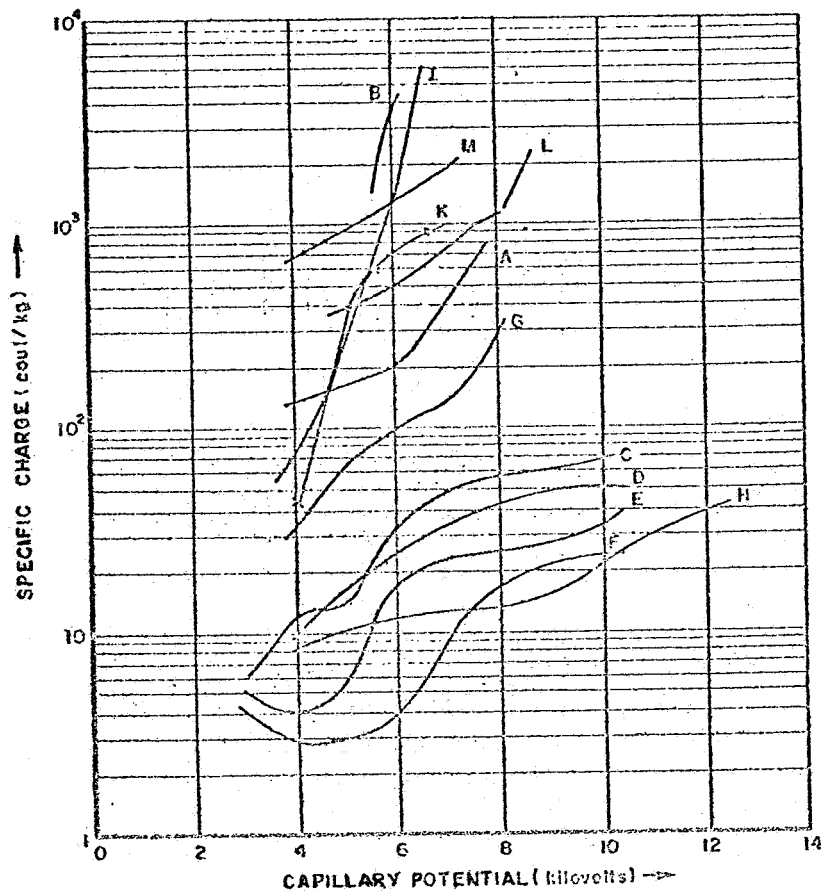


FIG. 5.2 (From Ref. 5.9, pages 32-33) Specific Charge vs. Capillary Potential.

Parameters for Curves:

Curve	Solution
A, B	15g NaI/100 ml glycerol
C, D, E, F	1.6g NaCl/100 ml glycerol
G	5 ml H <sub>2</sub> SO <sub>4</sub> /100 ml glycerol
H	0.78g NaCl/100 ml tetraethyleneglycol
I	0.35g NaOH/50 ml glycerol
J	20g NaI/50 ml glycerol
K	0.3ml H <sub>2</sub> SO <sub>4</sub> /50 ml glycerol
L	1.5gMgCl <sub>2</sub> -6H <sub>2</sub> O/50 ml glycerol
M	20g ZnCl <sub>2</sub> /50 ml glycerol